# CRACKING OF A HOMOGENEOUS HALF PLANE DUE TO SLIDING CONTACT

Fazil Erdogan
and
Serkan Dag

Lehigh University
Bethlehem, PA 18015

March 2001

AIR FORCE OFFICE OF SCIENTIFIC RESEARCH
GRANT F49620-98-1-0028

## DTIC CONVERSATION RECORD FOR DISTRIBUTION STATEMENT REQUEST

| DTIC Personnel Making Call | Date | Time |
|---|---|---|
| JACK RIKE | 17 Apr. 02 | 1430 |
| **Authorizing Official** | **Phone** | |
| F. Erdogan | | |

**Agency** LEHIGH Univ. MECH. Engineering & Mechanics

**Title**

**Internet Document URL** *(if applicable)*

**Distribution Statement** *(Please check one box)*

- ☑ DISTRIBUTION STATEMENT A: Approved for public release. Distribution is unlimited.
- ☐ DISTRIBUTION STATEMENT B: Distribution authorized to U.S. Government Agencies only.
- ☐ DISTRIBUTION STATEMENT C: Distribution authorized to U.S. Government Agencies and their contractors.
- ☐ DISTRIBUTION STATEMENT D: Distribution authorized to U.S. Department of Defense (DoD) and U.S DoD contractors only.
- ☐ DISTRIBUTION STATEMENT E: Distribution authorized to U.S. Department of Defense (DoD) components only.
- ☐ DISTRIBUTION STATEMENT F: Further dissemination only as directed by the controlling DoD office indicated below or by higher authority.
- ☐ DISTRIBUTION STATEMENT X: Distribution authorized to U.S. Government agencies and private individuals or enterprises eligible to obtain export-controlled technical data in accordance with DoD Directive 5230.25, Withholding of Unclassified Technical Data from Public Disclosure, 6 Nov 84.

**Reason for the above identified distribution statement** *(in accordance with DoD Directive 5230.24)*

| Controlling Office | Date of Distribution Statement Determination |
|---|---|
| | |

**AQ Number** *(For DTIC-OCA Use Only)*

# CRACKING OF A HOMOGENEOUS HALF PLANE DUE TO SLIDING CONTACT

Serkan Dag and Fazil Erdogan

*ME-MECH. Department, Lehigh University, Bethlehem, PA 18015*

**Abstract**

In this report the initiation and subcritical growth of surface cracks in homogeneous materials due to sliding contact are considered. The load is applied through a rigid stamp with an arbitrary profile. The problem is formulated and solved under the assumptions of plane elasticity and Coulomb friction. The stress state on the surface of the half plane is analyzed in the absence of any cracks in order to determine the crack initiation force and angle. A surface crack is then introduced and the resulting coupled crack/contact problem is investigated. Extensive results are presented regarding mostly the mixed mode stress intensity factors which constitute the main driving force for the subcritically growing cracks.

## 1. Introduction

In this report, the edge crack problem in a homogenous half-plane due to sliding contact will be considered. The problem geometry is shown in Figure 1. A homogeneous elastic half-plane is indented by a rigid stamp of arbitrary profile. The contact area extends from $x = a$ to $x = b$ at the surface and the half-plane contains an edge crack of length $d$. The crack is perpendicular to the boundary of the half-plane. The contact is assumed to transfer both normal and tangential forces. A normal force of $P$ is applied by the rigid stamp and sliding contact is assumed at the interface. Friction coefficient is denoted by $\eta$, hence the tangential force transferred by the contact is equal to $\eta P$. $\mu$ is the

shear modulus of the half-plane, $\kappa$ is the Kolosov's constant and for this plane strain problem, it is equal to $3 - 4\nu$ where $\nu$ is the Poisson's ratio.

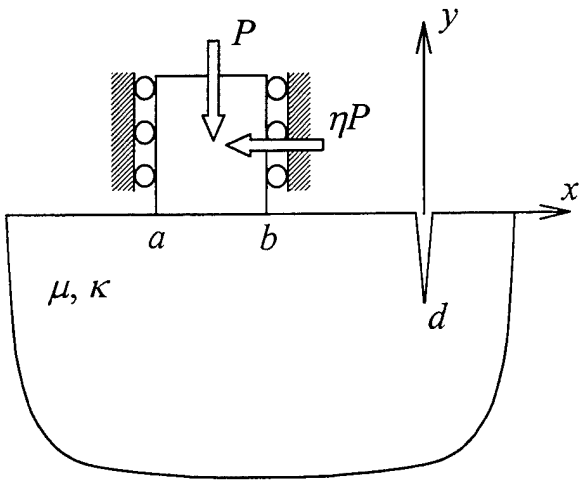


**Figure 1:** Geometry of the problem

In this report, the two dimensional elasticity problem will be formulated and solved using Navier's equations. By the use of Fourier Transforms, the problem will be reduced to a system of three integral equations, and these equations will then be solved numerically to determine the stress intensity factors at the crack tip and contact stresses.

## 2. Formulation of the problem

First, we will express the boundary conditions that must be satisfied in this problem. There are mixed boundary conditions at the surface $y = 0$ and at the crack plane $x = 0$. At the surface of the half-plane $y = 0$, shear and normal stresses are zero outside the contact area, in the contact area normal displacement component $v(x, 0)$ is known. At the crack plane $x = 0$, crack faces do not transfer any normal or shear stress and they displace relative to each other in normal and tangential directions, but outside the crack,

i.e. if $y < d$, there is no relative tangential or normal displacement at $x = 0$ plane. The conditions at the crack plane are valid only if the crack is open, under some loading conditions crack faces may contact. However, the problem will be solved by assuming an open crack and a negative mode I stress intensity factor will indicate that crack closure occurs for that loading condition. There are also additional boundary conditions, integration of the normal stresses in the contact area must give the total force $P$ applied to the contact and stresses must vanish as $(x^2 + y^2) \rightarrow \infty$. Since, sliding contact is assumed, shear stress in the contact area is given by Coulomb's Law. All the boundary conditions can be expressed mathematically in the following form,

$$\sigma_{yy}(x, 0) = 0, \qquad x < a \text{ and } x > b, \tag{1a}$$

$$\sigma_{xy}(x, 0) = 0, \qquad x < a \text{ and } x > b, \tag{1b}$$

$$\frac{4\mu}{\kappa + 1}\frac{\partial}{\partial x}v(x, 0) = f(x), \qquad a < x < b, \tag{1c}$$

$$\sigma_{xy}(x, 0) = \eta\sigma_{yy}(x, 0), \qquad a < x < b, \tag{1d}$$

$$\sigma_{xx}(0, y) = 0, \qquad d < y < 0, \tag{1e}$$

$$\sigma_{xy}(0, y) = 0, \qquad d < y < 0, \tag{1f}$$

$$\int_a^b \sigma_{yy}(x, 0)dx = -P, \tag{1g}$$

$$(\sigma_{yy}, \sigma_{xy}, \sigma_{xx}) \rightarrow 0 \text{ as } (x^2 + y^2) \rightarrow \infty, \tag{1h}$$

where $v(x, y)$ is the normal displacement component and $f(x)$ is a known function. Note that in (1d) $\sigma_{yy}(x, 0)$ is always negative and if the friction coefficient is taken as positive, the shear force transferred by the contact will be directed as shown in Figure 1. The problem will be formulated using three unknown functions and using superposition. Considering Figure 1 and boundary conditions (1), following unknown functions can be defined:

$$\frac{2\mu}{\kappa+1}\frac{\partial}{\partial y}(u(0^+,y)-u(0^-,y))=f_1(y), \qquad d<y<0, \tag{2a}$$

$$\frac{2\mu}{\kappa+1}\frac{\partial}{\partial y}(v(0^+,y)-v(0^-,y))=f_2(y), \qquad d<y<0, \tag{2b}$$

$$\sigma_{yy}(x,0)=f_3(x), \qquad a<x<b, \tag{2c}$$

where $u$ and $v$ are the displacement components in $x$ and $y$ directions respectively. The scheme that will be employed in the formulation is shown in Figure 2. Problem 1 is the contact problem without crack and in this case the stresses and displacements will be obtained in terms of the unknown contact stress which is given by (2c). In problem 2 stress and displacement fields will be obtained in terms of the relative displacement derivatives of the crack faces which are given by (2a) and (2b). This can also be viewed as the distributed dislocation solution for the homogenous half-plane. Note that $f_1$ and $f_2$ are zero in problem 1 and $f_3$ is zero in problem 2. The total stress and displacement fields for the original problem can then be obtained by summing the solutions of the problems 1 and 2, and satisfying the boundary conditions of the original coupled problem. The stresses and displacements may then be expressed as

$$\sigma_{ij}(x,y)=\sigma_{ij}^{(1)}(x,y)+\sigma_{ij}^{(2)}(x,y), \qquad i,j=x \text{ or } y, \tag{3a}$$

$$u(x,y)=u^{(1)}(x,y)+u^{(2)}(x,y), \tag{3b}$$

$$v(x,y)=v^{(1)}(x,y)+v^{(2)}(x,y). \tag{3c}$$

Superscripts (1) and (2) stand for problems (1) and (2) respectively. The stress and displacement fields given by (3) must satisfy the conditions given by (1). In the following sections problems 1 and 2 will be formulated to derive the stress and displacement fields in terms of a certain set of unknown functions.

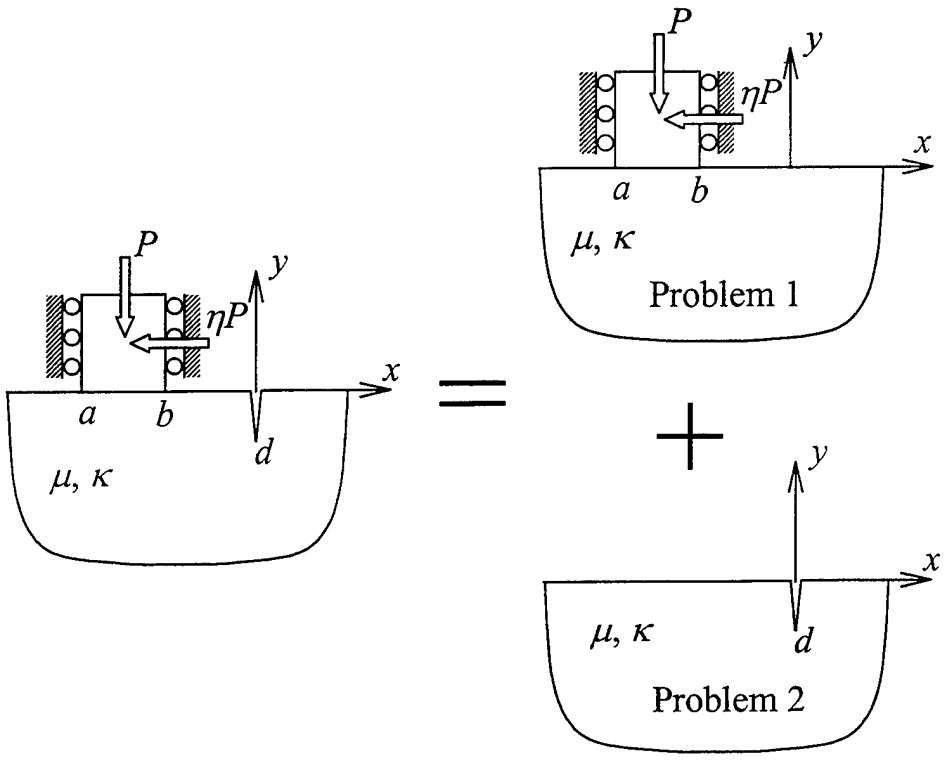


**Figure 2:** Superposition

2.1 *Problem 1 - The Contact Problem*

Geometry of the contact problem is shown in Figure 3. In this section stresses and displacements will be obtained in terms of the unknown contact stress, $\sigma_{yy}(x,0)$ at the surface. The equations of equilibrium can be written in the following form,

$$\frac{\partial \sigma_{xx}}{\partial x} + \frac{\partial \sigma_{xy}}{\partial y} = 0, \tag{4a}$$

$$\frac{\partial \sigma_{yy}}{\partial y} + \frac{\partial \sigma_{xy}}{\partial x} = 0. \tag{4b}$$

Assuming plane stress or plane strain and small deformations, for the linear elastic medium considered Hooke's law becomes

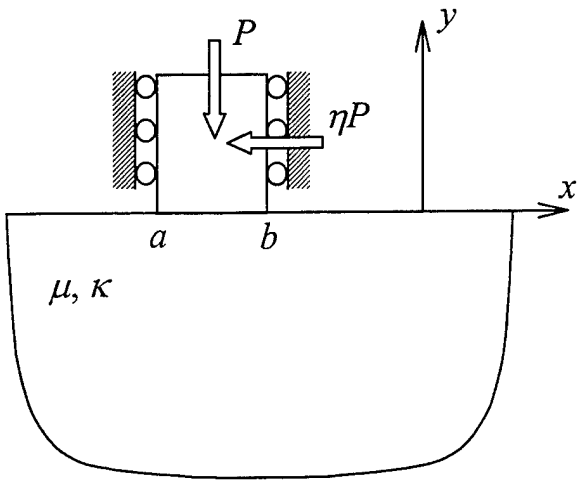


**Figure 3:** Contact Problem

$$\sigma_{yy}(x,y) = \frac{\mu}{\kappa-1}\Big\{(\kappa+1)\frac{\partial v}{\partial y} + (3-\kappa)\frac{\partial u}{\partial x}\Big\}, \tag{5a}$$

$$\sigma_{xx}(x,y) = \frac{\mu}{\kappa-1}\Big\{(\kappa+1)\frac{\partial u}{\partial x} + (3-\kappa)\frac{\partial v}{\partial y}\Big\}, \tag{5b}$$

$$\sigma_{xy}(x,y) = \mu\Big\{\frac{\partial u}{\partial y} + \frac{\partial v}{\partial x}\Big\}. \tag{5c}$$

Contact problem is a plane strain problem, hence for this case $\kappa$ is equal to $3-4\nu$. Substituting (5) in (4a) and (4b), governing equations for the displacements can be obtained as follows,

$$(\kappa+1)\frac{\partial^2 u}{\partial x^2} + (\kappa-1)\frac{\partial^2 u}{\partial y^2} + 2\frac{\partial^2 v}{\partial x \partial y} = 0, \tag{6a}$$

$$(\kappa-1)\frac{\partial^2 v}{\partial x^2} + (\kappa+1)\frac{\partial^2 v}{\partial y^2} + 2\frac{\partial^2 u}{\partial x \partial y} = 0. \tag{6b}$$

Considering Fourier Transformation in $x$, $u$ and $v$ can be expressed in the following form,

$$u(x,y) = \frac{1}{2\pi}\int_{-\infty}^{\infty} U(w,y)\exp(i\omega x)d\omega, \tag{7a}$$

$$v(x,y) = \frac{1}{2\pi}\int_{-\infty}^{\infty} V(w,y)\exp(i\omega x)d\omega, \tag{7b}$$

where, $i = \sqrt{-1}$ and $U(\omega, y)$ and $V(\omega,y)$ are Fourier transforms of $u(x, y)$ and $v(x, y)$ in $x$, respectively. Substituting (7) in (6) following ordinary differential equations are obtained

$$-\omega^2(\kappa+1)U + (\kappa-1)\frac{d^2U}{dy^2} + 2i\omega\frac{dV}{dy} = 0, \tag{8a}$$

$$-\omega^2(\kappa-1)V + (\kappa+1)\frac{d^2V}{dy^2} + 2i\omega\frac{dU}{dy} = 0. \tag{8b}$$

Solving equations (8), substituting the solution in (7) and considering the regularity condition given by (1h), displacements can be expressed as follows:

$$u(x,y) = \frac{1}{2\pi}\int_{-\infty}^{\infty} (A_1C_1 + A_2C_2y)\exp(|\omega|y + i\omega x)d\omega, \tag{9a}$$

$$v(x,y) = \frac{1}{2\pi}\int_{-\infty}^{\infty} (C_1 + C_2y)\exp(|\omega|y + i\omega x)d\omega. \tag{9b}$$

Note that in (9) $y < 0$, $C_1$ and $C_2$ are unknown constants and $A_1$ and $A_2$ are given by

$$A_1 = \frac{i\kappa}{\omega}\frac{C_2}{C_1} + \frac{i|\omega|}{\omega}, \qquad A_2 = \frac{i|\omega|}{\omega}. \tag{10a,b}$$

Substituting (9) in (5) stresses can also be obtained

$$\sigma_{xx}(x,y) = -\frac{\mu}{2\pi}\int_{-\infty}^{\infty}\Big[2|\omega|C_1 + ((\kappa+3) + 2|\omega|y)C_2\Big]\exp(|\omega|y + i\omega x)d\omega, \tag{11a}$$

$$\sigma_{yy}(x,y) = \frac{\mu}{2\pi}\int_{-\infty}^{\infty}\Big[2|\omega|C_1 + ((\kappa-1) + 2|\omega|y)C_2\Big]\exp(|\omega|y + i\omega x)d\omega, \tag{11b}$$

$$\sigma_{xy}(x,y) = \frac{\mu i}{2\pi}\int_{-\infty}^{\infty}\Big[2\omega C_1 + \big((\kappa+1)|\omega| + 2\omega^2 y\big)\frac{C_2}{\omega}\Big]\exp(|\omega|y + i\omega x)d\omega. \tag{11c}$$

The constants $C_1$ and $C_2$ will be determined using the conditions (1a), (1b) and (1d) and stresses and displacements will be expressed in terms of the contact stress $\sigma_{yy}(x,0)$. Considering boundary conditions (1a), (1b), (1d) and (2c) we can write

$$\sigma_{yy}(x,0)=\frac{\mu}{2\pi}\int_{-\infty}^{\infty}\Big[2|\omega|C_1+(\kappa-1)C_2\Big]\exp(i\omega x)d\omega=\begin{cases}f_3(x), & a<x<b\\ 0, & x<a,\,x>b\end{cases} \tag{12a}$$

$$\sigma_{xy}(x,0)=\frac{\mu i}{2\pi}\int_{-\infty}^{\infty}\Big[2\omega C_1+(\kappa+1)\frac{|\omega|}{\omega}C_2\Big]\exp(i\omega x)d\omega=\begin{cases}\eta f_3(x), & a<x<b\\ 0, & x<a,\,x>b\end{cases} \tag{12b}$$

Taking Fourier transforms of both sides in (12) we obtain the following equations,

$$\mu(2|\omega|C_1+(\kappa-1)C_2)=\int_a^b f_3(t)\exp(-i\omega t)dt, \tag{13a}$$

$$\mu\left(2i\omega C_1+i(\kappa+1)\frac{|\omega|}{\omega}C_2\right)=\int_a^b \eta f_3(t)\exp(-i\omega t)dt. \tag{13b}$$

$C_1$ and $C_2$ are determined in terms of $f_3$ solving the linear system of equations (13) and they are substituted in (11) to derive the expressions for the stresses. These operations are carried out using the symbolic manipulator MAPLE, some integrals are evaluated in closed form and following results are obtained:

$$\sigma_{xx}(x,y)=\frac{2}{\pi}\int_a^b\frac{\eta(t-x)^3-y(t-x)^2}{\left(y^2+(t-x)^2\right)^2}f_3(t)dt, \tag{14a}$$

$$\sigma_{yy}(x,y)=\frac{2}{\pi}\int_a^b\frac{\eta y^2(t-x)-y^3}{\left(y^2+(t-x)^2\right)^2}f_3(t)dt, \tag{14b}$$

$$\sigma_{xy}(x,y)=\frac{2}{\pi}\int_a^b\frac{-\eta y(t-x)^2+y^2(t-x)}{\left(y^2+(t-x)^2\right)^2}f_3(t)dt. \tag{14c}$$

the resulting system of ordinary differential equations the expressions for stresses and displacements for both half-planes $x > 0$ and $x < 0$ can be obtained by following the procedure described below.

*Half-Plane, $x > 0$*

In the following equations superscript 4 stands for the half-plane $x > 0$.

$$u^{(4)}(x,y) = \frac{1}{2\pi}\int_{-\infty}^{\infty}\left[\frac{i|\omega|}{\omega}C_1^{(4)} + \left(\frac{i\kappa}{\omega} + \frac{i|\omega|}{\omega}x\right)C_2^{(4)}\right]\exp(-|\omega|x + i\omega y)d\omega, \tag{15a}$$

$$v^{(4)}(x,y) = \frac{1}{2\pi}\int_{-\infty}^{\infty}\left(C_1^{(4)} + C_2^{(4)}x\right)\exp(-|\omega|x + i\omega y)d\omega, \tag{15b}$$

$$\sigma_{xx}^{(4)}(x,y) = -\frac{\mu i}{2\pi}\int_{-\infty}^{\infty}\left[2\omega C_1^{(4)} + \left((\kappa+1)|\omega| + 2\omega^2 x\right)\frac{C_2^{(4)}}{\omega}\right]\exp(-|\omega|x + i\omega y)d\omega, \tag{15c}$$

$$\sigma_{yy}^{(4)}(x,y) = \frac{\mu i}{2\pi}\int_{-\infty}^{\infty}\left[2\omega C_1^{(4)} + \left(-(3-\kappa)|\omega| + 2\omega^2 x\right)\frac{C_2^{(4)}}{\omega}\right]\exp(-|\omega|x + i\omega y)d\omega, \tag{15d}$$

$$\sigma_{xy}^{(4)}(x,y) = -\frac{\mu}{2\pi}\int_{-\infty}^{\infty}\left[2|\omega|C_1^{(4)} + ((\kappa-1) + 2|\omega|x)C_2^{(4)}\right]\exp(-|\omega|x + i\omega y)d\omega, \tag{15e}$$

where $C_1^{(4)}$ and $C_2^{(4)}$ are unknown constants. Similarly the solution for $x < 0$ is obtained in the following form:

*Half-Plane, $x < 0$*

In the following equations superscript 3 stands for the half-plane $x < 0$.

$$u^{(3)}(x,y) = \frac{1}{2\pi}\int_{-\infty}^{\infty}\left[-\frac{i|\omega|}{\omega}C_1^{(3)} + \left(\frac{i\kappa}{\omega} - \frac{i|\omega|}{\omega}x\right)C_2^{(3)}\right]\exp(|\omega|x + i\omega y)d\omega, \tag{16a}$$

$$v^{(3)}(x,y) = \frac{1}{2\pi}\int_{-\infty}^{\infty}\Big(C_1^{(3)} + C_2^{(3)}x\Big)\exp(|\omega|x + i\omega y)d\omega, \tag{16b}$$

$$\sigma_{xx}^{(3)}(x,y) = \frac{\mu i}{2\pi}\int_{-\infty}^{\infty}\Big[-2\omega C_1^{(3)} + \big((\kappa+1)|\omega| - 2\omega^2 x\big)\frac{C_2^{(3)}}{\omega}\Big]\exp(|\omega|x + i\omega y)d\omega, \tag{16c}$$

$$\sigma_{yy}^{(3)}(x,y) = -\frac{\mu i}{2\pi}\int_{-\infty}^{\infty}\Big[-2\omega C_1^{(3)} - \big((3-\kappa)|\omega| + 2\omega^2 x\big)\frac{C_2^{(3)}}{\omega}\Big]\exp(|\omega|x + i\omega y)d\omega, \tag{16d}$$

$$\sigma_{xy}^{(3)}(x,y) = \frac{\mu}{2\pi}\int_{-\infty}^{\infty}\Big[2|\omega|C_1^{(3)} + \big(-(\kappa-1) + 2|\omega|x\big)C_2^{(3)}\Big]\exp(|\omega|x + i\omega y)d\omega, \tag{16e}$$

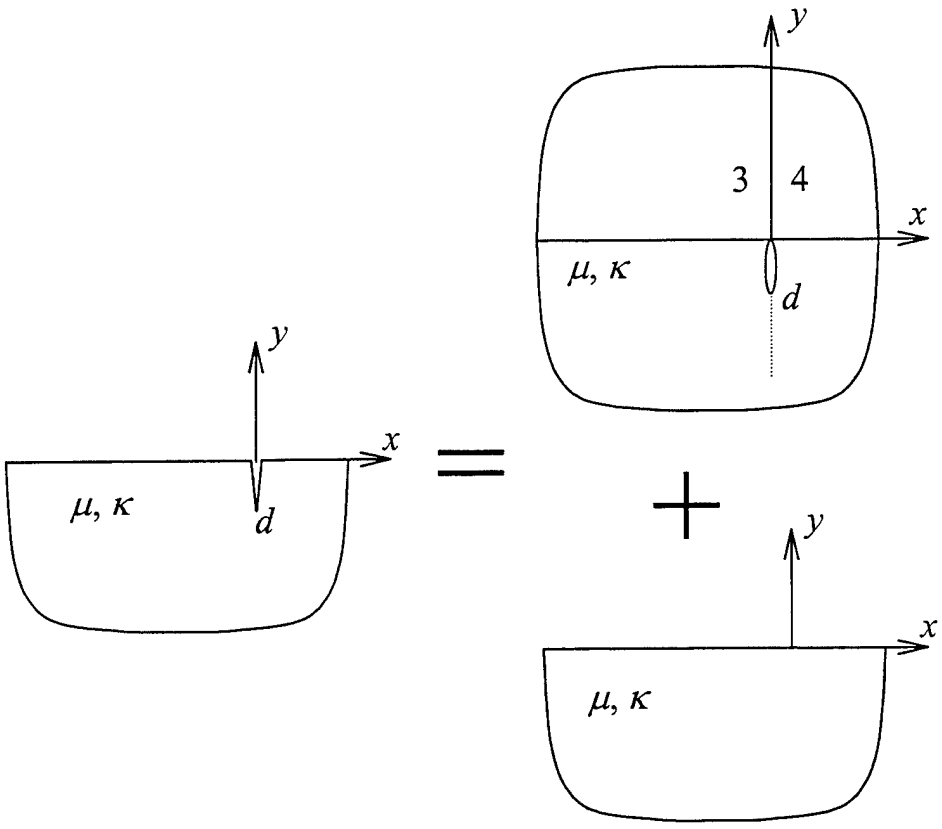


**Figure 5:** Superposition for the crack problem

where $C_1^{(3)}$ and $C_2^{(3)}$ are unknown constants. The boundary conditions for the infinite plane problem are in the following form,

$$\sigma_{xx}^{(3)}(0,y) = \sigma_{xx}^{(4)}(0,y), \qquad -\infty < y < \infty, \tag{17a}$$

$$\sigma_{xy}^{(3)}(0,y) = \sigma_{xy}^{(4)}(0,y), \qquad -\infty < y < \infty, \tag{17b}$$

$$\frac{2\mu}{\kappa+1}\frac{\partial}{\partial y}\left(u^{(4)}(0,y) - u^{(3)}(0,y)\right) = \begin{cases} f_1(y), & d < y < 0 \\ 0, & y < d,\ y > 0 \end{cases} \tag{17c}$$

$$\frac{2\mu}{\kappa+1}\frac{\partial}{\partial y}\left(v^{(4)}(0,y) - v^{(3)}(0,y)\right) = \begin{cases} f_2(y), & d < y < 0 \\ 0, & y < d,\ y > 0 \end{cases} \tag{17d}$$

Using the expressions (15), (16) and boundary conditions (17), the four unknown constants are determined in terms of $f_1$ and $f_2$ using the symbolic manipulator MAPLE. The constants are then substituted in the expressions for stresses and displacements, and the stresses and normal displacement derivative for the infinite plane containing a crack are obtained as follows:

$$\sigma_{yy}^{(i)}(x,y) = \frac{1}{\pi}\int_d^0 \frac{(y-t)\left(x^2-(y-t)^2\right)}{\left(x^2+(y-t)^2\right)^2} f_1(t)dt$$

$$+\frac{1}{\pi}\int_d^0 \frac{x\left(x^2+3(y-t)^2\right)}{\left(x^2+(y-t)^2\right)^2} f_2(t)dt, \tag{18a}$$

$$\sigma_{xx}^{(i)}(x,y) = -\frac{1}{\pi}\int_d^0 \frac{(y-t)\left(3x^2+(y-t)^2\right)}{\left(x^2+(y-t)^2\right)^2} f_1(t)dt$$

$$-\frac{1}{\pi}\int_d^0 \frac{x\left(-x^2+(y-t)^2\right)}{\left(x^2+(y-t)^2\right)^2} f_2(t)dt, \tag{18b}$$

$$\sigma_{xy}^{(i)}(x,y) = \frac{1}{\pi}\int_d^0 \frac{x\left(x^2-(y-t)^2\right)}{\left(x^2+(y-t)^2\right)^2} f_1(t)dt$$

$$+\frac{1}{\pi}\int_d^0 \frac{(y-t)\left(x^2-(y-t)^2\right)}{\left(x^2+(y-t)^2\right)^2} f_2(t)dt, \tag{18c}$$

$$\frac{\partial}{\partial x}v^{(i)}(x,y) = \frac{1}{4\pi\mu}\int_d^0 \frac{(1-\kappa)x^3 - (3+\kappa)x(y-t)^2}{\left(x^2+(y-t)^2\right)^2} f_1(t)dt$$

$$+ \frac{1}{4\pi\mu}\int_d^0 \frac{(y-t)\left[(1-\kappa)x^2 - (3+\kappa)(y-t)^2\right]}{\left(x^2+(y-t)^2\right)^2} f_2(t)dt, \tag{18d}$$

where superscript $(i)$ stands for the infinite plane. Half-plane $y < 0$ solution, can now be superimposed on the solution for the crack in the infinite plane to obtain the required solution. The half plane $y < 0$ solution is given by equations (9) and (11) in terms of two unknown constants $C_1$ and $C_2$. These constants are determined in this case by imposing the following free surface conditions:

$$\sigma_{yy}(x,0) = 0, \qquad -\infty < x < \infty, \tag{19a}$$

$$\sigma_{xy}(x,0) = 0, \qquad -\infty < x < \infty. \tag{19b}$$

Note that these conditions must be satisfied, by the total solution, i.e., the sum of the solutions for infinite and half-planes have to satisfy the boundary conditions. The constants $C_1$ and $C_2$ are determined using the symbolic manipulator MAPLE, by imposing the above mentioned boundary conditions, the stresses and normal displacement derivative for a crack in a half plane as depicted in Figure 4, are then obtained as follows:

$$\sigma_{xx}(x,y) = \frac{1}{\pi}\left\{\int_d^0 S_{xx1}(x,y,t)f_1(t)dt + \int_d^0 S_{xx2}(x,y,t)f_2(t)dt\right\} + \sigma_{xx}^{(i)}(x,y), \tag{20a}$$

$$\sigma_{yy}(x,y) = \frac{1}{\pi}\left\{\int_d^0 S_{yy1}(x,y,t)f_1(t)dt + \int_d^0 S_{yy2}(x,y,t)f_2(t)dt\right\} + \sigma_{yy}^{(i)}(x,y), \tag{20b}$$

$$\sigma_{xy}(x,y) = \frac{1}{\pi}\left\{\int_d^0 S_{xy1}(x,y,t)f_1(t)dt + \int_d^0 S_{xy2}(x,y,t)f_2(t)dt\right\} + \sigma_{xy}^{(i)}(x,y), \tag{20c}$$

$$\frac{\partial v(x,y)}{\partial x} = \frac{1}{4\pi\mu}\left\{\int_d^0 S_{v1}(x,y,t)f_1(t)dt + \int_d^0 S_{v2}(x,y,t)f_2(t)dt\right\} + \frac{\partial v^{(i)}(x,y)}{\partial x}, \tag{20d}$$

$$S_{xx1}(x,y,t) = \Big\{16yt(y+t)^3 - 2(y+t)\big(y^2+10yt+3t^2\big)\big((y+t)^2+x^2\big)$$

$$+ (3y+5t)\big((y+t)^2+x^2\big)^2\Big\}/\big((y+t)^2+x^2\big)^3, \tag{20e}$$

$$S_{xx2}(x,y,t) = \Big\{16xyt(y+t)^2 - 2x(3t^2+4yt-y^2)\big((y+t)^2+x^2\big)$$

$$- x\big((y+t)^2+x^2\big)^2\Big\}/\big((y+t)^2+x^2\big)^3, \tag{20f}$$

$$S_{yy1}(x,y,t) = \Big\{-16yt(y+t)^3 - 2(y+t)\big(-y^2-6yt+t^2\big)\big((y+t)^2+x^2\big)$$

$$+ (-y+t)\big((y+t)^2+x^2\big)^2\Big\}/\big((y+t)^2+x^2\big)^3, \tag{20g}$$

$$S_{yy2}(x,y,t) = \Big\{-16xyt(y+t)^2 - 2x(y^2+t^2)\big((y+t)^2+x^2\big)$$

$$- x\big((y+t)^2+x^2\big)^2\Big\}/\big((y+t)^2+x^2\big)^3, \tag{20h}$$

$$S_{xy1}(x,y,t) = \Big\{-16xyt(y+t)^2 + 2x\big(4yt+y^2+t^2\big)\big((y+t)^2+x^2\big)$$

$$- x\big((y+t)^2+x^2\big)^2\Big\}/\big((y+t)^2+x^2\big)^3, \tag{20i}$$

$$S_{xy2}(x,y,t) = \Big\{16yt(y+t)^3 - 2(y+t)\big(-y^2+6yt+t^2\big)\big((y+t)^2+x^2\big)$$

$$+ (t-y)\big((y+t)^2+x^2\big)^2\Big\}/\big((y+t)^2+x^2\big)^3, \tag{20j}$$

$$S_{v1}(x,y,t) = x\Big\{(\kappa+3)(y^4-8yt^3) - 6(\kappa+8)y^2t^2 + (\kappa-1)x^4$$

$$+ 2(\kappa+1)x^2(y^2-t^2) - (1+3\kappa)t^4$$

$$+ 8yt(x^2-2y^2)\Big\}/\big((y+t)^2+x^2\big)^3, \tag{20k}$$

$$S_{v2}(x,y,t)=\Big\{(\kappa+3)y^5+2(\kappa+1)x^2(y^3+t^3)+(\kappa-1)x^4(y-t)$$

$$+6(\kappa-3)yx^2t(y+t)+2(9\kappa+23)t^2y^3+2(11\kappa+21)t^3y^2$$

$$+(13\kappa+5)t^4y+(7\kappa+21)ty^4+(1+3\kappa)t^5\Big\}/\big((y+t)^2+x^2\big)^3. \qquad (20l)$$

2.3 *Solution for the coupled crack - contact problem*

Since the expressions for the contact and crack problems are derived, stresses and normal displacement derivative for the coupled crack and contact problem can now be obtained by using equations (14) and (20). For the coupled problem stresses on the crack plane, and normal displacement derivative at the contact surface are found to be

$$\sigma_{xx}(0,y)=\frac{1}{\pi}\int_d^0\Big(\frac{1}{t-y}+\frac{1}{t+y}+\frac{2t}{(t+y)^2}-\frac{4t^2}{(t+y)^3}\Big)f_1(t)dt$$

$$+\frac{2}{\pi}\int_a^b\frac{\eta t^3-yt^2}{(y^2+t^2)^2}f_3(t)dt, \qquad -\infty<y<0, \qquad (21a)$$

$$\sigma_{xy}(0,y)=\frac{1}{\pi}\int_d^0\Big(\frac{1}{t-y}+\frac{1}{t+y}+\frac{2t}{(t+y)^2}-\frac{4t^2}{(t+y)^3}\Big)f_2(t)dt$$

$$+\frac{2}{\pi}\int_a^b\frac{-\eta yt^2+y^2t}{(y^2+t^2)^2}f_3(t)dt, \qquad -\infty<y<0, \qquad (21b)$$

$$\frac{4\mu}{\kappa+1}\frac{\partial}{\partial x}v(x,0)=-\frac{4}{\pi}\int_d^0\frac{t^2x}{(x^2+t^2)^2}f_1(t)+\frac{4}{\pi}\int_d^0\frac{t^3}{(x^2+t^2)^2}f_2(t)dt$$

$$-\eta\frac{\kappa-1}{\kappa+1}f_3(x)+\frac{1}{\pi}\int_a^b\frac{f_3(t)}{t-x}dt, \qquad -\infty<x<\infty. \qquad (21c)$$

## 3. Integral equations and singular behavior of the unknown functions

Using the boundary conditions (1c), (1e) and (1f) and equation (21), following system of integral equations can be obtained to determine the unknown functions $f_1$, $f_2$ and $f_3$ for the coupled crack and contact problem,

$$\sigma_{xx}(0,y) = \frac{1}{\pi}\int_d^0 \frac{f_1(t)}{t-y}dt + \frac{1}{\pi}\int_d^0 K_{11}(t,y)f_1(t)dt + \frac{1}{\pi}\int_a^b K_{13}(t,y)f_3(t)dt = 0,$$

$$d < y < 0, \qquad (22a)$$

$$\sigma_{xy}(0,y) = \frac{1}{\pi}\int_d^0 \frac{f_2(t)}{t-y}dt + \frac{1}{\pi}\int_d^0 K_{22}(t,y)f_2(t)dt + \frac{1}{\pi}\int_a^b K_{23}(t,y)f_3(t)dt = 0,$$

$$d < y < 0, \qquad (22b)$$

$$\frac{4\mu}{(\kappa+1)}\frac{\partial}{\partial x}v(x,0) = \frac{1}{\pi}\int_d^0 K_{31}(t,x)f_1(t)dt + \frac{1}{\pi}\int_d^0 K_{32}(t,x)f_2(t)dt - \eta\frac{\kappa-1}{\kappa+1}f_3(x)$$

$$+ \frac{1}{\pi}\int_a^b \frac{f_3(t)}{t-x}dt = f(x), \qquad a < x < b. \qquad (22c)$$

The kernels are given by

$$K_{11}(t,y) = K_{22}(t,y) = \frac{1}{t+y} + \frac{2t}{(t+y)^2} - \frac{4t^2}{(t+y)^3}, \qquad (23a)$$

$$K_{13}(t,y) = \frac{2(\eta t^3 - yt^2)}{(y^2+t^2)^2}, \qquad (23b)$$

$$K_{23}(t,y) = \frac{2(-\eta y t^2 + y^2 t)}{(y^2+t^2)^2}, \qquad (23c)$$

$$K_{31}(t,x) = -\frac{4t^2 x}{(x^2+t^2)^2}, \qquad (23d)$$

$$K_{32}(t,x) = \frac{4t^3}{(x^2+t^2)^2}, \qquad (23e)$$

All the singular integral equations contain a Cauchy integral and also the kernels $K_{11}$, $K_{22}$, $K_{13}$ and $K_{23}$ become singular as $t$ and $y$ simultaneously go to zero. Similarly, the kernels $K_{31}$ and $K_{32}$ become singular as $x$ and $t$ simultaneously go to zero. Since, $\sigma_{xx}(0,y)$, $\sigma_{xy}(0,y)$ and $\partial v(x,0)/\partial x$ are bounded at all points in their respective intervals, the unknown functions may have a special behavior in the form of a power singularity at the end points. In this section the singular behavior of the unknown functions will be examined using a function-theoretic method. In this analysis, there are two cases. If $b<0$, in addition to the Cauchy singularities only terms that can become singular are $K_{11}$ and $K_{22}$. Other kernels are bounded at all points of their respective intervals. If $b=0$, all of the kernels have to be examined to determine the singular behavior of unknown functions. We will begin with the case of $b<0$ in the next section.

3.1. *Singular behavior of the unknown functions for,* $b<0$

We will examine the possibility of a power singularity in the unknown functions for the case $b<0$. Initially we assume the following form for the unknown functions,

$$f_1(t)=F_1(t)(-t)^{\alpha_1}(t-d)^{\gamma_1}, \qquad d<t<0, \tag{24a}$$

$$f_2(t)=F_2(t)(-t)^{\alpha_2}(t-d)^{\gamma_2}, \qquad d<t<0, \tag{24b}$$

$$f_3(t)=F_3(t)(b-t)^{\omega}(t-a)^{\beta}, \qquad a<t<b. \tag{24c}$$

where $F_j(t)$, $(j=1,2,3)$ is Hölder-continuous in its respective interval and it is assumed that $-1<\Re(\alpha_1,\alpha_2,\gamma_1,\gamma_2,\omega,\beta)<0$. Consider now the following sectionally holomorphic functions

$$\psi_1(z)=\frac{1}{\pi}\int_d^0 \frac{f_1(t)}{t-z}dt, \tag{25a}$$

$$\psi_2(z) = \frac{1}{\pi}\int_d^0 \frac{f_2(t)}{t-z}dt, \tag{25b}$$

$$\psi_3(z) = \frac{1}{\pi}\int_a^b \frac{f_3(t)}{t-z}dt. \tag{25c}$$

The singular behavior of $\psi_j(z),\ (j=1,2,3)$ around the end points is in the following form, (see, for example Erdogan [1] or Muskhelishvili [2]),

$$\psi_1(z) = -F_1(d)(-d)^{\alpha_1}\frac{\exp(-\pi i\gamma_1)}{\sin(\pi\gamma_1)}(z-d)^{\gamma_1} + F_1(0)(-d)^{\gamma_1}\frac{z^{\alpha_1}}{\sin(\pi\alpha_1)} + F^*(z), \tag{26a}$$

$$\psi_2(z) = -F_2(d)(-d)^{\alpha_2}\frac{\exp(-\pi i\gamma_2)}{\sin(\pi\gamma_2)}(z-d)^{\gamma_2} + F_2(0)(-d)^{\gamma_2}\frac{z^{\alpha_2}}{\sin(\pi\alpha_2)} + F^*(z), \tag{26b}$$

$$\psi_3(z) = -F_3(a)(b-a)^{\omega}\frac{\exp(-\pi i\beta)}{\sin(\pi\beta)}(z-a)^{\beta} + F_3(b)(b-a)^{\beta}\frac{(z-b)^{\omega}}{\sin(\pi\omega)} + F^*(z). \tag{26c}$$

The function $F^*(z), (n=1,2,3)$ is bounded everywhere except possibly at the end points, where it may have a weaker singularity. Using Plemelj formulas and equations (26) the singular behavior of the Cauchy integrals at the end points, for the given form of unknown functions is obtained as follows:

$$\frac{1}{\pi}\int_d^0 \frac{f_1(t)}{t-y}dt = -F_1(d)(-d)^{\alpha_1}\cot(\pi\gamma_1)(y-d)^{\gamma_1} + F_1(0)(-d)^{\gamma_1}\cot(\pi\alpha_1)(-y)^{\alpha_1} + H_1(y), \qquad d<y<0, \tag{27a}$$

$$\frac{1}{\pi}\int_d^0 \frac{f_2(t)}{t-y}dt = -F_2(d)(-d)^{\alpha_2}\cot(\pi\gamma_2)(y-d)^{\gamma_2} + F_2(0)(-d)^{\gamma_2}\cot(\pi\alpha_2)(-y)^{\alpha_2} + H_2(y), \qquad d<y<0, \tag{27b}$$

$$\frac{1}{\pi}\int_a^b \frac{f_3(t)}{t-x}dt = -F_3(a)(b-a)^{\omega}\cot(\pi\beta)(x-a)^{\beta} + F_3(b)(b-a)^{\beta}\cot(\pi\omega)(b-x)^{\omega} + H_3(x), \qquad a<x<b. \tag{27c}$$

$H_1(y)$, $H_2(y)$ and $H_3(x)$ are bounded in their respective intervals, and at the end points their behavior is similar to that of $F^*(z)$ in equations (26). Now, consider equations (25) and assume that complex variables $z_1$, $z_2$ and $z_3$ satisfy the following conditions:

$$z_1 \notin (d < y < 0), \tag{28a}$$

$$z_2 \notin (d < y < 0), \tag{28b}$$

$$z_3 \notin (a < x < b). \tag{28c}$$

Under these conditions, $\psi_1(z_1)$, $\psi_2(z_2)$ and $\psi_3(z_3)$ are holomorphic. Thus, we can write,

$$\psi_1(z_1) = \frac{1}{\pi}\int_d^0 \frac{f_1(t)}{t - z_1}dt, \tag{29a}$$

$$\psi_2(z_2) = \frac{1}{\pi}\int_d^0 \frac{f_2(t)}{t - z_2}dt, \tag{29b}$$

$$\psi_3(z_3) = \frac{1}{\pi}\int_a^b \frac{f_3(t)}{t - z_3}dt. \tag{29c}$$

For the case $b < 0$, other than the Cauchy integrals whose singular behavior are given by (27), the kernels that can become singular are $K_{11}$ and $K_{22}$ and all the other kernels of the integral equation remain bounded. It can be seen that, as $y$ and $t$ simultaneously go to zero $K_{11}$ and $K_{22}$ become singular. Equations (29) will be used to determine the singular behavior of $K_{11}$ and $K_{22}$ in the following analysis. $K_{11}$ can also be expressed in the following form:

$$K_{11}(t,y) = -\frac{1}{(t+y)} + \frac{6y}{(t+y)^2} - \frac{4y^2}{(t+y)^3}. \tag{30}$$

Also note that,

$$\frac{1}{(t+y)^2} = -\frac{d}{dy}\left(\frac{1}{t+y}\right), \tag{31a}$$

$$\frac{1}{(t+y)^3} = \frac{1}{2}\frac{d^2}{dy^2}\left(\frac{1}{t+y}\right). \tag{31b}$$

Then, using (29a) and (30)-(31) we can write

$$\frac{1}{\pi}\int_d^0 K_{11}(t,y)f_1(t)dt = -\psi_1(-y) - 6y\frac{d}{dy}\psi_1(-y) - 2y^2\frac{d^2}{dy^2}\psi_1(-y). \tag{32}$$

Using (26a), singular behavior of this term near $y = 0$ can be expressed as follows:

$$\frac{1}{\pi}\int_d^0 K_{11}(t,y)f_1(t)dt \cong -\frac{2\alpha_1^2 + 4\alpha_1 + 1}{\sin(\pi\alpha_1)}(-d)^{\gamma_1}(-y)^{\alpha_1}F_1(0). \tag{33a}$$

Similarly for $K_{22}$ we obtain,

$$\frac{1}{\pi}\int_d^0 K_{22}(t,y)f_2(t)dt \cong -\frac{2\alpha_2^2 + 4\alpha_2 + 1}{\sin(\pi\alpha_2)}(-d)^{\gamma_2}(-y)^{\alpha_2}F_2(0). \tag{33b}$$

Note that instead of showing the bounded terms, $\cong$ sign is used in (33). Since singular behavior of all the terms are determined, using (27) and (33) the singular behavior of the integral equations given by (22) can be expressed as follows:

$$\sigma_{xx}(0,y) \cong F_1(0)(-d)^{\gamma_1}\left[\cot(\pi\alpha_1) - \frac{2\alpha_1^2 + 4\alpha_1 + 1}{\sin(\pi\alpha_1)}\right](-y)^{\alpha_1}$$

$$- F_1(d)(-d)^{\alpha_1}\cot(\pi\gamma_1)(y-d)^{\gamma_1}, \tag{34a}$$

$$\sigma_{xy}(0,y) \cong F_2(0)(-d)^{\gamma_2}\left[\cot(\pi\alpha_2) - \frac{2\alpha_2^2 + 4\alpha_2 + 1}{\sin(\pi\alpha_2)}\right](-y)^{\alpha_2}$$

$$- F_2(d)(-d)^{\alpha_2}\cot(\pi\gamma_2)(y-d)^{\gamma_2}, \tag{34b}$$

$$\frac{4\mu}{\kappa+1}\frac{\partial}{\partial x}v(x,0) \cong -F_3(a)(b-a)^{\omega}\cot(\pi\beta)(x-a)^{\beta} + F_3(b)(b-a)^{\beta}\cot(\pi\omega)(b-x)^{\omega}$$

$$- \eta\frac{\kappa-1}{\kappa+1}F_3(x)(b-x)^{\omega}(x-a)^{\beta}. \tag{34c}$$

Now, the characteristic equations can be derived by using (34) to determine the unknown exponents. Multiplying (34a) by $(-y)^{-\alpha_1}$ and letting $y \to 0$ we obtain,

$$\cot(\pi\alpha_1) - \frac{2\alpha_1^2 + 4\alpha_1 + 1}{\sin(\pi\alpha_1)} = 0, \tag{35}$$

and multiplying (34a) by $(y-d)^{-\gamma_1}$ and letting $y \to d$ we have,

$$\cot(\pi\gamma_1) = 0. \tag{36}$$

It is assumed that $F_1(0)$ and $F_1(d)$ are not equal to zero. Similarly using equation (34b) we obtain

$$\cot(\pi\alpha_2) - \frac{2\alpha_2^2 + 4\alpha_2 + 1}{\sin(\pi\alpha_2)} = 0, \tag{37a}$$

$$\cot(\pi\gamma_2) = 0. \tag{37b}$$

Again $F_2(0)$ and $F_2(d)$ are assumed not to be zero. Multiplying (34c) by $(x-a)^{-\beta}$ and letting $x \to a$ we have the following equation

$$\cot(\pi\beta) = -\eta\frac{\kappa - 1}{\kappa + 1}, \tag{38}$$

and multiplying (34c) by $(b-x)^{-\omega}$ and letting $x \to b$ we have another characteristic equation to determine $\omega$

$$\cot(\pi\omega) = \eta\frac{\kappa - 1}{\kappa + 1}. \tag{39}$$

$F_3(a)$ and $F_3(b)$ are assumed not to be zero. Equations (35) and (37a) have no roots in the interval $-1 < \alpha_1, \alpha_2 < 0$, hence the unknowns $f_1$ and $f_2$ have no power singularity at the end point at $y = 0$. This is the well known result for an edge crack and from equations (36) and (37b) we obtain, $\gamma_1 = \gamma_2 = -1/2$. Equations (38) and (39) give the strength of singularity at the ends of the contact area. These exponents are less than zero if the half-plane is in contact with a flat stamp as shown in Figure 1. If the half-plane is indented by a circular stamp at the end points contact stress is zero and the exponents are

greater then zero. Since, there is no singularity at $y = 0$ for $f_1$ and $f_2$, they can be expressed in the following form

$$f_1(t) = \frac{F_1(t)}{(t-d)^{1/2}}, \qquad f_2(t) = \frac{F_2(t)}{(t-d)^{1/2}}. \tag{40a,b}$$

In this case the asymptotic behavior of the sectionally holomorphic functions $\psi_1(z)$ and $\psi_2(z)$ near the end point 0, can be written as follows (see, for example Muskhelishvili, [2]),

$$\psi_1(z) \cong \frac{F_1(0)}{\pi\sqrt{-d}}\ln(z), \qquad \psi_2(z) \cong \frac{F_2(0)}{\pi\sqrt{-d}}\ln(z). \tag{41a,b}$$

Singular behavior of the Cauchy integrals at the end point 0, then can be written as

$$\frac{1}{\pi}\int_d^0 \frac{f_1(t)}{t-y}dt \cong \frac{F_1(0)}{\pi\sqrt{-d}}\ln(-y), \tag{42a}$$

$$\frac{1}{\pi}\int_d^0 \frac{f_2(t)}{t-y}dt \cong \frac{F_2(0)}{\pi\sqrt{-d}}\ln(-y). \tag{42b}$$

For this case, integral equations must be examined to search for a logarithmic singularity. Considering equation (30), the only term that causes a logarithmic singularity is the first term and we can write,

$$-\frac{1}{\pi}\int_d^0 \frac{f_1(t)}{t+y}dt \cong -\frac{F_1(0)}{\pi\sqrt{-d}}\ln(-y). \tag{43}$$

Hence, in integral equation (22a) the only terms that have logarithmic singularity are given by (42a) and (43), but as can be seen these terms cancel each other. So there is no additional condition to eliminate the existence of a logarithmic singularity in (22a) and similarly it can be shown that this is also the case for (22b).

3.2. *Singular behavior of the unknown functions for,* $b = 0$ .

In this section, first we will examine the possibility of a power singularity in the unknown functions for $b = 0$ using the function-theoretic method. If $b = 0$, $K_{11}$, $K_{22}$, $K_{13}$ and $K_{23}$ become singular as $y$ and $t$ go to 0 and $K_{31}$ and $K_{32}$ become singular as $x$ and $t$ approach 0. Hence, all the kernels must be examined to determine the strength of singularity at the point, $x = 0$, $y = 0$. The unknown functions can expressed in the following form,

$$f_1(t) = G_1(t)(-t)^{\alpha}(t-d)^{\gamma_1}, \qquad d < t < 0, \tag{44a}$$

$$f_2(t) = G_2(t)(-t)^{\alpha}(t-d)^{\gamma_2}, \qquad d < t < 0, \tag{44b}$$

$$f_3(t) = G_3(t)(-t)^{\alpha}(t-a)^{\beta}, \qquad a < t < 0. \tag{44c}$$

The function $G_j(t)$, $(j = 1, 2, 3)$ is Holder-continuous in its respective interval, and it is assumed that $-1 < \Re(\alpha, \gamma_1, \gamma_2, \beta) < 0$. The definition of the sectionally holomorphic functions is given by equations (25) and the singular behavior of these functions near the end points is given by,

$$\psi_1(z) = -G_1(d)(-d)^{\alpha}\frac{\exp(-\pi i\gamma_1)}{\sin(\pi\gamma_1)}(z-d)^{\gamma_1} + G_1(0)(-d)^{\gamma_1}\frac{z^{\alpha}}{\sin(\pi\alpha)} + G_1^*(z), \tag{45a}$$

$$\psi_2(z) = -G_2(d)(-d)^{\alpha}\frac{\exp(-\pi i\gamma_2)}{\sin(\pi\gamma_2)}(z-d)^{\gamma_2} + G_2(0)(-d)^{\gamma_2}\frac{z^{\alpha}}{\sin(\pi\alpha)} + G_2^*(z), \tag{45b}$$

$$\psi_3(z) = -G_3(a)(-a)^{\alpha}\frac{\exp(-\pi i\beta)}{\sin(\pi\beta)}(z-a)^{\beta} + G_3(0)(-a)^{\beta}\frac{z^{\alpha}}{\sin(\pi\alpha)} + G_3^*(z). \tag{45c}$$

$G_n^*(z)$ is bounded everywhere except possibly at the end points where it may have a weaker singularity. Using Plemelj formulas and equations (45) singular behavior of the Cauchy integrals at the end points can be expressed as,

$$\frac{1}{\pi}\int_d^0 \frac{f_1(t)}{t-y}dt = -G_1(d)(-d)^{\alpha}\cot(\pi\gamma_1)(y-d)^{\gamma_1} + G_1(0)(-d)^{\gamma_1}\cot(\pi\alpha)(-y)^{\alpha} + H_1(y), \qquad d<y<0, \tag{46a}$$

$$\frac{1}{\pi}\int_d^0 \frac{f_2(t)}{t-y}dt = -G_2(d)(-d)^{\alpha}\cot(\pi\gamma_2)(y-d)^{\gamma_2} + G_2(0)(-d)^{\gamma_2}\cot(\pi\alpha)(-y)^{\alpha} + H_2(y), \qquad d<y<0, \tag{46b}$$

$$\frac{1}{\pi}\int_a^0 \frac{f_3(t)}{t-x}dt = -G_3(a)(-a)^{\alpha}\cot(\pi\beta)(x-a)^{\beta} + G_3(0)(-a)^{\beta}\cot(\pi\alpha)(b-x)^{\alpha} + H_3(x), \qquad a<x<0. \tag{46c}$$

If we assume complex variables $z_1$, $z_2$ and $z_3$ satisfy the following conditions

$$z_1 \notin (d<y<0), \tag{47a}$$

$$z_2 \notin (d<y<0), \tag{47b}$$

$$z_3 \notin (a<x<0), \tag{47c}$$

then, $\psi_1(z_1)$, $\psi_2(z_2)$ and $\psi_3(z_3)$ are holomorphic and equations (29) are valid. In order to determine the asymptotic behavior of the integral equations, the kernels will be expanded into partial fractions in the following form,

$$K_{11}(t,y) = K_{22}(t,y) = -\frac{1}{(t+y)} + \frac{6y}{(t+y)^2} - \frac{4y^2}{(t+y)^3}, \tag{48a}$$

$$K_{13}(t,y) = \eta\Big(\frac{1}{t+iy} + \frac{1}{t-iy} + \frac{iy}{2(t-iy)^2} - \frac{iy}{2(t+iy)^2}\Big) - \frac{i}{2(t+iy)} + \frac{i}{2(t-iy)} - \frac{y}{2(t+iy)^2} - \frac{y}{2(t-iy)^2}, \tag{48b}$$

$$K_{23}(t,y) = \eta\Big( - \frac{i}{2(t+iy)} + \frac{i}{2(t-iy)} - \frac{y}{2(t+iy)^2} - \frac{y}{2(t-iy)^2}\Big)$$

$$+ \frac{iy}{2(t+iy)^2} - \frac{iy}{2(t-iy)^2}, \tag{48c}$$

$$K_{31}(t,x) = \frac{-i}{(t+xi)} - \frac{x}{(t+xi)^2} + \frac{i}{(t-xi)} - \frac{x}{(t-xi)^2}, \tag{48d}$$

$$K_{32}(t,x) = \frac{2}{t+xi} - \frac{ix}{(t+xi)^2} + \frac{2}{t-xi} + \frac{ix}{(t-xi)^2}. \tag{48e}$$

Using (29) and (48) we can write the following expressions

$$\frac{1}{\pi}\int_d^0 K_{11}(t,y)f_1(t)dt = \ -\psi_1(-y) - 6y\frac{d}{dy}\psi_1(-y) - 2y^2\frac{d^2}{dy^2}\psi_1(-y), \tag{49a}$$

$$\frac{1}{\pi}\int_d^0 K_{22}(t,y)f_2(t)dt = \ -\psi_2(-y) - 6y\frac{d}{dy}\psi_2(-y) - 2y^2\frac{d^2}{dy^2}\psi_2(-y), \tag{49b}$$

$$\frac{1}{\pi}\int_a^0 K_{13}(t,y)f_3(t)dt = \eta\Big(\psi_3(-iy) + \psi_3(iy) + \frac{y}{2}\frac{d}{dy}(\psi_3(iy) + \psi_3(-iy))\Big)$$

$$+ \frac{i}{2}(\psi_3(iy) - \psi_3(-iy)) - \frac{y}{2i}\frac{d}{dy}(\psi_3(iy) - \psi_3(-iy)), \tag{49c}$$

$$\frac{1}{\pi}\int_a^0 K_{23}(t,y)f_3(t)dt = \eta\Big(\frac{i}{2}(\psi_3(iy) - \psi_3(-iy)) - \frac{y}{2i}\frac{d}{dy}(\psi_3(iy) - \psi_3(-iy))\Big)$$

$$- \frac{y}{2}\frac{d}{dy}(\psi_3(iy) + \psi_3(-iy)), \tag{49d}$$

$$\frac{1}{\pi}\int_d^0 K_{31}(t,x)f_1(t)dt = i(\psi_1(ix) - \psi_1(-ix)) + xi\frac{d}{dx}(\psi_1(ix) - \psi_1(-ix)), \tag{49e}$$

$$\frac{1}{\pi}\int_d^0 K_{32}(t,x)f_2(t)dt = 2(\psi_2(ix) + \psi_2(-ix)) + x\frac{d}{dx}(\psi_2(ix) + \psi_2(-ix)). \tag{49f}$$

The asymptotic behavior of the expressions given above near $y = 0$ and $x = 0$ can now be obtained by using equations (45) as follows:

$$\frac{1}{\pi}\int_d^0 K_{11}(t,y)f_1(t)dt \cong -\frac{2\alpha^2+4\alpha+1}{\sin(\pi\alpha)}(-d)^{\gamma_1}G_1(0)(-y)^{\alpha}, \tag{50a}$$

$$\frac{1}{\pi}\int_d^0 K_{22}(t,y)f_2(t)dt \cong -\frac{2\alpha^2+4\alpha+1}{\sin(\pi\alpha)}(-d)^{\gamma_2}G_2(0)(-y)^{\alpha}, \tag{50b}$$

$$\frac{1}{\pi}\int_a^0 K_{13}(t,y)f_3(t)dt \cong \left(\frac{\eta\cos(\pi\alpha/2)(\alpha+2)+\sin(\pi\alpha/2)(\alpha+1)}{\sin(\pi\alpha)}\right)\times$$

$$\times(-a)^{\beta}G_3(0)(-y)^{\alpha}, \tag{50c}$$

$$\frac{1}{\pi}\int_a^0 K_{23}(t,y)f_3(t)dt \cong \left(\frac{\eta\sin(\pi\alpha/2)(\alpha+1)-\alpha\cos(\pi\alpha/2)}{\sin(\pi\alpha)}\right)(-a)^{\beta}G_3(0)(-y)^{\alpha}, \tag{50d}$$

$$\frac{1}{\pi}\int_d^0 K_{31}(t,x)f_1(t)dt \cong 2\frac{\sin(\pi\alpha/2)}{\sin(\pi\alpha)}(\alpha+1)(-d)^{\gamma_1}G_1(0)(-x)^{\alpha}, \tag{50e}$$

$$\frac{1}{\pi}\int_d^0 K_{32}(t,x)f_2(t)dt \cong 2\frac{\cos(\pi\alpha/2)}{\sin(\pi\alpha)}(\alpha+2)(-d)^{\gamma_2}G_2(0)(-x)^{\alpha}. \tag{50f}$$

Using (46) and (50), we can express the singular behavior of the integral equations (22) near the end points as

$$\sigma_{xx}(0,y) \cong -\cot(\pi\gamma_1)(-d)^{\alpha}G_1(d)(y-d)^{\gamma_1}+\cot(\pi\alpha)(-d)^{\gamma_1}G_1(0)(-y)^{\alpha}$$

$$-\frac{2\alpha^2+4\alpha+1}{\sin(\pi\alpha)}(-d)^{\gamma_1}G_1(0)(-y)^{\alpha}$$

$$+\left(\frac{\eta\cos(\pi\alpha/2)(\alpha+2)+\sin(\pi\alpha/2)(\alpha+1)}{\sin(\pi\alpha)}\right)(-a)^{\beta}G_3(0)(-y)^{\alpha}, \tag{51a}$$

$$\sigma_{xy}(0,y) \cong -\cot(\pi\gamma_2)(-d)^{\alpha}G_2(d)(y-d)^{\gamma_2}+\cot(\pi\alpha)(-d)^{\gamma_2}G_2(0)(-y)^{\alpha}$$

$$-\frac{2\alpha^2+4\alpha+1}{\sin(\pi\alpha)}(-d)^{\gamma_2}G_2(0)(-y)^{\alpha}$$

$$+\left(\frac{\eta\sin(\pi\alpha/2)(\alpha+1)-\alpha\cos(\pi\alpha/2)}{\sin(\pi\alpha)}\right)(-a)^{\beta}G_3(0)(-y)^{\alpha}, \tag{51b}$$

$$\frac{4\mu}{(\kappa+1)}\frac{\partial v(x,0)}{\partial x} \cong -\cot(\pi\beta)(-a)^{\alpha}G_3(a)(x-a)^{\beta}+\cot(\pi\alpha)(-a)^{\beta}G_3(0)(-x)^{\alpha}$$

$$-\eta\frac{\kappa-1}{\kappa+1}G_3(x)(-x)^{\alpha}(x-a)^{\beta}$$

$$+2\frac{\sin(\pi\alpha/2)}{\sin(\pi\alpha)}(\alpha+1)(-d)^{\gamma_1}G_1(0)(-x)^{\alpha}$$

$$+2\frac{\cos(\pi\alpha/2)}{\sin(\pi\alpha)}(\alpha+2)(-d)^{\gamma_2}G_2(0)(-x)^{\alpha}. \tag{51c}$$

The expressions given by (51), are bounded at all points in the intervals $a < x < 0$ and $d < y < 0$. Using this condition characteristic equations can be obtained to determine the unknown exponents. If we multiply equation (51a) by $(y-d)^{-\gamma_1}$ and let $y \to d$ and then multiply by $(-y)^{-\alpha}$ and let $y \to 0$, we obtain two equations in the following form

$$\cot(\pi\gamma_1) = 0, \tag{52a}$$

$$\frac{1}{\sin(\pi\alpha)}\Big[\cos(\pi\alpha)-\big(2\alpha^2+4\alpha+1\big)\Big](-d)^{\gamma_1}G_1(0)$$

$$+\frac{1}{\sin(\pi\alpha)}\Big[\eta\cos(\pi\alpha/2)(\alpha+2)+\sin(\pi\alpha/2)(\alpha+1)\Big](-a)^{\beta}G_3(0)=0. \tag{52b}$$

Multiplying equation (51b) by $(y-d)^{-\gamma_2}$ and letting $y \to d$ and then multiplying by $(-y)^{-\alpha}$ and letting $y \to 0$ we obtain the following equations

$$\cot(\pi\gamma_2) = 0, \tag{53a}$$

$$\frac{1}{\sin(\pi\alpha)}\Big[\cos(\pi\alpha)-\big(2\alpha^2+4\alpha+1\big)\Big](-d)^{\gamma_2}G_2(0)$$

$$+\frac{1}{\sin(\pi\alpha)}\Big[\eta\sin(\pi\alpha/2)(\alpha+1)-\alpha\cos(\pi\alpha/2)\Big](-a)^{\beta}G_3(0)=0. \tag{53b}$$

Multiplying (51c) by $(x-a)^{-\beta}$ and letting $x \to a$, then multiplying by $(-x)^{-\alpha}$ and letting $x \to 0$, following equations are obtained

$$\cot(\pi\beta) = -\eta\frac{\kappa-1}{\kappa+1}, \tag{54a}$$

$$2\frac{\sin(\pi\alpha/2)}{\sin(\pi\alpha)}(\alpha+1)(-d)^{\gamma_1}G_1(0) + 2\frac{\cos(\pi\alpha/2)}{\sin(\pi\alpha)}(\alpha+2)(-d)^{\gamma_2}G_2(0)$$

$$+\left[\cot(\pi\alpha) - \eta\frac{\kappa-1}{\kappa+1}\right](-a)^{\beta}G_3(0) = 0. \tag{54b}$$

Using equations (52a) and (53a) $\gamma_1$ and $\gamma_2$ can be obtained as $-1/2$ and $\beta$ can be obtained from (54a). As for $\alpha$, (52b), (53b) and (54b) constitute an eigenvalue problem which yields a characteristic equation to determine $\alpha$ and two additional equations that relate $G_1(0)$, $G_2(0)$ and $G_3(0)$. The eigenvalue problem can be expressed in the following form using (52b), (53b) and (54b),

$$\begin{bmatrix} a_{11}(\alpha) & 0 & a_{13}(\alpha) \\ 0 & a_{22}(\alpha) & a_{23}(\alpha) \\ a_{31}(\alpha) & a_{32}(\alpha) & a_{33}(\alpha) \end{bmatrix} \begin{bmatrix} \sqrt{-d}G_1(0) \\ \sqrt{-d}G_2(0) \\ (-a)^{\beta}G_3(0) \end{bmatrix} = \begin{bmatrix} 0 \\ 0 \\ 0 \end{bmatrix} \tag{55}$$

The coefficients $a_{ij}(\alpha)$ are given in Appendix A. Assuming $G_1(0) \neq 0$, $G_2(0) \neq 0$ and $G_3(0) \neq 0$ and solving the eigenvalue problem given by (55) we obtain the following characteristic equation,

$$\frac{2\alpha^2+4\alpha+1-\cos(\pi\alpha)}{(\kappa+1)\sin^2(\pi\alpha)} \times$$

$$\times \left(\eta\left(4\alpha^2+10\alpha+5+(\kappa-1)\cos(\pi\alpha)+\kappa(2\alpha+3)\right)+(\kappa+1)\sin(\pi\alpha)\right) = 0. \tag{56}$$

The eigenvalue problem (55) yields two more equations which relate $G_1(0)$, $G_2(0)$ and $G_3(0)$ as follows:

$$G_1(0)\sqrt{-d} = \frac{\eta\cos(\pi\alpha/2)(2+\alpha)+\sin(\pi\alpha/2)(1+\alpha)}{2\alpha^2+4\alpha+1-\cos(\pi\alpha)}G_3(0)(-a)^{\beta}, \tag{57a}$$

$$G_2(0)\sqrt{-d} = \frac{\eta\sin(\pi\alpha/2)(1+\alpha)-\cos(\pi\alpha/2)\alpha}{2\alpha^2+4\alpha+1-\cos(\pi\alpha)}G_3(0)(-a)^{\beta}. \tag{57b}$$

For $\eta \neq 0$ the characteristic equation (56) can further be reduced to following form,

$$\eta(4\alpha^2 + 10\alpha + 5 + (\kappa - 1)\cos(\pi\alpha) + \kappa(2\alpha + 3)) + (\kappa + 1)\sin(\pi\alpha) = 0. \quad (58)$$

In order to verify the solution method and the resulting characteristic equation, the analysis to determine the strength of singularity is also carried out by considering a $90^0$ elastic wedge and using Mellin transformation. It is shown that equation (58) can also be obtained using Mellin transforms. This analysis is described in Appendix B. Strength of singularity $\alpha$ is a function of $\kappa$ and friction coefficient $\eta$. Equation (58) can be solved to determine $\alpha$ for different values of $\kappa$ and $\eta$. $\beta$ is the strength of singularity at the other end of the contact area, and for the case $b < 0$ strength of singularities for the contact stresses are $\beta$ and $\omega$. For a flat stamp, the stresses are singular at both ends of the contact area and for this case equation (58) is solved for different values of friction coefficient and for $\nu = 0.25$. The results for $\alpha$, $\beta$ and $\omega$ are shown in Figure 6. If the friction coefficient is greater than zero the tangential force is directed as shown in Figure 1 and $\alpha$ is the strength of singularity at the trailing end of the contact. Figure 6 shows that, if $\eta > 0$, $\alpha$ is real and negative and it is a strong function of the friction coefficient $\eta$. For the frictionless case, $\alpha = 0$ and no power singularity exists, and for higher values of friction coefficient there is a strong singularity at the trailing end of the contact. $\omega$ is the strength of singularity at the trailing end of the contact for $b < 0$ and $\alpha$ is less than $\omega$ for larger values of friction coefficient. $\eta > 0$ is the practically important case, because in the other case, i.e., $\eta < 0$, crack faces are forced to close by the tangential force. In this case no singularity exists for $b = 0$, instead there is a complex zero, and its imaginary and real parts are shown in Figure 6. The effect of the Poisson's ratio on the strength of singularity, $\alpha$ is shown in Figure 7. As can be seen, the effect of the Poisson's ration is not very significant especially if $\eta > 0$, but the singularity becomes stronger as $\nu$ decreases. If $\eta = 0$, no power singularity exists hence for this case the integral equations have to be

checked in order to determine the conditions not to have a logarithmic singularity. In this case the unknown functions can be expressed in the following form

$$f_1(t) = G_1(t)(t-d)^{-1/2}, \quad d < t < 0, \tag{59a}$$

$$f_2(t) = G_2(t)(t-d)^{-1/2}, \quad d < t < 0, \tag{59b}$$

$$f_3(t) = G_3(t)(t-a)^{\beta}, \quad a < t < 0. \tag{59c}$$

The asymptotic behavior of the sectionally holomorphic functions near point 0 is found to be,

$$\psi_1(z) \cong \frac{G_1(0)}{\pi\sqrt{-d}}\ln(z), \quad \psi_2(z) \cong \frac{G_2(0)}{\pi\sqrt{-d}}\ln(z), \quad \psi_3(z) \cong \frac{G_3(0)}{\pi(-a)^{\beta}}\ln(z). \tag{60}$$

The asymptotic behavior of the Cauchy integrals can then be written as follows:

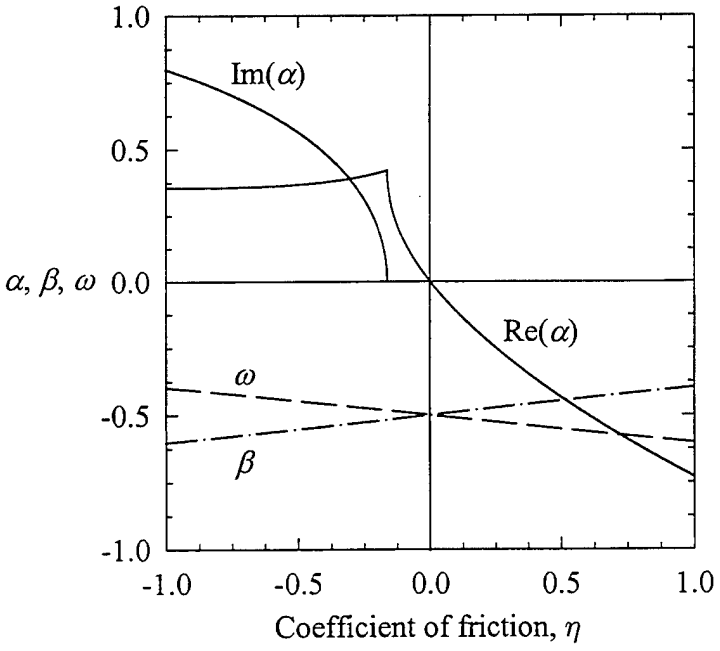


**Figure 6:** Strengths of singularity, $\alpha$, $\beta$ and $\omega$, $\nu = 0.25$.

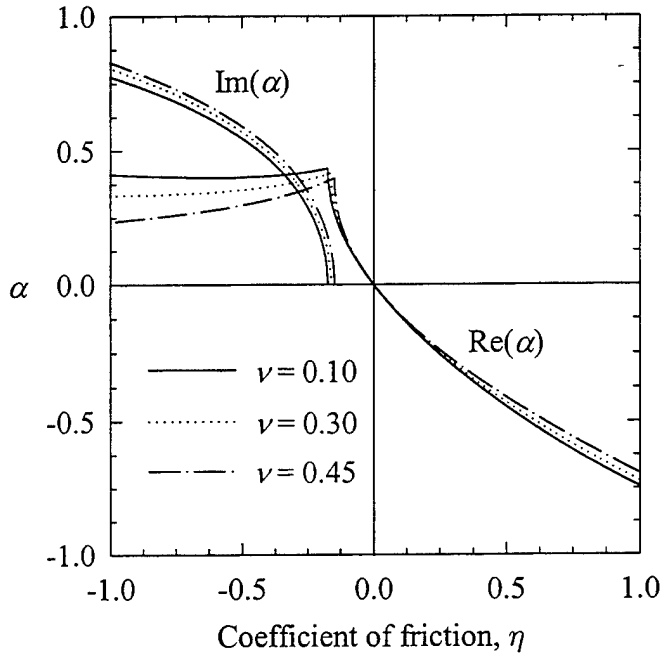


**Figure 7:** Effect of the Poisson's ratio on strength of singularity, $\alpha$.

$$\frac{1}{\pi}\int_d^0 \frac{f_1(t)}{t-y}dt \cong \frac{F_1(0)}{\pi\sqrt{-d}}\ln(-y), \tag{61a}$$

$$\frac{1}{\pi}\int_d^0 \frac{f_2(t)}{t-y}dt \cong \frac{F_2(0)}{\pi\sqrt{-d}}\ln(-y), \tag{61b}$$

$$\frac{1}{\pi}\int_a^0 \frac{f_3(t)}{t-y}dt \cong \frac{F_3(0)}{\pi(-a)^{\beta}}\ln(-y). \tag{61c}$$

Using the partial fractions (48) and (60), integral equations (22) are examined and it is seen that logarithmic terms cancel in equations (22a) and (22b). However, the analysis also shows that, in equation (22c) in order to cancel the logarithmic singularity following condition has to be satisfied,

$$G_2(0)\sqrt{-d} = -\frac{1}{4}G_3(0)(-a)^{\beta}. \tag{62}$$

Hence, if $\eta = 0$, there is no power singularity, but there is a relationship between $G_2(0)$ and $G_3(0)$ as given by (62).*

## 4. Numerical solution of the singular integral equations

In this section, numerical solution methods will be developed to solve the singular integral equations given by (22) in order to determine the stress intensity factors at the crack tip and contact stresses. Three cases will be considered. First, we will consider a flat stamp, with $b = 0$. The strength of singularity $\alpha$, determined in section 3.2, will be used in this solution. In the second case, a flat stamp with $b < 0$ will be considered. Finally, a numerical solution method will be developed for a circular stamp with smooth end points. The numerical solution methods are based on the expansion of the unknown functions in Jacobi polynomials. Using the properties of Jacobi polynomials, Cauchy integrals can be evaluated in closed form. The integral equations will then be reduced to a system of linear algebraic equations which can be solved to determine the stress intensity factors and contact stresses.

### 4.1 *Flat stamp,* $b = 0$

The geometry of the problem is shown in Figure 1. In this section only the problem for $b = 0$ will be considered. The methods of solution for both problems $b = 0$ and $b < 0$ are similar; but in the case of $b = 0$, the strength of singularity $\alpha$ must be considered and there are compatibility relations between $G_1(0)$, $G_2(0)$ and $G_3(0)$ that must be satisfied

* Note that for $\eta = 0$, the 90-degree wedge $x < 0$, $y < 0$ under boundary conditions $v(x,0) = 0$, $\sigma_{xy}(x,0) = 0$, $\sigma_{xx}(0,y) = 0$, $\sigma_{xy}(0,y) = 0$ are equivalent to an elastic half plane $x < 0$ loaded in such a way that $y = 0$ is a plane of symmetry and near $x = 0$, $y = 0$ surface tractions $\sigma_{xx}(0,y)$, $\sigma_{xy}(0,y)$ are zero. Hence, at and near $x = 0$, $y = 0$ the stresses are bounded.

as shown in section 3.2. In order to solve the problem numerically, first the integral equations (22) and equation (1g) are written in normalized form as follows

$$-\frac{1}{\pi}\int_{-1}^{1}\frac{g_1(r)dr}{r-s_1}+\int_{-1}^{1}G_{11}(r,s_1)g_1(r)dr+\int_{-1}^{1}G_{13}(r,s_1)g_3(r)dr=0, \tag{63a}$$

$$-\frac{1}{\pi}\int_{-1}^{1}\frac{g_2(r)dr}{r-s_2}+\int_{-1}^{1}G_{22}(r,s_2)g_2(r)dr+\int_{-1}^{1}G_{23}(r,s_2)g_3(r)dr=0, \tag{63b}$$

$$\int_{-1}^{1}G_{31}(r,s_3)g_1(r)dr+\int_{-1}^{1}G_{32}(r,s_3)g_2(r)dr-\frac{\kappa-1}{\kappa+1}\eta g_3(s_3)-\frac{1}{\pi}\int_{-1}^{1}\frac{g_3(r)}{r-s_3}dr=0, \tag{63c}$$

$$\int_{-1}^{1}g_3(r)dr=-2, \tag{63d}$$

where, following transformations are used

$$y=\frac{d}{2}s_1+\frac{d}{2}, \qquad \text{(for equation 22a)}, \tag{64a}$$

$$y=\frac{d}{2}s_2+\frac{d}{2}, \qquad \text{(for equation 22b)}, \tag{64b}$$

$$x=\frac{a}{2}s_3+\frac{a}{2}, \qquad \text{(for equation 22c)}, \tag{64c}$$

and,

$$\mathrm{g}_1(r)=-\frac{a}{P}f_1\left(\frac{d}{2}r+\frac{d}{2}\right), \tag{65a}$$

$$g_2(r)=-\frac{a}{P}f_2\left(\frac{d}{2}r+\frac{d}{2}\right), \tag{65b}$$

$$g_3(r)=-\frac{a}{P}f_3\left(\frac{a}{2}r+\frac{a}{2}\right). \tag{65c}$$

Note that, right-hand side of equation (63c) is zero, since for a flat stamp normal displacement beneath the stamp is constant. The normalized kernels $G_{ij}$ are given in

Appendix C. In order to solve the problem, the unknown functions are expanded into series of Jacobi polynomials in the following form

$$g_1(r) = (1-r)^{-1/2}(1+r)^{\alpha}\sum_{n=0}^{\infty}A_n P_n^{(-1/2,\alpha)}(r), \tag{66a}$$

$$g_2(r) = (1-r)^{-1/2}(1+r)^{\alpha}\sum_{n=0}^{\infty}B_n P_n^{(-1/2,\alpha)}(r), \tag{66b}$$

$$g_3(r) = (1-r)^{\beta}(1+r)^{\alpha}\sum_{n=0}^{\infty}C_n P_n^{(\beta,\alpha)}. \tag{66c}$$

$P_n$ is the Jacobi polynomial, and the exponents $\alpha$ and $\beta$ are given by equations (56) and (54a) respectively. Substituting (66c) in equilibrium equation (63d) and evaluating the integral we obtain the first constant in the expansion of $g_3(r)$ in the following form,

$$C_0 = -2/\theta_0, \qquad \theta_0 = \frac{2^{\alpha+\beta+1}\Gamma(\beta+1)\Gamma(\alpha+1)}{\Gamma(\alpha+\beta+2)}. \tag{67a,b}$$

where $\Gamma$ is the Gamma function. Substituting (66) in (63) evaluating the Cauchy principal value integrals in closed form, truncating all the infinite series at $n = N$, and using (67), integral equations (63) can be written in the following form,

$$\sum_{n=0}^{N}A_n\Big\{\Gamma_{1n}(\alpha)\mathrm{F}\big(n+1,\,-n+\frac{1}{2}-\alpha;\frac{3}{2};\frac{1-s_1}{2}\big)+h_{11n}(s_1)\Big\}+\sum_{n=1}^{N}C_n h_{13n}(s_1) =$$

$$= -C_0 h_{130}(s_1), \qquad -1 < s_1 < 1, \tag{68a}$$

$$\sum_{n=0}^{N}B_n\Big\{\Gamma_{2n}(\alpha)\mathrm{F}\big(n+1,\,-n+\frac{1}{2}-\alpha;\frac{3}{2};\frac{1-s_2}{2}\big)+h_{22n}(s_2)\Big\}+\sum_{n=1}^{N}C_n h_{23n}(s_2) =$$

$$= -C_0 h_{230}(s_2), \qquad -1 < s_2 < 1, \tag{68b}$$

$$\sum_{n=0}^{N} A_n h_{31n}(s_3) + \sum_{n=0}^{N} B_n h_{32n}(s_3) +$$

$$+ \sum_{n=1}^{N} C_n \Gamma_{3n}(\alpha) \mathrm{F}\big(n+1, -n-\beta-\alpha; 1-\beta; \frac{1-s_3}{2}\big) =$$

$$= -C_0 \Gamma_{30}(\alpha) \mathrm{F}\big(1, -\beta-\alpha; 1-\beta; \frac{1-s_3}{2}\big), \qquad -1 < s_3 < 1, \tag{68c}$$

where F() is the Hypergeometric function, for the definition and mathematical properties of the Hypergeometric function see for example Abramowitz and Stegun [3] and for the numerical computation of the Hypergeometric function one may refer to Luke [4]. Functions $h_{ijn}(s_i), (i,j=1,2,3)$ are given in Appendix C. The formulas used in the evaluation of the Cauchy principal value integrals are given in Appendix D. Functions $\Gamma_{in}(i=1,2,3)$ are given by,

$$\Gamma_{1n}(\alpha) = \Gamma_{2n}(\alpha) = \frac{2^{(\alpha-1/2)}\Gamma(-1/2)\Gamma(n+\alpha+1)}{\pi\Gamma(n+\alpha+1/2)}, \tag{69a}$$

$$\Gamma_{3n}(\alpha) = \frac{2^{(\alpha+\beta)}\Gamma(\beta)\Gamma(n+\alpha+1)}{\pi\Gamma(n+\alpha+\beta+1)}. \tag{69b}$$

In the solution of the flat stamp problem with $b=0$, compatibility conditions given by (57a), (57b) and (62) must also be considered. Substituting (66) in the compatibility conditions and truncating the infinite series, for $\eta \neq 0$ we obtain the following additional equations

$$\sum_{n=0}^{N} A_n P_n^{(-1/2,\alpha)}(-1) = p_1(\alpha)\Big(\frac{a}{d}\Big)^{-\alpha}\Big(\frac{1}{2}\Big)^{-(\beta+1/2)} \sum_{n=0}^{N} C_n P_n^{(\beta,\alpha)}(-1), \tag{70a}$$

$$\sum_{n=0}^{N} B_n P_n^{(-1/2,\alpha)}(-1) = p_2(\alpha)\Big(\frac{a}{d}\Big)^{-\alpha}\Big(\frac{1}{2}\Big)^{-(\beta+1/2)} \sum_{n=0}^{N} C_n P_n^{(\beta,\alpha)}(-1), \tag{70b}$$

where,

$$p_1(\alpha) = \frac{\eta\cos(\pi\alpha/2)(2+\alpha) + \sin(\pi\alpha/2)(1+\alpha)}{2\alpha^2 + 4\alpha + 1 - \cos(\pi\alpha)}, \tag{71a}$$

$$p_2(\alpha) = \frac{\eta\sin(\pi\alpha/2)(1+\alpha) - \cos(\pi\alpha/2)\alpha}{2\alpha^2 + 4\alpha + 1 - \cos(\pi\alpha)}. \tag{71b}$$

If $\eta = 0$, there is only one additional condition

$$\sum_{n=0}^{N} B_n P_n^{(-1/2,\alpha)}(-1) = -\frac{1}{4}\left(\frac{a}{d}\right)^{-\alpha}\left(\frac{1}{2}\right)^{-(\beta+1/2)} \sum_{n=0}^{N} C_n P_n^{(\beta,\alpha)}(-1). \tag{72}$$

Equations (68) can now be numerically solved together with (70) or (72) to determine the unknown constants $A_n$, $B_n$ and $C_n$. In the numerical solution the equations are converted to a linear system of algebraic equations by using collocation points. If $\eta \neq 0$, $N$ collocation points are used for (68a) and (68b) and considering (70) we have two sets of $(N+1)$ equations. Since, $C_0$ is known, $(N)$ collocation points are used for (68c), hence total number of linear equations is $(3N+2)$ for $(3N+2)$ unknowns. The following roots of the Chebyshev polynomials are selected as collocation points,

$$s_{1i} = s_{2i} = s_{3i} = \cos\left(\frac{\pi(2i-1)}{2N}\right), \qquad i = 1, ..., N. \tag{73}$$

Note that if $\eta = 0$, there is one compatibility equation and in this case $(N+1)$ collocation points are used for equation (68a) and $s_{1i}$ is in the following form,

$$s_{1i} = \cos\left(\frac{\pi(2i-1)}{2(N+1)}\right), \qquad i = 1, ..., N+1. \tag{74}$$

*Stress intensity factors at the crack tip*

Modes I and II stress intensity factors at the crack tip are defined by

$$k_I = \lim_{y \to d} \sqrt{2(d-y)}\,\sigma_{xx}(0, y), \tag{75a}$$

$$k_{II} = \lim_{y \to d} \sqrt{2(d-y)}\sigma_{xy}(0,y). \tag{75b}$$

The dominant terms, for $\sigma_{xx}(0,y)$ and $\sigma_{xy}(0,y)$ near $d$ can be written as follows:

$$\sigma_{xx}(0,y) \cong \frac{1}{\pi}\int_d^0 \frac{f_1(t)dt}{t-y}, \tag{76a}$$

$$\sigma_{xy}(0,y) \cong \frac{1}{\pi}\int_d^0 \frac{f_2(t)dt}{t-y}. \tag{76b}$$

Considering the definition of the sectionally holomorphic functions given by, (25a,b) the asymptotic behavior of (76) near $d$ can be written as,

$$\sigma_{xx}(0,y) \cong G_1(d)(-d)^{\alpha}(d-y)^{-1/2}, \tag{77a}$$

$$\sigma_{xy}(0,y) \cong G_2(d)(-d)^{\alpha}(d-y)^{-1/2}. \tag{77b}$$

Note that (77) is valid for, $y < d$ and $(d-y) \to 0$. Using the equations given above, and (65a,b), and (66a,b) normalized stress intensity factors can be expressed as follows,

$$\frac{k_I\sqrt{-a}}{P} = 2^{\alpha}\sqrt{\frac{d}{a}}\sum_{n=0}^{N} A_n P_n^{(-1/2,\alpha)}(1), \tag{78a}$$

$$\frac{k_{II}\sqrt{-a}}{P} = 2^{\alpha}\sqrt{\frac{d}{a}}\sum_{n=0}^{N} B_n P_n^{(-1/2,\alpha)}(1). \tag{78b}$$

After solving the system of linear equations for $A_n$, $B_n$ and $C_n$, stress intensity factors can be obtained using equations (78) and contact stresses can be obtained using equation (66c).

4.2 *Flat stamp,* $b < 0$.

The geometry of the problem is shown in Figure 1. Integral equations (22) can be written in normalized form as follows:

$$-\frac{1}{\pi}\int_{-1}^{1}\frac{m_1(r)dr}{r-s_1}+\int_{-1}^{1}M_{11}(r,s_1)m_1(r)dr+\int_{-1}^{1}M_{13}(r,s_1)m_3(r)dr=0, \tag{79a}$$

$$-\frac{1}{\pi}\int_{-1}^{1}\frac{m_2(r)dr}{r-s_2}+\int_{-1}^{1}M_{22}(r,s_2)m_2(r)dr+\int_{-1}^{1}M_{23}(r,s_2)m_3(r)dr=0, \tag{79b}$$

$$\int_{-1}^{1}M_{31}(r,s_3)m_1(r)dr+\int_{-1}^{1}M_{32}(r,s_3)m_2(r)dr-\frac{\kappa-1}{\kappa+1}\eta m_3(s_3)$$

$$-\frac{1}{\pi}\int_{-1}^{1}\frac{m_3(r)}{r-s_3}dr=0, \tag{79c}$$

$$\int_{-1}^{1}m_3(r)dr=-2. \tag{79d}$$

In this case following transformations are used,

$$y=\frac{d}{2}s_1+\frac{d}{2}, \qquad \text{(for equation 22a)}, \tag{80a}$$

$$y=\frac{d}{2}s_2+\frac{d}{2}, \qquad \text{(for equation 22b)}, \tag{80b}$$

$$x=\frac{a-b}{2}s_3+\frac{a+b}{2}, \qquad \text{(for equation 22c)}, \tag{80c}$$

and,

$$m_1(r)=\frac{b-a}{P}f_1\left(\frac{d}{2}r+\frac{d}{2}\right), \tag{81a}$$

$$m_2(r)=\frac{b-a}{P}f_2\left(\frac{d}{2}r+\frac{d}{2}\right), \tag{81b}$$

$$m_3(r)=\frac{b-a}{P}f_3\left(\frac{a-b}{2}r+\frac{a+b}{2}\right). \tag{81c}$$

The normalized kernels $M_{ij}$ are given in Appendix C. The unknown functions are expanded into series of Jacobi polynomials as follows:

$$m_1(r) = (1-r)^{-1/2}\sum_{n=0}^{\infty} A_n P_n^{(-1/2,0)}(r), \tag{82a}$$

$$m_2(r) = (1-r)^{-1/2}\sum_{n=0}^{\infty} B_n P_n^{(-1/2,0)}(r), \tag{82b}$$

$$m_3(r) = (1-r)^{\beta}(1+r)^{\omega}\sum_{n=0}^{\infty} C_n P_n^{(\beta,\omega)}. \tag{82c}$$

The exponents $\beta$ and $\omega$ are given by equations (38) and (39) respectively and note that, $\beta < 0$, $\omega < 0$, $\beta + \omega = -1$. Substituting (82c) in equilibrium equation (79d) and evaluating the integral we obtain the first constant in the expansion of $m_3(r)$ as follows:

$$C_0 = 2\sin(\pi\beta)/\pi. \tag{83}$$

Substituting (82) in (79), evaluating the Cauchy integrals in closed from and truncating the infinite series at $N$, we obtain the following equations,

$$\sum_{n=0}^{N} A_n\Big\{\Omega_n \mathrm{F}\big(n+1, -n+\frac{1}{2}; \frac{3}{2}; \frac{1-s_1}{2}\big) + p_{11n}(s_1)\Big\} + \sum_{n=1}^{N} C_n p_{13n}(s_1) =$$

$$= -C_0 p_{130}(s_1), \qquad -1 < s_1 < 1, \tag{84a}$$

$$\sum_{n=0}^{N} B_n\Big\{\Omega_n \mathrm{F}\big(n+1, -n+\frac{1}{2}; \frac{3}{2}; \frac{1-s_2}{2}\big) + p_{22n}(s_2)\Big\} + \sum_{n=1}^{N} C_n p_{23n}(s_2) =$$

$$= -C_0 p_{230}(s_2), \qquad -1 < s_2 < 1, \tag{84b}$$

$$\sum_{n=0}^{N} A_n p_{31n}(s_3) + \sum_{n=0}^{N} B_n p_{32n}(s_3) + \frac{1}{2\sin(\pi\beta)}\sum_{n=1}^{N} C_n P_{n-1}^{(-\beta,-\omega)}(s_3) = 0,$$

$$-1 < s_3 < 1. \tag{84c}$$

Functions $p_{ijn}(s_i), (i,j=1,2,3)$ are given in Appendix C. The formulas used in the evaluation of the Cauchy principal value integrals are given in Appendix D and $\Omega_n$ is given by

$$\Omega_n = \frac{\Gamma(-1/2)\Gamma(n+1)}{\pi\sqrt{2}\Gamma(n+1/2)}. \tag{85}$$

By using the collocation technique equations (84), can now be converted to a linear system of algebraic equations. There are a total of $(3N+2)$ unknowns in this problem. Hence in the numerical solution $(N+1)$ collocation points are used for each of the equations (84a) and (84b) and $(N)$ collocation points are used in equation (84c). The following roots of Chebyshev polynomials are selected as the collocation points,

$$s_{1i} = s_{2i} = \cos\Big(\frac{\pi(2i-1)}{2(N+1)}\Big), \qquad i = 1, ..., N+1, \tag{86a}$$

$$s_{3i} = \cos\Big(\frac{\pi(2i-1)}{2N}\Big), \qquad i = 1, ..., N. \tag{86b}$$

*Stress intensity factors at the crack tip*

Definition of the modes I and II stress intensity factors are given by equations (75). The dominant terms, for $\sigma_{xx}(0,y)$ and $\sigma_{xy}(0,y)$ near $d$ are given by equations (76). Using these equations, asymptotic behavior of the stresses near the crack tip can be written as,

$$\sigma_{xx}(0,y) \cong F_1(d)(d-y)^{-1/2}, \tag{87a}$$

$$\sigma_{xy}(0,y) \cong F_2(d)(d-y)^{-1/2}. \tag{87b}$$

By using the equations (81a), (81b), (82a), (82b) and (87) normalized stress intensity factors at the crack tip can then be expressed as follows:

$$\frac{k_I\sqrt{-d}}{P} = \frac{-d}{(b-a)}\sum_{n=0}^{N} A_n P_n^{(-1/2,0)}(1), \tag{88a}$$

$$\frac{k_{II}\sqrt{-d}}{P} = \frac{-d}{(b-a)}\sum_{n=0}^{N} B_n P_n^{(-1/2,0)}(1). \tag{88b}$$

After solving the linear system of equations, stress intensity factors can be determined using (88) and contact stresses can be obtained using (82c).

### 4.3 *Circular stamp*

The geometry of the problem is shown in Figure 8. A homogenous half-plane is indented by a rigid stamp of circular profile. The radius of the stamp is denoted as $R$, and it is assumed that contact area $(b-a)$ is much smaller then the radius $R$. $c$ denotes the position of the centerline of the stamp. In this problem the contact area is not constant and it depends on the force applied to the stamp. There are four parameters in the contact problem which are $P$, $a$, $b$ and c. Once two of these parameters are specified, the other two have to be determined from the solution of the problem.

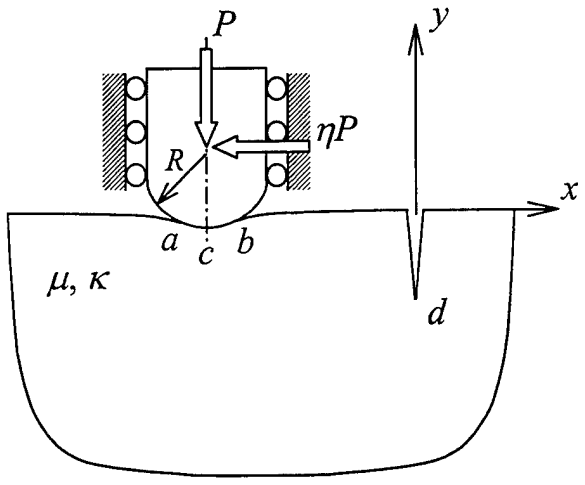


**Figure 8:** Circular stamp problem

If we assume that $P$ and one of the end points for instance $a$ is known, then $b$ and $c$ can be determined using an iterative solution method. In order to avoid iterations and longer computation time, in this study $a$ and $b$ will be specified and corresponding values of $P$ and $c$ will be determined without iterations. Considering Figure 8, if contact area is much smaller than the radius $R$, derivative of the normal displacement $v(x,0)$ can be written in the following form,

$$\frac{\partial}{\partial x}v(x,0) = \frac{x-c}{R}, \qquad a < x < b, \tag{89}$$

then, the integral equations given by (22) and the equilibrium equation given by (1.9) can be written in normalized form as follows:

$$-\frac{1}{\pi}\int_{-1}^{1}\frac{w_1(r)dr}{r-s_1} + \int_{-1}^{1}W_{11}(r,s_1)w_1(r)dr + \int_{-1}^{1}W_{13}(r,s_1)w_3(r)dr = 0, \tag{90a}$$

$$-\frac{1}{\pi}\int_{-1}^{1}\frac{w_2(r)dr}{r-s_2} + \int_{-1}^{1}W_{22}(r,s_2)w_2(r)dr + \int_{-1}^{1}W_{23}(r,s_2)w_3(r)dr = 0, \tag{90b}$$

$$\int_{-1}^{1}W_{31}(r,s_3)w_1(r)dr + \int_{-1}^{1}W_{32}(r,s_3)w_2(r)dr - \frac{\kappa-1}{\kappa+1}\eta w_3(s_3) - \frac{1}{\pi}\int_{-1}^{1}\frac{w_3(r)}{r-s_3}dr = \frac{2}{\kappa+1}\Big(\frac{a-b}{R}s_3 + \frac{a+b}{R} - \frac{2c}{R}\Big), \tag{90c}$$

$$\frac{a-b}{2R}\int_{-1}^{1}w_3(r)dr = \frac{P}{\mu R}. \tag{90d}$$

In this case following transformations are used,

$$y = \frac{d}{2}s_1 + \frac{d}{2}, \qquad \text{(for equation 22a)}, \tag{91a}$$

$$y = \frac{d}{2}s_2 + \frac{d}{2}, \qquad \text{(for equation 22b)}, \tag{91b}$$

$$x = \frac{a-b}{2}s_3 + \frac{a+b}{2}, \qquad \text{(for equation 22c)}, \tag{91c}$$

and,

$$w_1(r) = \frac{1}{\mu} f_1\left(\frac{d}{2}r + \frac{d}{2}\right), \tag{92a}$$

$$w_2(r) = \frac{1}{\mu} f_2\left(\frac{d}{2}r + \frac{d}{2}\right), \tag{92b}$$

$$w_3(r) = \frac{1}{\mu} f_3\left(\frac{a-b}{2}r + \frac{a+b}{2}\right). \tag{92c}$$

The normalized kernels $W_{ij}$ are given in Appendix C. The unknown functions are expanded into series of Jacobi polynomials in the following form,

$$w_1(r) = (1-r)^{-1/2}\sum_{n=0}^{\infty} A_n P_n^{(-1/2,0)}(r), \tag{93a}$$

$$w_2(r) = (1-r)^{-1/2}\sum_{n=0}^{\infty} B_n P_n^{(-1/2,0)}(r), \tag{93b}$$

$$w_3(r) = (1-r)^{\beta}(1+r)^{\omega}\sum_{n=0}^{\infty} C_n P_n^{(\beta,\omega)}(r). \tag{93c}$$

The exponents $\beta$ and $\omega$ are given by equations (38) and (39) respectively and in this case $\beta > 0$, $\omega > 0$ and $\beta + \omega = 1$. Substituting (93c) in equilibrium equation (90d) and evaluating the integral, normalized force can be expressed in the following form,

$$\frac{P}{\mu R} = \frac{a-b}{2R} C_0 \theta_0, \qquad \theta_0 = \frac{2\omega(1-\omega)\pi}{\sin(\pi\omega)}. \tag{94}$$

In the numerical solution, $a/R$, $b/R$ and $d/R$ will be specified and once the problem is solved the corresponding value of the normalized force will be obtained by using the equilibrium equation, i.e., equation (94). In order to determine $c/R$ we will consider the consistency condition. First consider the last two terms on the left-hand side of equation (90c), they can be written in the following form,

$$F(s_3) = \frac{\kappa - 1}{\kappa + 1}\eta w_3(s_3) + \frac{1}{\pi}\int_{-1}^{1} \frac{w_3(r)}{r - s_3} dr. \tag{95}$$

If $F(s_3)$ is divided by the weight function and integrated from $-1$ to 1, following result is obtained

$$\int_{-1}^{1} \frac{F(s_3)}{(1 - s_3)^{\beta}(1 + s_3)^{\omega}} ds_3 = 0. \tag{96}$$

Other terms in equation (90c) must also satisfy this condition, and integrating the other terms we obtain the following expression,

$$\sum_{n=0}^{\infty} A_n \widehat{W}_{31n} + \sum_{n=0}^{\infty} B_n \widehat{W}_{32n} = \frac{2}{\kappa + 1}\Big(\frac{a - b}{R}(1 - 2\omega) + \frac{a + b}{R} - \frac{2c}{R}\Big)\frac{\pi}{\sin(\pi\omega)}, \tag{97}$$

where,

$$\widehat{W}_{31n} = \int_{-1}^{1} \Big\{ \int_{-1}^{1} W_{31}(r, s_3)(1 - r)^{-1/2} P_n^{(-1/2,0)}(r) dr \Big\} (1 - s_3)^{-\beta}(1 + s_3)^{-\omega} ds_3, \tag{98a}$$

$$\widehat{W}_{32n} = \int_{-1}^{1} \Big\{ \int_{-1}^{1} W_{32}(r, s_3)(1 - r)^{-1/2} P_n^{(-1/2,0)}(r) dr \Big\} (1 - s_3)^{-\beta}(1 + s_3)^{-\omega} ds_3. \tag{98b}$$

Once the problem is solved for a given $a/R$ and $b/R$, $c/R$ can be obtained using equation (97). Substituting (93) in (90a,c), evaluating the Cauchy integrals in closed from, eliminating $c/R$ from (90c) using the consistency condition given by (97) and truncating the infinite series at $N$, we obtain the following equations:

$$\sum_{n=0}^{N} A_n \Big\{ \Omega_n \mathrm{F}\big(n + 1, -n + \frac{1}{2}; \frac{3}{2}; \frac{1 - s_1}{2}\big) + q_{11n}(s_1) \Big\} + \sum_{n=0}^{N} C_n q_{13n}(s_1) = 0, \quad -1 < s_1 < 1, \tag{99a}$$

$$\sum_{n=0}^{N} B_n \Big\{ \Omega_n \mathrm{F}\big(n + 1, -n + \frac{1}{2}; \frac{3}{2}; \frac{1 - s_2}{2}\big) + q_{22n}(s_2) \Big\} + \sum_{n=0}^{N} C_n q_{23n}(s_2) = 0, \quad -1 < s_2 < 1, \tag{99b}$$

$$\sum_{n=0}^{N} A_n \left( q_{31n}(s_3) - \frac{\sin(\pi\omega)}{\pi} \widehat{W}_{31n} \right) + \sum_{n=0}^{N} B_n \left( q_{32n}(s_3) - \frac{\sin(\pi\omega)}{\pi} \widehat{W}_{32n} \right)$$

$$+ \frac{1}{2\sin(\pi\omega)} \sum_{n=0}^{N} C_n P_{n+1}^{(-\beta,-\omega)}(s_3) = \frac{4}{\kappa+1} \frac{a-b}{R} P_1^{(-\beta,-\omega)}(s_3), \quad -1 < s_3 < 1. \tag{99c}$$

Functions $q_{ijn}(s_i), (i,j = 1,2,3)$ are given in Appendix C. The formulas used in the evaluation of the Cauchy principal value integrals are given in Appendix D and $\Omega_n$ is given by equation (85). Equations (99) can now be converted to a linear system of algebraic equations using collocation points. There are a total of $(3N+3)$ unknowns in this problem, hence $(N+1)$ collocation points are used for each of the equations. The following roots of the Chebyshev polynomials are selected as the collocation points,

$$s_{1i} = s_{2i} = s_{3i} = \cos\left(\frac{\pi(2i-1)}{2(N+1)}\right), \qquad i = 1, ..., N+1. \tag{100}$$

For given values of $a/R$, $b/R$ and $d/R$ equations (99) can be solved and normalized force $P/\mu R$ and $c/R$ can be obtained using equations (94) and (97) respectively.

*Stress intensity factors at the crack tip*

Definition of the modes I and II stress intensity factors are given by equations (75). Using the sectionally holomorphic functions, asymptotic expressions can be derived for the stresses and the stress intensity factors can be shown to be in the following form,

$$\frac{k_I\sqrt{R}}{P} = \sqrt{-\frac{d}{R}} \frac{1}{C_0\theta_0} \frac{2R}{a-b} \sum_{n=0}^{N} A_n P_n^{(-1/2,0)}(1), \tag{101a}$$

$$\frac{k_{II}\sqrt{R}}{P} = \sqrt{-\frac{d}{R}} \frac{1}{C_0\theta_0} \frac{2R}{a-b} \sum_{n=0}^{N} B_n P_n^{(-1/2,0)}(1). \tag{101b}$$

Contact stresses can be obtained using equation (93c).

## 5 Results

In this section, numerical results obtained for the three different cases will be presented and the effect of the friction coefficient $\eta$, stamp location and crack length on the stress intensity factors at the crack tip and contact stresses will be examined. The numerical solution methods are described in Section 4. Computer programs are developed for the implementation of the numerical procedures and results are presented in the following sections for flat and circular stamps. Before, giving the results for the stress intensity factors, we examine surface stresses in the half plane in the absence of a crack. Figures 9 and 10 show the contact stress $\sigma_{yy}(x,0)$ and in-plane stress $\sigma_{xx}(x,0)$ for a half-plane loaded by a circular stamp. The expressions for the stresses in the absence of a crack are obtained in closed form as shown in Appendix E. Figure 10 shows the tensile peak for $\sigma_{xx}(x,0)$ at the trailing end of the contact region. At the leading end in-plane stress is compressive. The tensile peak at the trailing end of the contact area is the reason of surface crack initiation in sliding contact problems. In the following sections we will present the results for stress intensity factors and contact stresses for a half-plane containing a crack at the trailing end of the contact area.

### 5.1 *Flat stamp*, $b = 0$

Figures 11 and 12 show a comparison of the results for normalized mode I and II stress intensity factors with those of Hasebe et. *al* [5] for the case of a flat stamp with $b = 0$ and $\nu = 0.25$. Mode I and II stress intensity factors are given in intervals, $d/a = 0...1$ and $a/d = 1...0$. Hasebe *et.* al [5] solved this problem using the complex stress function technique and by mapping the half-plane with a crack into a unit circle. As also stated in the paper by Hasebe *et.* al [5], since the half-plane is mapped into a unit

circle by using a rational mapping function, the crack tips at $y = 0$ and $y = d$, have roundness after mapping. However, as can be seen in Figures 11 and 12 the results agree very well. In the paper mentioned, the signs of the mode II stress intensity factors are given as negative, but for a flat stamp with $b = 0$, it is clear that mode II stress intensity factors have to be positive at the crack tip. Figures 11 and 12 show that, for low values of friction coefficient, i.e., for a smaller tangential force, mode I stress intensity factors are negative. As the tangential force increases mode I stress intensity factors increase and they become positive. Hence, if the applied tangential force is not sufficiently large there will be contact between the crack faces and crack closure will occur. In this case, crack faces transfer compressive normal stresses and the assumption of zero crack surface tractions is not valid. Figure 12 shows that, for a flat stamp with $b = 0$, mode II stress intensity factors are positive for all values of friction coefficient which is an expected result and if the applied tangential force is smaller, mode II stress intensity factor increases. During numerical solution, it was observed that as $a/d$ or $d/a$ approaches zero, it is becoming increasingly difficult to obtain convergent results, but using relatively larger number of Gaussian points and weights in the numerical integration of the kernels of integral equations, convergent results could be obtained. In Figures 13 and 14 a flat stamp with $b = 0$ is considered and stress intensity factors are normalized with respect to contact area length $a$, in both of the intervals $d/a = 0...1$ and $a/d = 0...1$. Hence for a constant contact area length $a$, the effect of crack length $d$ on the stress intensity factors is obtained. It can be seen that, as $d \to \infty$, both modes I and mode II stress intensity factors go to zero. It is known that when a brittle material is indented by an indenter which at the same time translates laterally across the surface and applies frictional forces, tensile stresses intensify at the trailing edge, and this results in the generation of partial cone cracks, (see for example Lawn [6]). The cone cracks extend into the material and they bend backwards, i.e. opposite to the applied tangential force direction. An analysis of the

results given in Figure 14 shows that this is the case for the problem under consideration. Mode II stress intensity factors are positive for all values of friction coefficient and crack length. If we consider a small element at the crack tip as shown in Figure 15, the crack will bend backwards and it will propagate in a direction opposite to the applied frictional force.

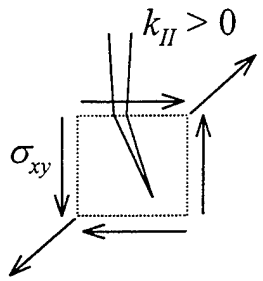


**Figure 15:** Direction of crack growth

Figures 16 and 17 show the effect of the Poisson's ratio on mode I and II stress intensity factors for a constant friction coefficient $\eta = 0.8$. The effect of the Poisson's ratio on mode I stress intensity factors is not significant as shown in Figure 16. The effect on mode II stress intensity factors, however, is larger especially for shorter crack lengths and as the Poisson's ratio decreases mode II stress intensity factors increase. Figures 18 and 19 show the normalized contact stresses for a flat stamp with $b = 0$. The contact stresses are infinite at the ends of the contact area except for the case $\eta = 0$, for which there is no singularity at the end $x = 0$.

5.2 *Flat stamp,* $b < 0$

The effect of the stamp location on mode I and mode II stress intensity factors for a flat stamp are shown in Figures 20 and 21. In these figures $(a - b)/d$ is kept constant as

0.1 and $\nu = 0.25$, and stress intensity factors are given for different values of $b/d$. Since, stress intensity factors are normalized with respect to $d$, the effect of the stamp location $b$ on stress intensity factors can be clearly observed in these figures. The full circles at $b/d = 0$ are obtained using the strength of singularity $\alpha$ and the numerical solution method described in section 4.1, while the full lines are obtained using the numerical solution method described in section 4.2. It can be seen that, full lines approach the circles at $b/d = 0$, which is a verification of both of the numerical methods developed. As $b$ increases from 0, mode I stress intensity factors initially increase and they go through a peak for larger values of friction coefficient $\eta$. Further increase in $b$ results in a decline in mode I stress intensity factors and they approach zero for larger values of $b/d$ which is an expected result. Similarly, mode II stress intensity factors approach zero, for larger values of $b/d$. It can also be seen that, if there is no tangential force, i.e., $\eta = 0$, mode I stress intensity factors are negative and mode II stress intensity factors are positive for all values of $b/d$. In Figures 22 and 23 the effect of the stamp location on mode I and mode II stress intensity factors are shown for $(a-b)/d = 1.0$ and $\nu = 0.25$. Figures 24 and 25, show the effect of the stamp location on stress intensity factors for $(a-b)/d = 10.0$ and $\nu = 0.25$. The trends are similar and self-explanatory in Figures 22-25. Figures 26 and 27 show the effect of the Poisson's ration on mode I and mode II stress intensity factors for $(a-b)/d = 1.0$ and $\eta = 0.8$. Figures show that for this value of $(a-b)/d$, the effect of the Poisson's ratio is not significant, however for a larger value of $(a-b)/d$ which is taken as 10.0 in Figures 28 and 29, the effect of the Poisson's ratio is larger. Mode I stress intensity factors increase as $\nu$ decreases as shown in Figure 28. The effect on mode II stress intensity factors is shown in Figure 29. Contact stresses for different values of $(a-b)/d$ are shown in Figures 30-32. Contact stresses are singular at the end points of the contact area. Figures 30-32 show the effect of the friction coefficient on contact stresses

5.3 *Circular stamp*

Mode I and II stress intensity factors for a circular stamp are shown in Figures 33 and 34 for different values of $b/R$. In these figures $(b-a)/R$ is kept constant as 0.05 and normalized crack length $d/R$ is $-0.1$. It can be seen that the variation of the normalized stress intensity factors is similar to that of the flat stamp case. Stress intensity factors approach zero, as $b/R$ increases. In the solution of the circular stamp problem the stress intensity factors are obtained for known values of $a/R$, $b/R$ and $d/R$ then the corresponding value of the normalized force $P/\mu R$ is determined using the equilibrium equation. Variation of the normalized force with $b/R$, for $(b-a)/R = 0.05$ and $d/R = -0.1$ is shown in Figure 35. It can be seen that normalized force approaches a constant value as $b/R$ decreases and this constant value can be obtained by solving the contact problem in a homogenous half-plane without a crack, which has a closed form solution. This solution is shown by the full circles in Figure 35, and our numerical results approach the closed form solution for small values of $b/R$. Closed form solution for the contact problem is given in Appendix E. As $b/R$ goes to zero, normalized force increases for smaller values of friction coefficient and it decreases for larger values. The increase for smaller values is due to more compressive stresses at the crack tip, as the tangential force decreases crack closure occurs and the normal force required for contact increases. For larger values of friction coefficient, mode I stress intensity factors are positive and normalized force decreases significantly with the increase in $b/R$. It can also be seen that, for a given contact length the normal force required is smaller for a larger friction coefficient. Figure 36 shows the contact stresses for $a/R = -0.1$, $b/R = -0.15$ and $d/R = -0.1$. The contact stresses are zero at the ends of the contact area and the effect of the friction coefficient on contact stresses is shown in this figure. Another set of results for stress intensity factors, normalized force and contact stresses are shown in Figures 37-

40, for $(b-a)/R = 0.1$. The trends are similar to those given in Figures 33-35. The effect of Poisson's ratio on stress intensity factors and normalized force is also examined. Figure 41 and 42 show the modes I and II stress intensity factors for different values of Poisson's ratio and for $\eta = 0.8$ and $(b-a)/R = 0.1$. It can be seen that the results are very close for all three values of the Poisson's ratio. However, Figure 43 shows that the effect of the Poisson's ratio on normalized force is significant and the normal force required is larger for a larger Poisson's ratio. Figures 44-46 show the effect of the crack length $d/R$ on stress intensity factors and normalized force for a circular stamp whose location is given by $b/R = -0.05$ and $a/R = -0.1$. Both normalized modes I and II stress intensity factors approach zero as $d/R$ go to zero and after a steep variation in stress intensity factors for large values of $d/R$, they eventually go to zero for small values of $d/R$ as seen in Figures 44 and 45. Figure 46 shows the variation of the normalized force with crack length, it can be seen that for small friction coefficients, $P/\mu R$ initially increases as crack length increases and then goes to a constant value as crack length increases further. For higher values of friction coefficient normalized force decreases initially and then approaches a constant value. Figures 47-49 show the variation of stress intensity factors and normalized force with crack length, for $b/R = -0.1$ and $a/R = -0.05$. The results are similar to those obtained in Figures 44-46.

## REFERENCES


[1] F. Erdogan, in *Mechanics Today*, S. Nemat-Nasser (ed.), Pergamon Press, Oxford, v.4 (1978) 1-86.

[2] N.I. Muskhelishvili, *Singular Integral Equations*, Noordhoff, Groningen, The Netherlands (1958).

[3] M. Abramowitz and I.A. Stegun, *Handbook of Mathematical Functions*, Dover Publications, Inc., New York (1965).

[4] Y.L. Luke, *Algorithms for the Computation of Mathematical Functions*, Academic Press, New York (1977).

[5] N. Hasebe, M. Okumura and T. Nakamura, "Frictional punch and crack in plane elasticity", *ASCE, Journal of Engineering Mechanics*, 115 (1989) 1137-1149.

[6] B. Lawn, *Fracture of Brittle Solids*, Cambridge Solid State Science Series, (1993).

[7] V.L. Hein and F. Erdogan, "Stress singularities in a two-material wedge", *International Journal of Fracture Mechanics*, 7 (1971) 317-330.

[8] F.G. Tricomi, "On the Finite Hilbert Transformation", *The Quarterly Journal of Mathematics Oxford Series*, 2 (1951) 199-211.

[9] M.A. Guler, "Contact mechanics of FGM coatings", Ph.D. Dissertation, Lehigh University, Bethlehem, PA, USA, (2000).

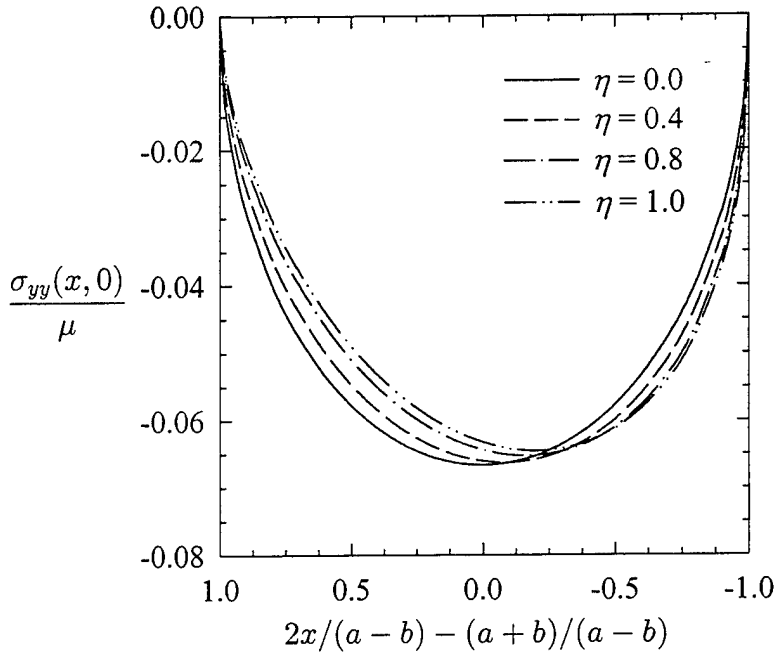


**Figure 9:** Contact stress, $\sigma_{yy}(x,0)$ for a homogeneous half-plane indented by a circular stamp as shown in Figure 8. $\nu = 0.25$, $d = 0$, $(b-a)/R = 0.1$.

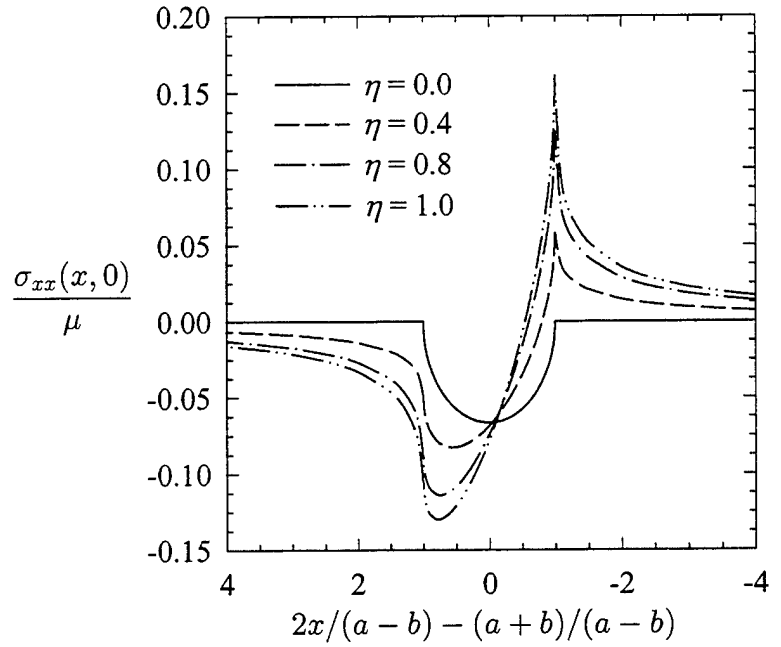


**Figure 10:** In-plane stress, $\sigma_{xx}(x,0)$ for a homogeneous half-plane indented by a circular stamp as shown in Figure 8. $\nu = 0.25$, $d = 0$, $(b-a)/R = 0.1$.

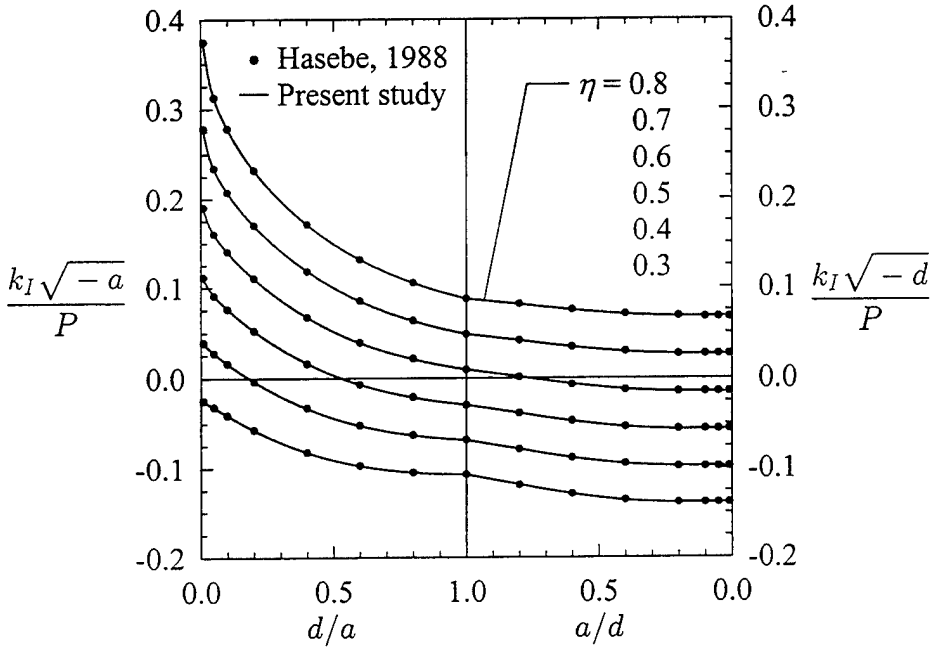


**Figure 11:** Mode I stress intensity factors for an edge crack in a homogeneous half-plane indented by a flat stamp as shown in Figure 1, $b = 0$, $\nu = 0.25$.

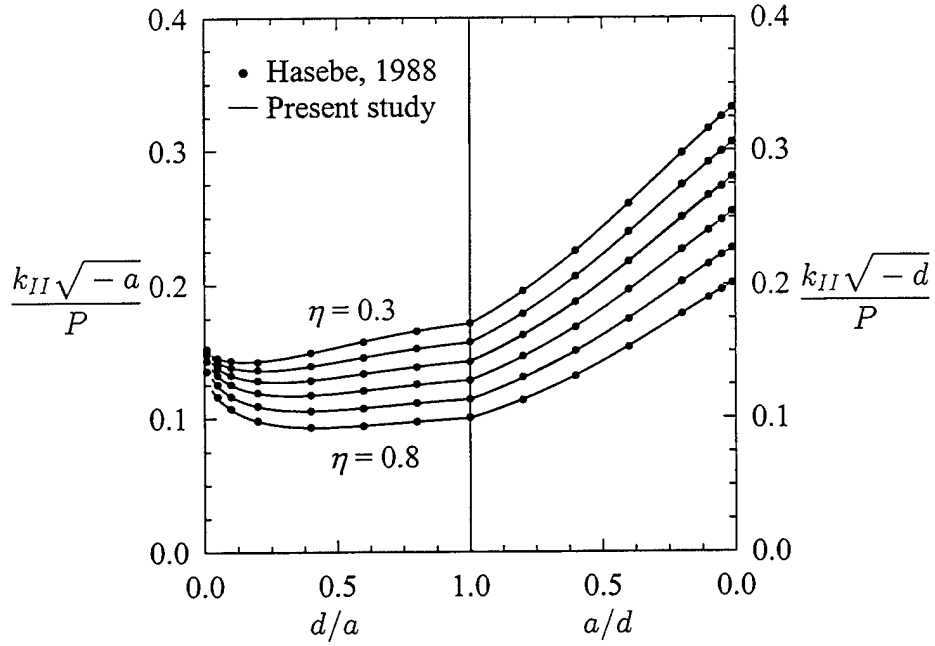


**Figure 12:** Mode II stress intensity factors for an edge crack in a homogeneous half-plane indented by a flat stamp as shown in Figure 1, $b = 0$, $\nu = 0.25$.

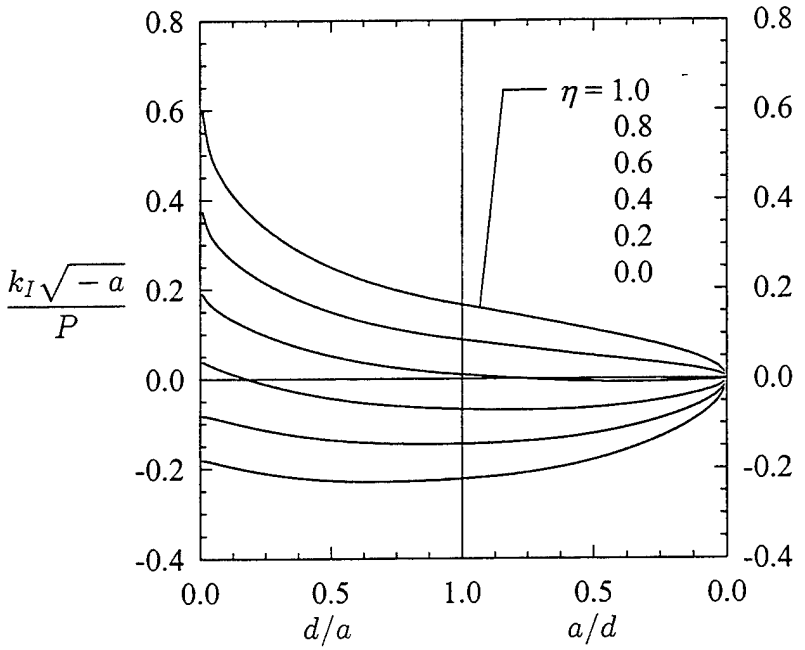


**Figure 13:** Mode I stress intensity factors for an edge crack in a homogeneous half-plane indented by a flat stamp as shown in Figure 1, $b = 0$, $\nu = 0.25$.

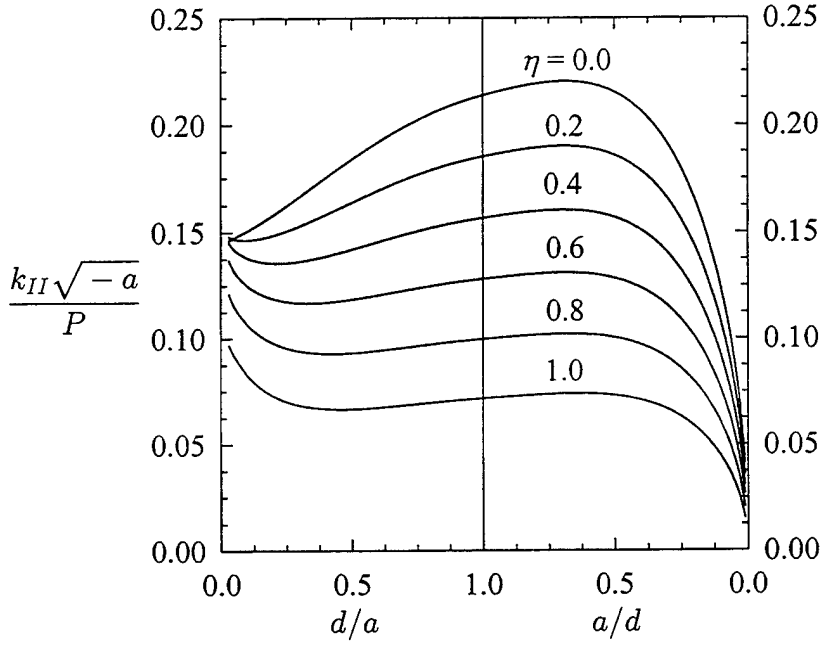


**Figure 14:** Mode II stress intensity factors for an edge crack in a homogeneous half-plane indented by a flat stamp as shown in Figure 1, $b = 0$, $\nu = 0.25$.

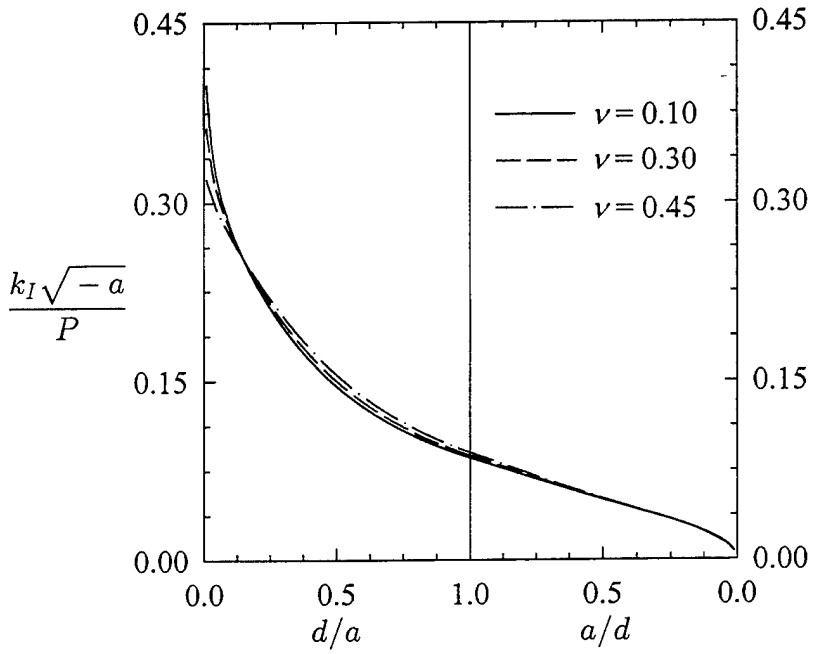


**Figure 16:** Effect of the Poisson's ratio on Mode I stress intensity factors for an edge crack in a homogeneous half-plane indented by a flat stamp as shown in Figure 1, $b = 0$, $\eta = 0.8$.

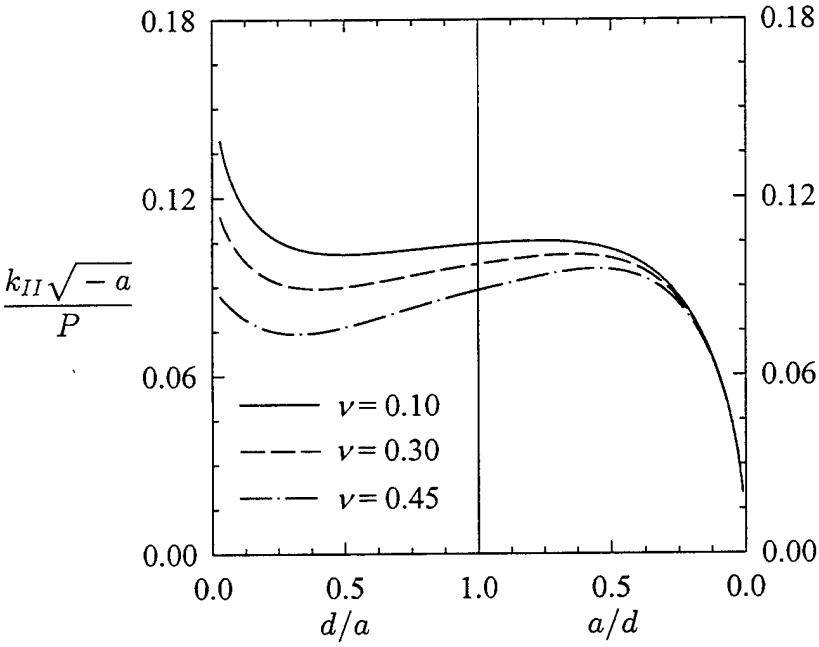


**Figure 17:** Effect of the Poisson's ratio on Mode II stress intensity factors for an edge crack in a homogeneous half-plane indented by a flat stamp as shown in Figure 1, $b = 0$, $\eta = 0.8$.

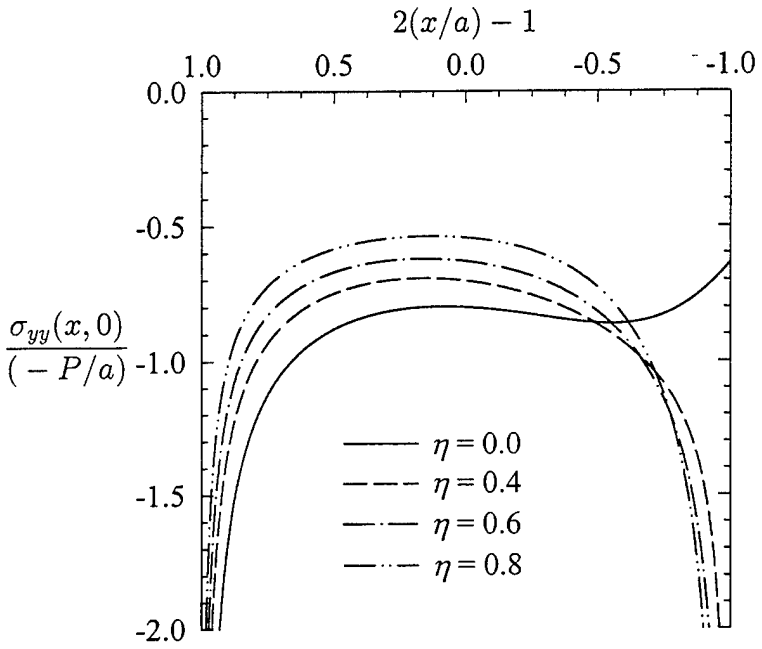


**Figure 18:** Contact stresses for a homogeneous half-plane with an edge crack indented by a flat stamp as shown in Figure 1, $b = 0$, $\nu = 0.25$, $d/a = 0.4$.

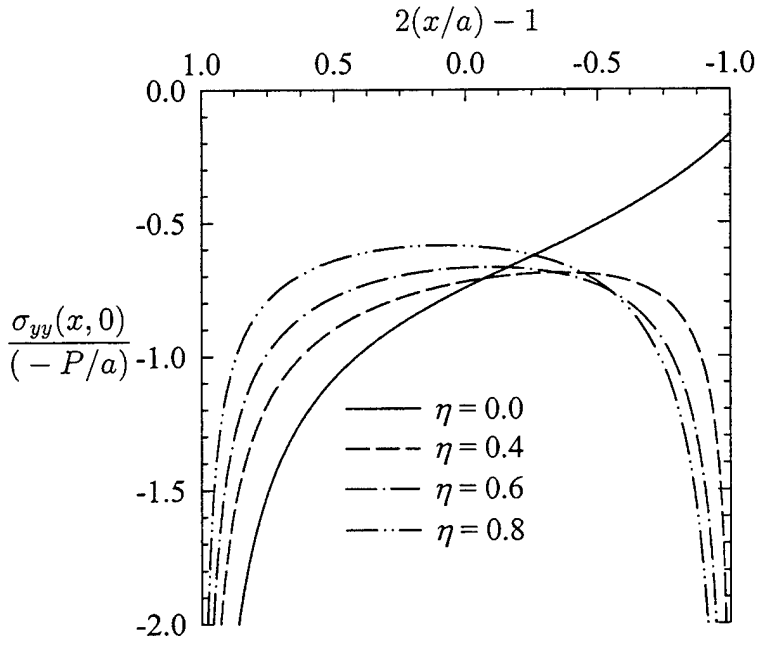


**Figure 19:** Contact stresses for a homogeneous half-plane with an edge crack indented by a flat stamp as shown in Figure 1. $\nu = 0.25$, $a/d = 0.4$.

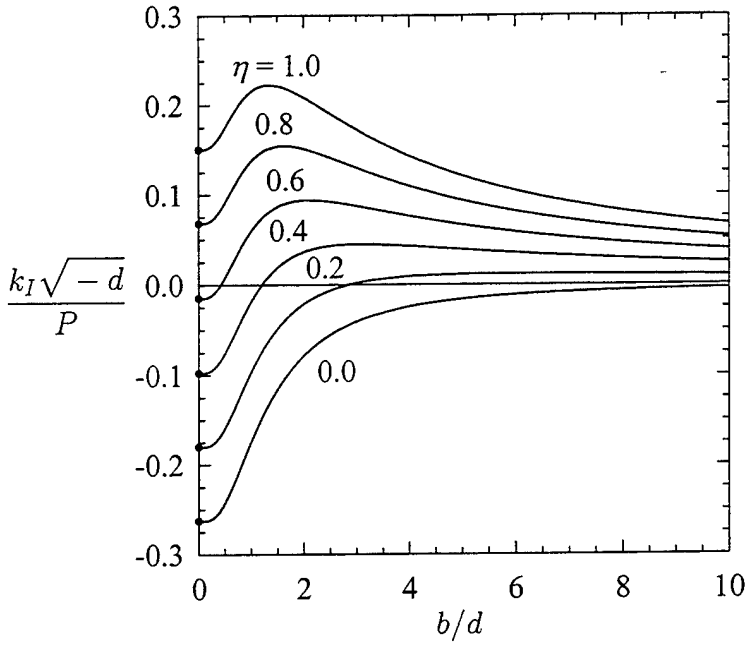


**Figure 20:** Mode I stress intensity factors for an edge crack in a homogeneous half-plane indented by a flat stamp as shown in Figure 1. $(a-b)/d = 0.1, \nu = 0.25$.

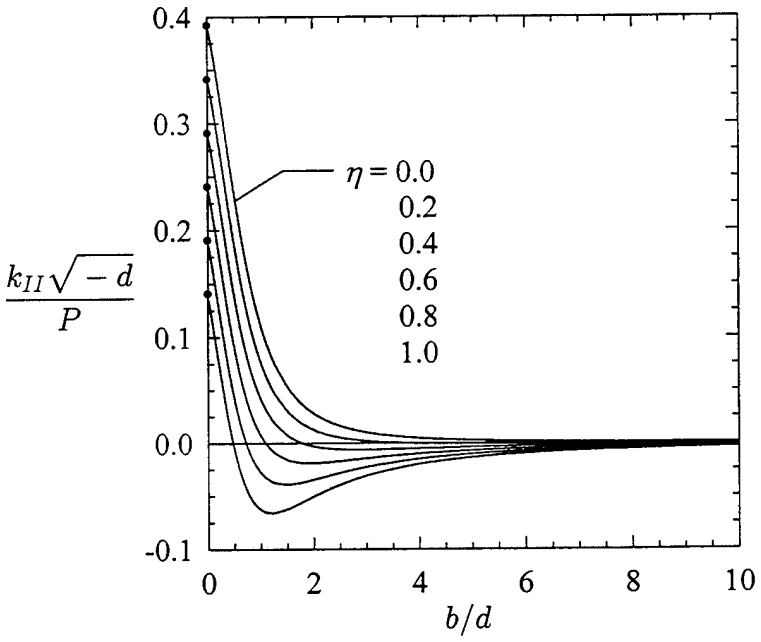


**Figure 21:** Mode II stress intensity factors for an edge crack in a homogeneous half-plane indented by a flat stamp as shown in Figure 1. $(a-b)/d = 0.1, \nu = 0.25$.

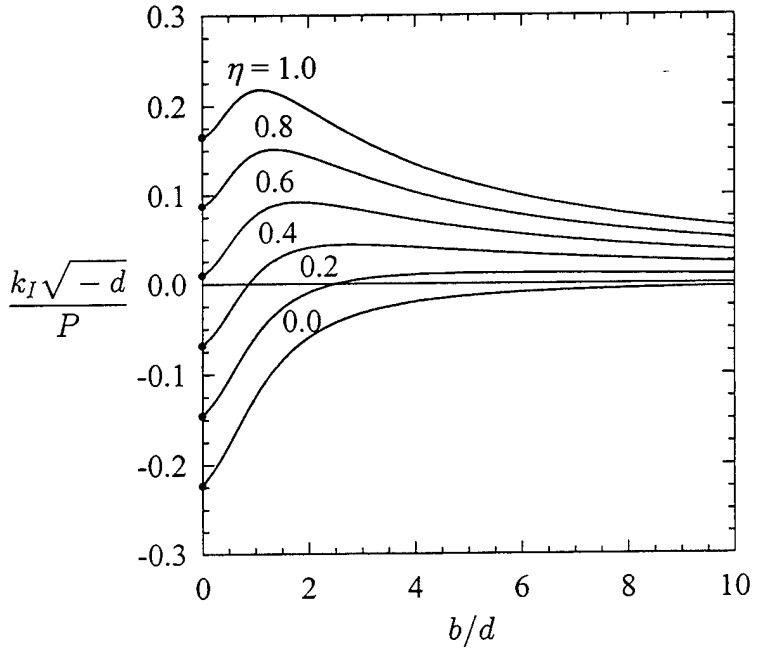


**Figure 22:** Mode I stress intensity factors for an edge crack in a homogeneous half-plane indented by a flat stamp as shown in Figure 1. $(a-b)/d = 1.0$, $\nu = 0.25$.

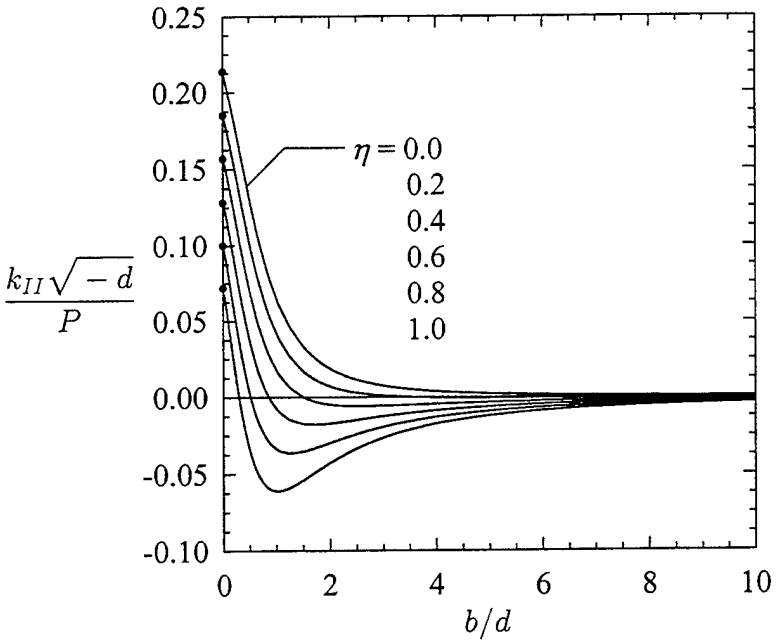


**Figure 23:** Mode II stress intensity factors for an edge crack in a homogeneous half-plane indented by a flat stamp as shown in Figure 1. $(a-b)/d = 1.0$, $\nu = 0.25$.

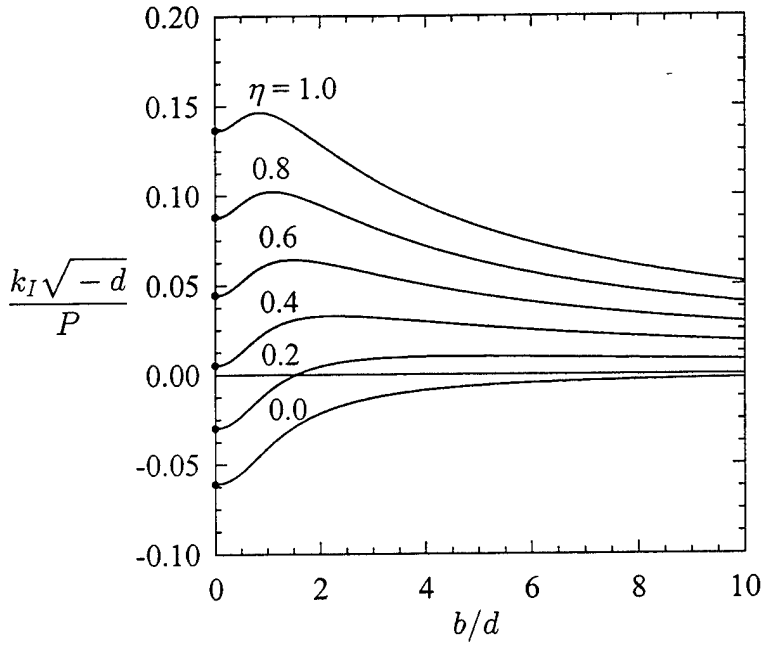


**Figure 24:** Mode I stress intensity factors for an edge crack in a homogeneous half-plane indented by a flat stamp as shown in Figure 1. $(a-b)/d = 10.0$, $\nu = 0.25$.

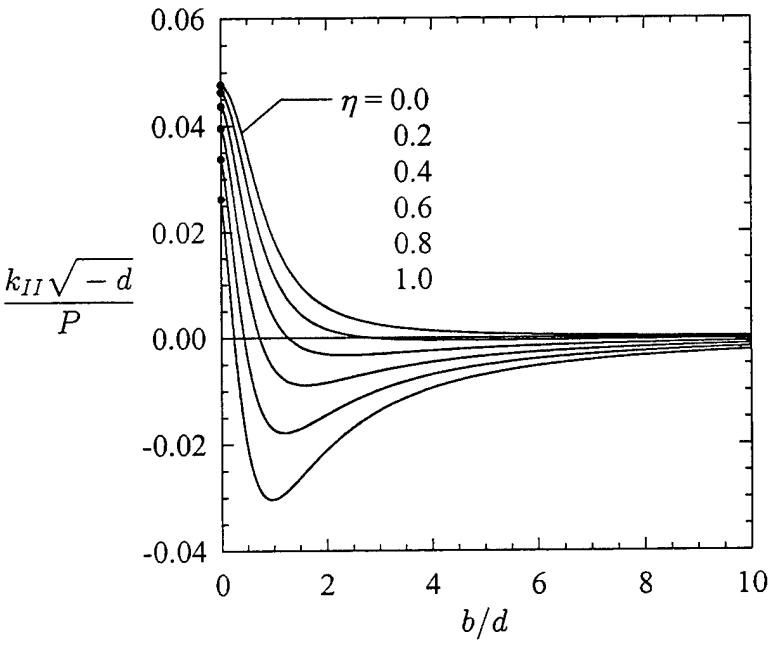


**Figure 25:** Mode II stress intensity factors for an edge crack in a homogeneous half-plane indented by a flat stamp as shown in Figure 1. $(a-b)/d = 10.0$, $\nu = 0.25$.

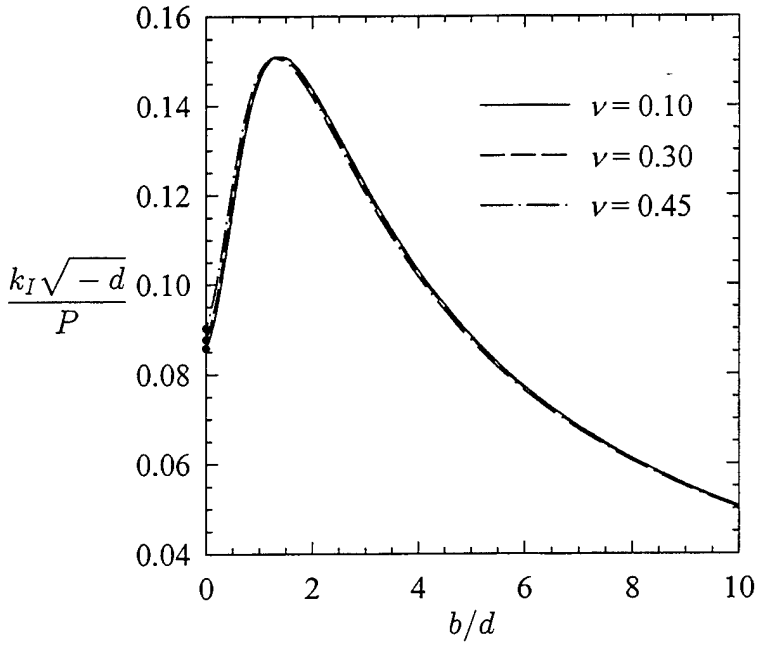


**Figure 26:** Effect of the Poisson's ratio on mode I stress intensity factors for an edge crack in a homogeneous half-plane indented by a flat stamp as shown in Figure 1. $(a-b)/d = 1.0, \eta = 0.8$.

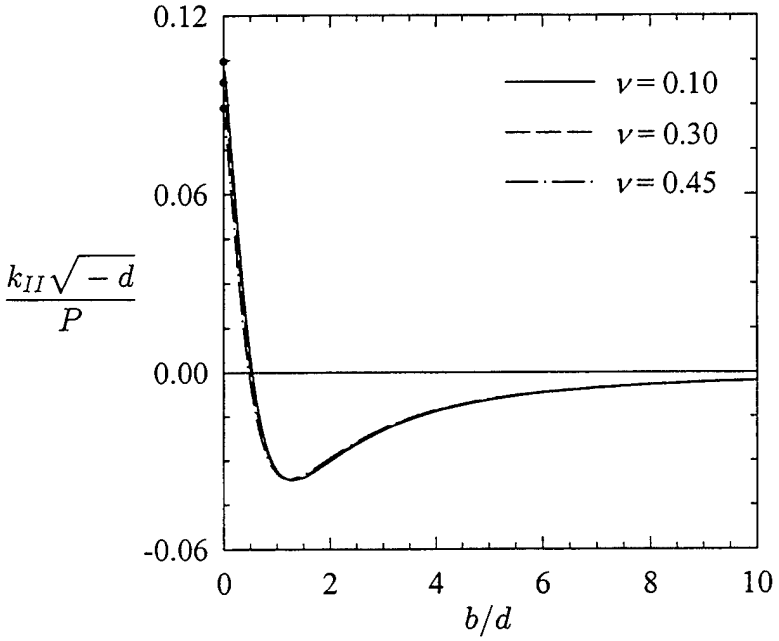


**Figure 27:** Effect of the Poisson's ratio on mode II stress intensity factors for an edge crack in a homogeneous half-plane indented by a flat stamp as shown in Figure 1. $(a-b)/d = 1.0, \eta = 0.8$.

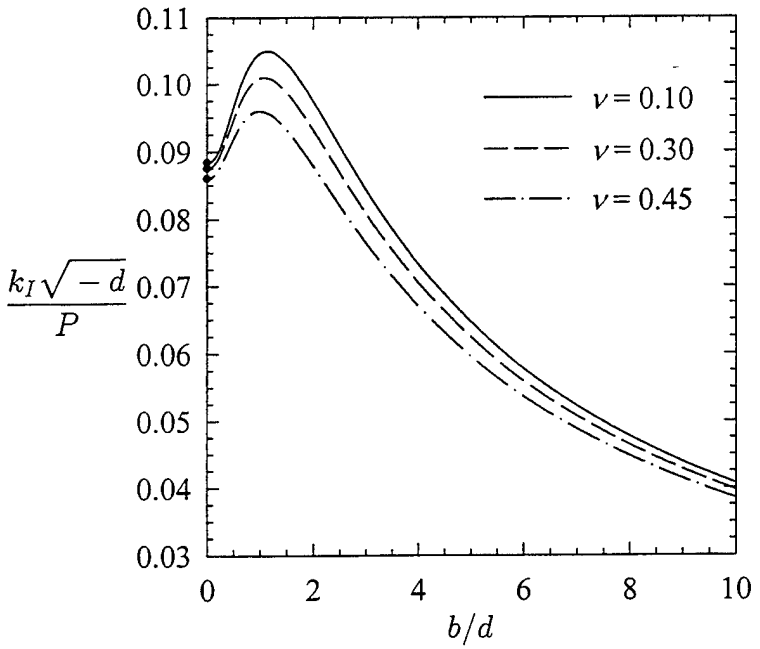


**Figure 28:** Effect of the Poisson's ratio on mode I stress intensity factors for an edge crack in a homogeneous half-plane indented by a flat stamp as shown in Figure 1. $(a-b)/d = 10.0, \eta = 0.8$.

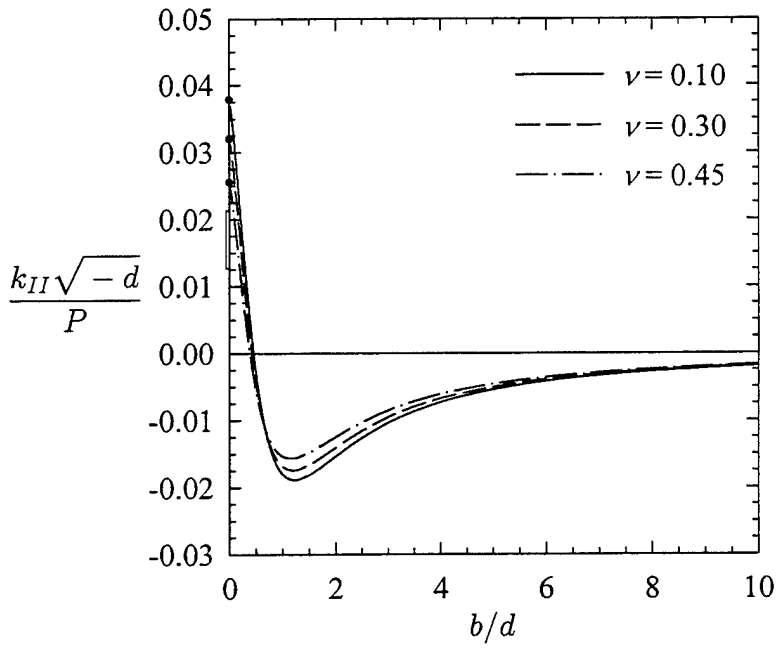


**Figure 29:** Effect of the Poisson's ratio on mode II stress intensity factors for an edge crack in a homogeneous half-plane indented by a flat stamp as shown in Figure 1. $(a-b)/d = 10.0, \eta = 0.8$.

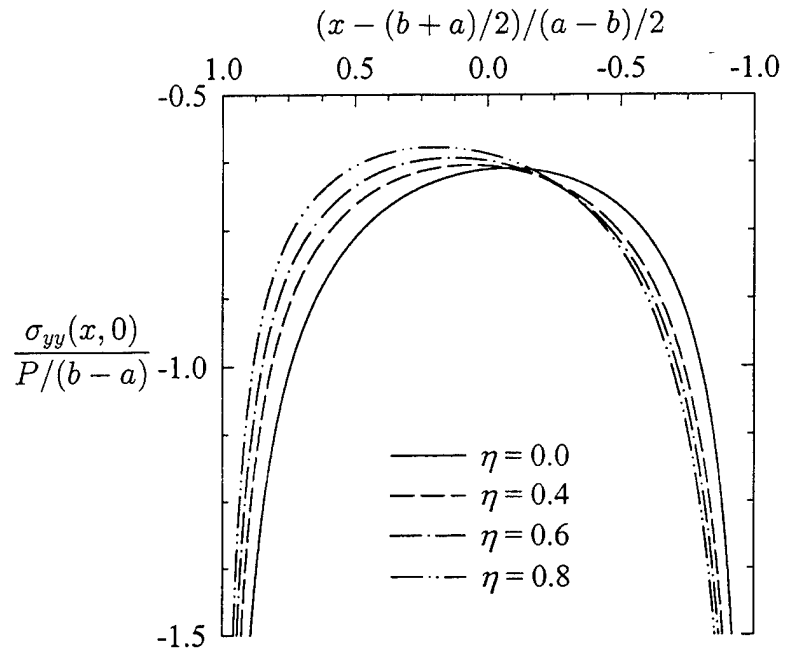


**Figure 30:** Contact stresses for a homogeneous half-plane with an edge crack indented by a flat stamp as shown in Figure 1. $\nu = 0.25$, $b/d = 0.4$, $(a-b)/d = 0.1$.

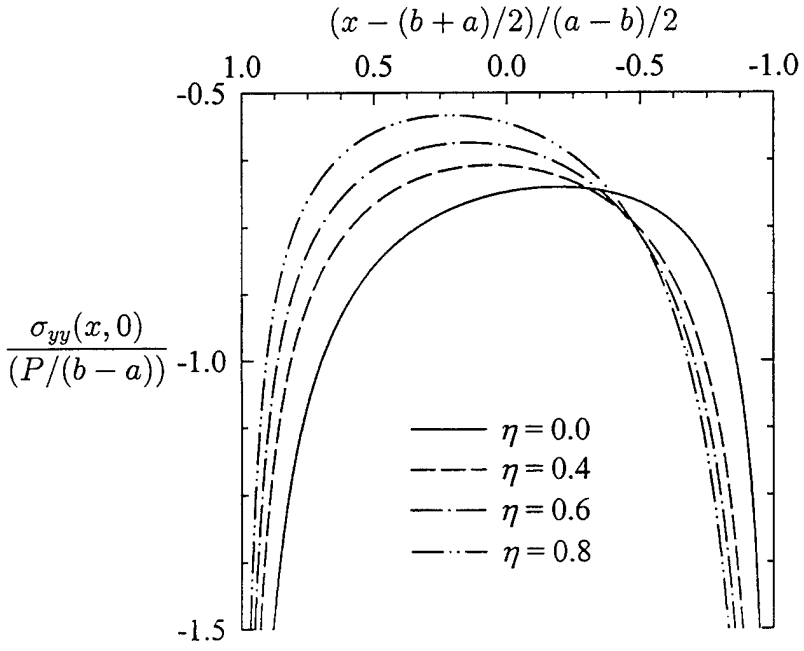


**Figure 31:** Contact stresses for a homogeneous half-plane with an edge crack indented by a flat stamp as shown in Figure 1. $\nu = 0.25$, $b/d = 0.4$, $(a-b)/d = 1.0$.

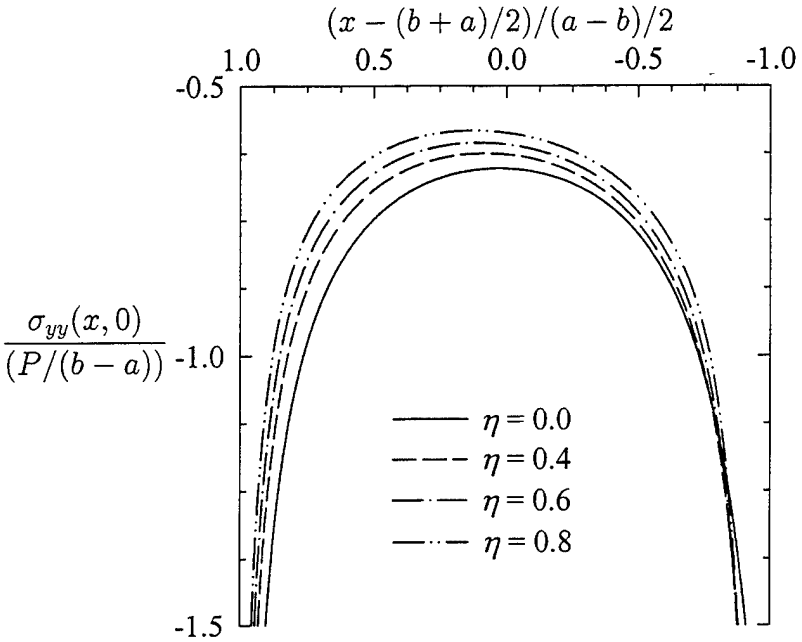


**Figure 32:** Contact stresses for a homogeneous half-plane with an edge crack indented by a flat stamp as shown in Figure 1. $\nu = 0.25$, $b/d = 0.4$, $(a-b)/d = 10.0$.

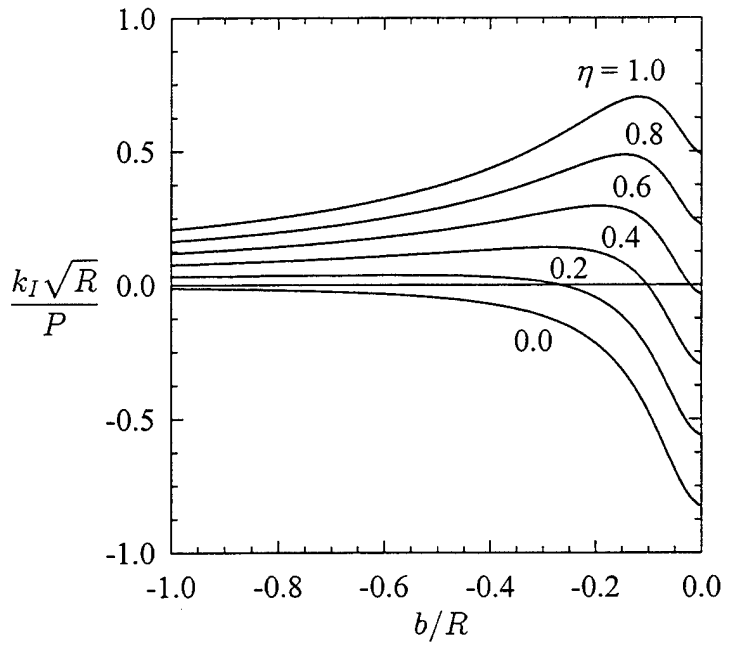


**Figure 33:** Mode I stress intensity factors for an edge crack in a homogeneous half-plane indented by a circular stamp as shown in Figure 8. $(b-a)/R = 0.05$, $d/R = -0.1$, $\nu = 0.25$.

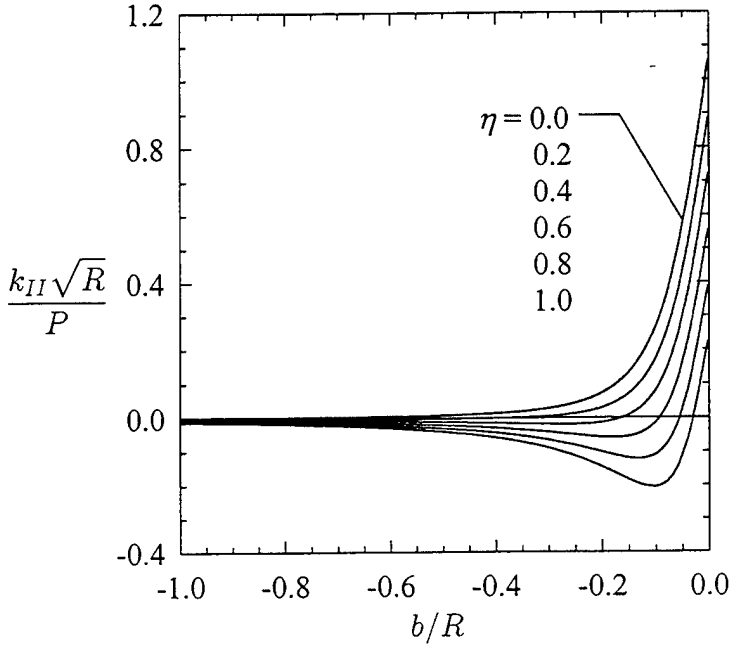


**Figure 34:** Mode II stress intensity factors for an edge crack in a homogeneous half-plane indented by a circular stamp as shown in Figure 8. $(b-a)/R = 0.05$, $d/R = -0.1$, $\nu = 0.25$.

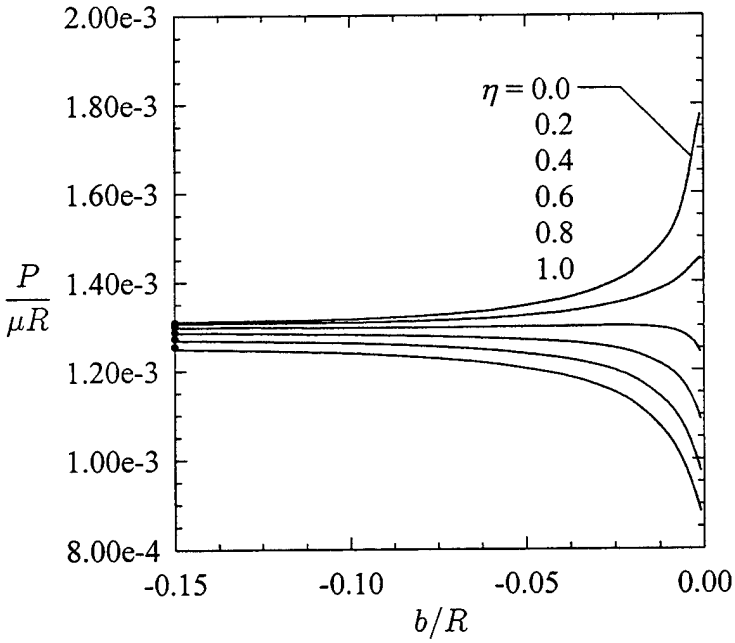


**Figure 35:** Normalized force for a homogeneous half-plane containing an edge crack and indented by a circular stamp as shown in Figure 8. $(b-a)/R = 0.05$, $d/R = -0.1$, $\nu = 0.25$.

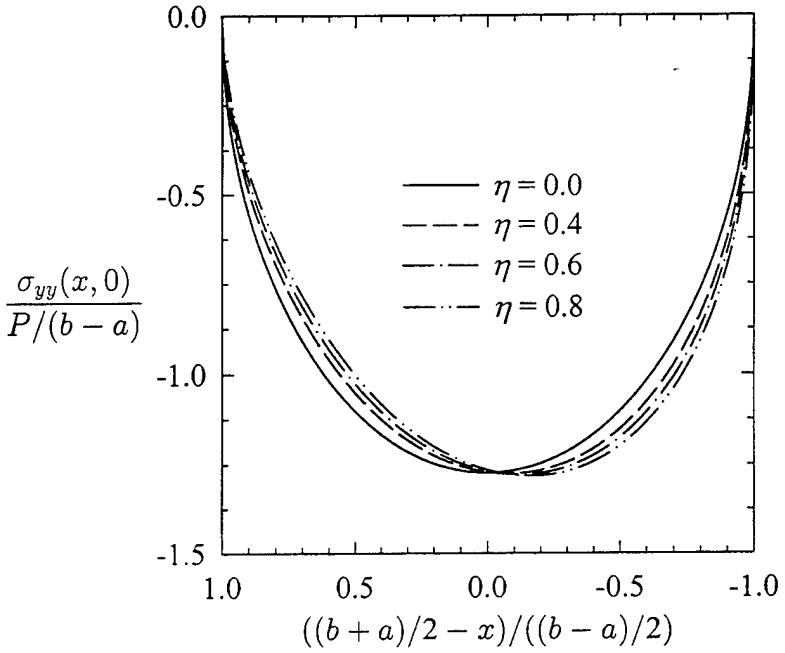


**Figure 36:** Contact stresses for a homogeneous half-plane with an edge crack indented by a circular stamp as shown in Figure 8. $\nu = 0.25$, $d/R = -0.1$, $b/R = -0.1$, $a/R = -0.15$

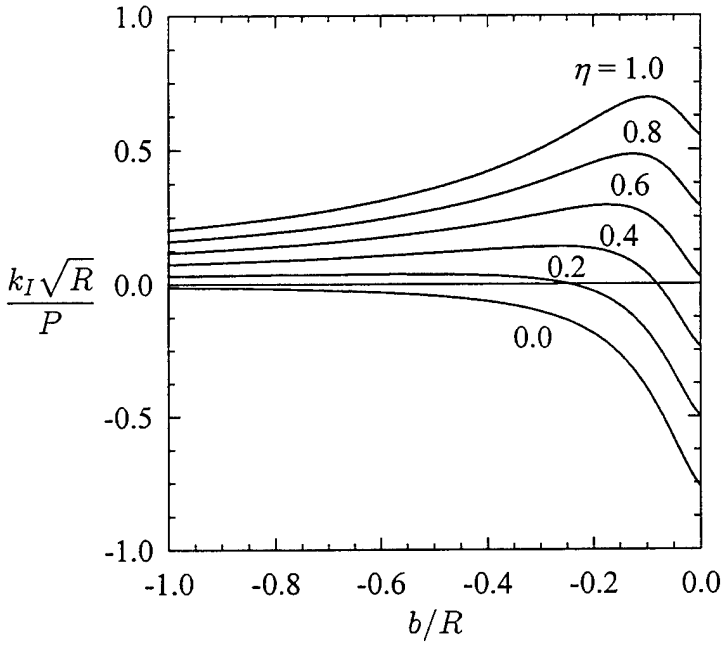


**Figure 37:** Mode I stress intensity factors for an edge crack in a homogeneous half-plane indented by a circular stamp as shown in Figure 8. $(b-a)/R = 0.1$, $d/R = -0.1$, $\nu = 0.25$.

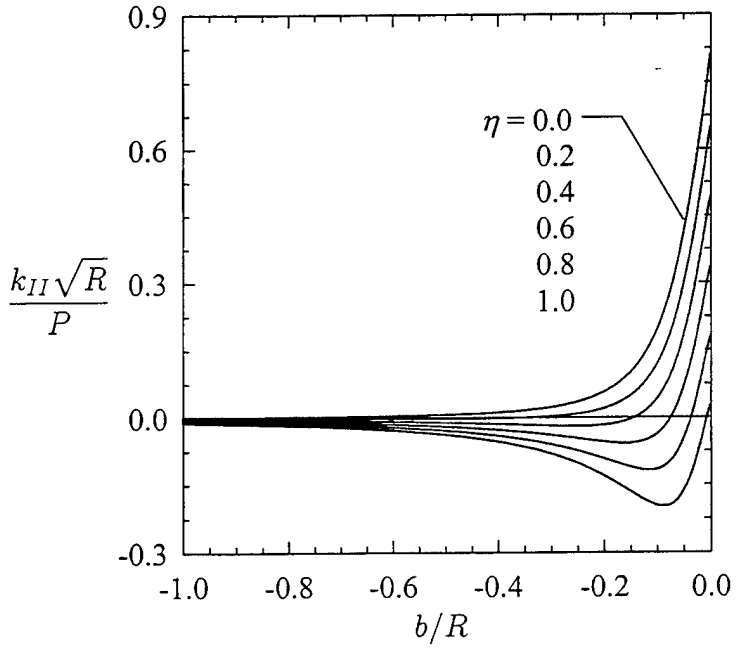


**Figure 38:** Mode II stress intensity factors for an edge crack in a homogeneous half-plane indented by a circular stamp as shown in Figure 8. $(b-a)/R = 0.1$, $d/R = -0.1$, $\nu = 0.25$.

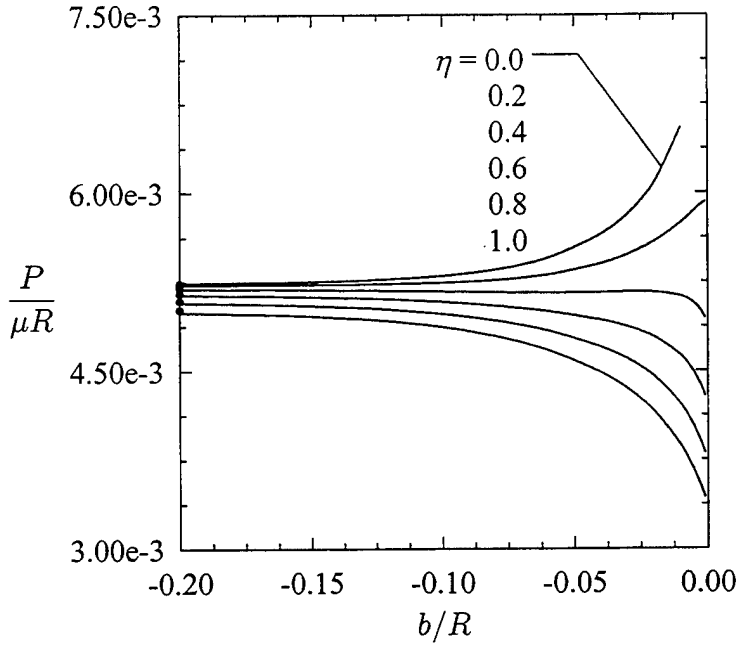


**Figure 39:** Normalized force for a homogeneous half-plane containing an edge crack and indented by a circular stamp as shown in Figure 8. $(b-a)/R = 0.1$, $d/R = -0.1$, $\nu = 0.25$.

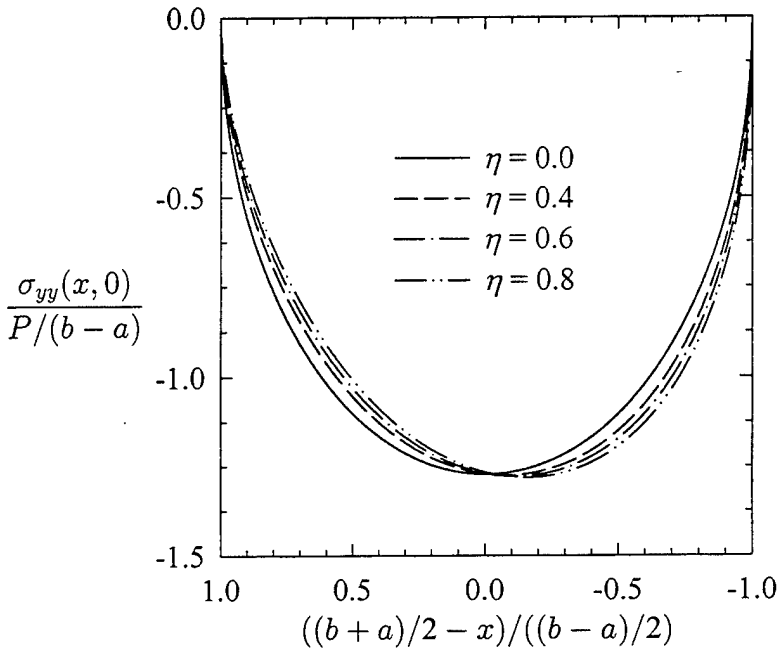


**Figure 40:** Contact stresses for a homogeneous half-plane with an edge crack indented by a circular stamp as shown in Figure 8. $\nu = 0.25$, $d/R = -0.1$, $b/R = -0.1$, $a/R = -0.2$.

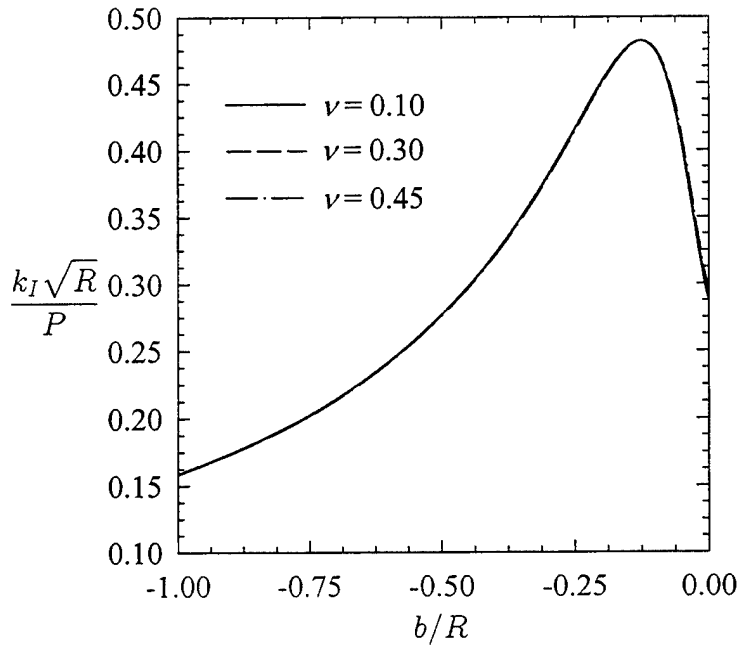


**Figure 41:** Effect of the Poisson's ratio on mode I stress intensity factors for an edge crack in a homogeneous half-plane indented by a circular stamp as shown in Figure 8. $(b-a)/R = 0.1$, $\eta = 0.8$, $d/R$ = -0.1.

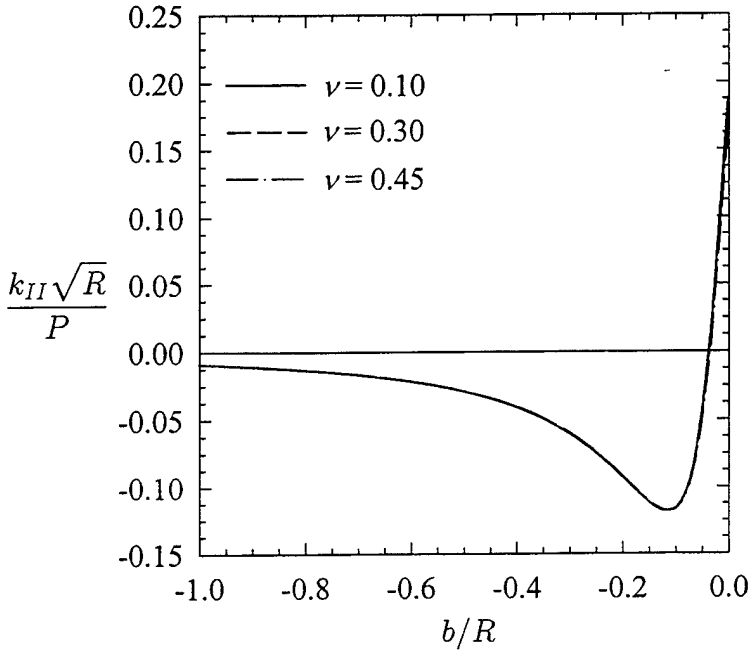


**Figure 42:** Effect of the Poisson's ratio on mode II stress intensity factors for an edge crack in a homogeneous half-plane indented by a circular stamp as shown in Figure 8. $(b-a)/R = 0.1, \eta = 0.8, d/R = -0.1$.

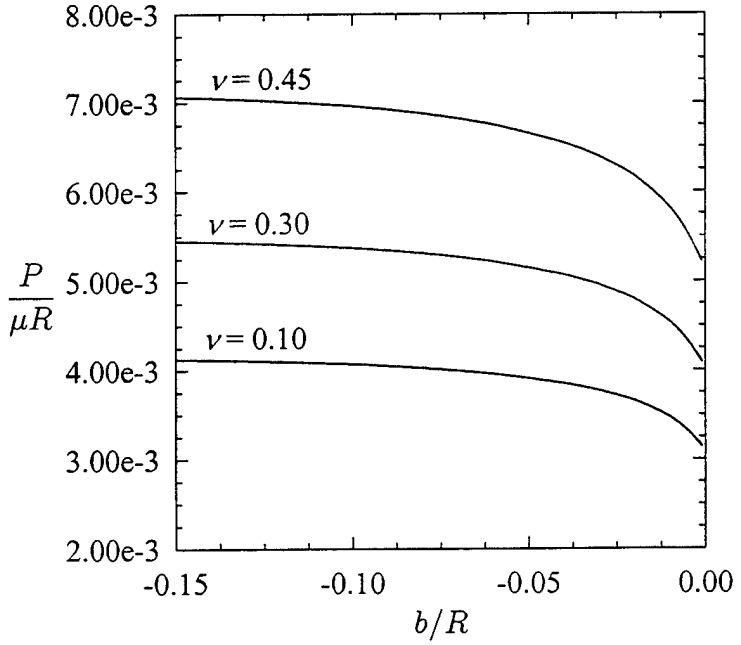


**Figure 43:** Effect of the Poisson's ration on the normalized force for a homogeneous half-plane containing an edge crack and indented by a circular stamp as shown in Figure 8. $(b-a)/R = 0.1, d/R = -0.1, \eta = 0.8$.

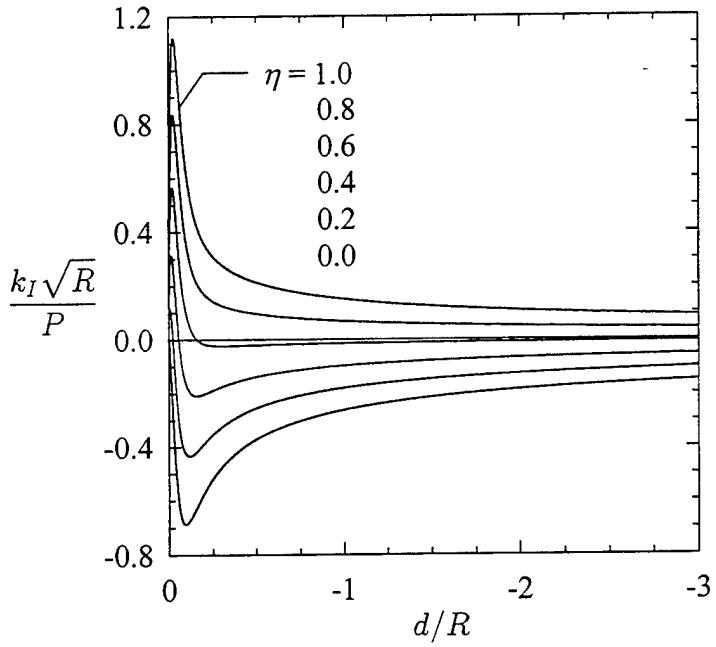


**Figure 44:** Mode I stress intensity factors for an edge crack in a homogeneous half-plane indented by a circular stamp as shown in Figure 8. $b/R = -0.05$, $a/R = -0.1$, $\nu = 0.25$.

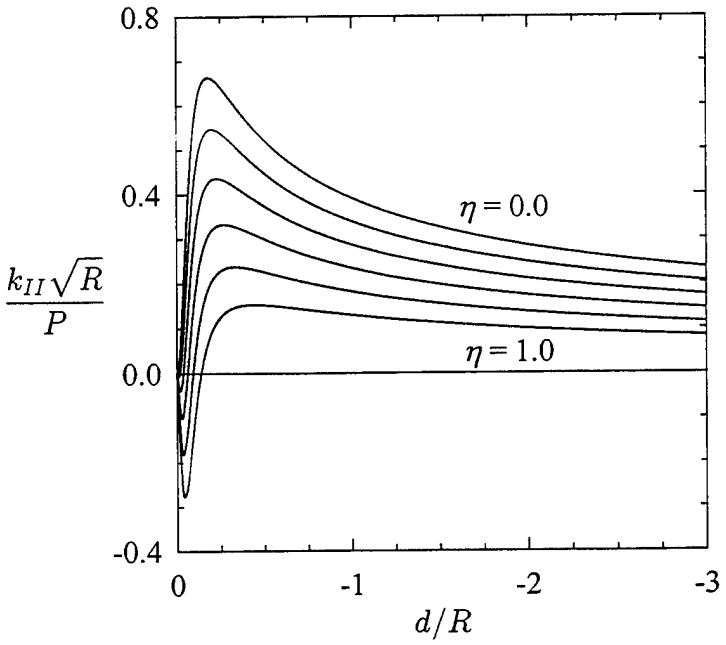


**Figure 45:** Mode II stress intensity factors for an edge crack in a homogeneous half-plane indented by a circular stamp as shown in Figure 8. $b/R = -0.05$, $a/R = -0.1$, $\nu = 0.25$.

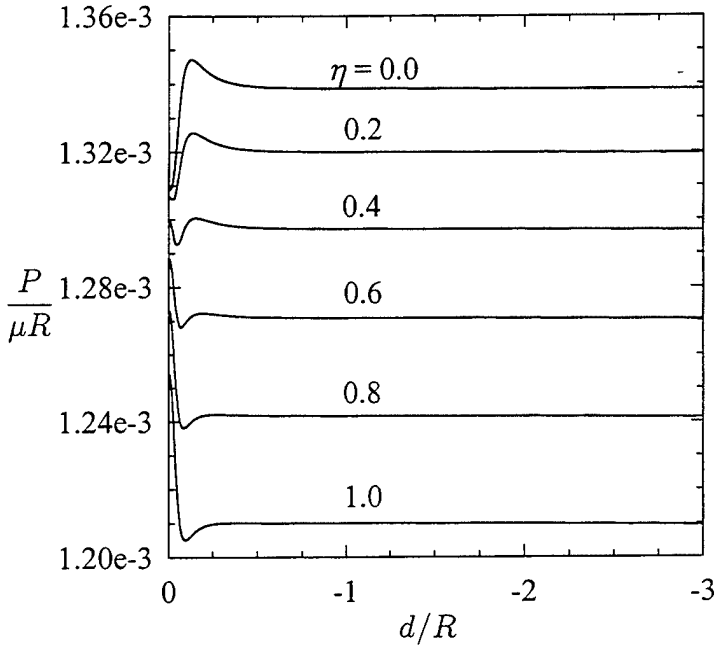


**Figure 46:** Normalized force for a homogeneous half-plane containing an edge crack and indented by a circular stamp as shown in Figure 8. $b/R = -0.05$, $a/R = -0.1$, $\nu = 0.25$.

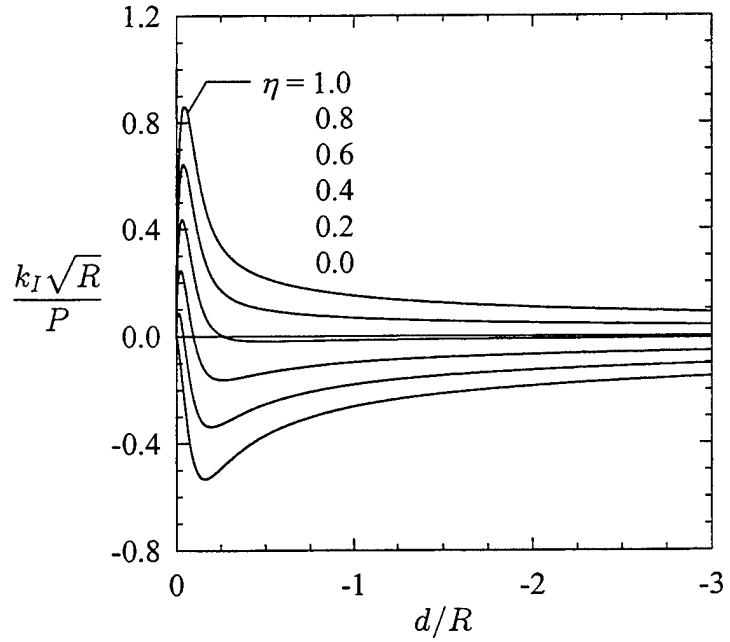


**Figure 47:** Mode I stress intensity factors for an edge crack in a homogeneous half-plane indented by a circular stamp as shown in Figure 8. $b/R = -0.1$, $a/R = -0.15$, $\nu = 0.25$.

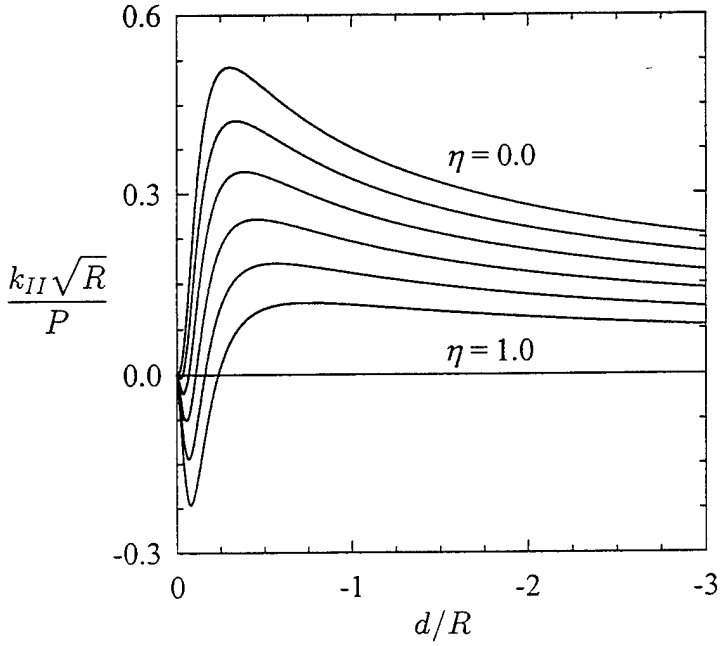


**Figure 48:** Mode II stress intensity factors for an edge crack in a homogeneous half-plane indented by a circular stamp as shown in Figure 8. $b/R = -0.1$, $a/R = -0.15$, $\nu = 0.25$.

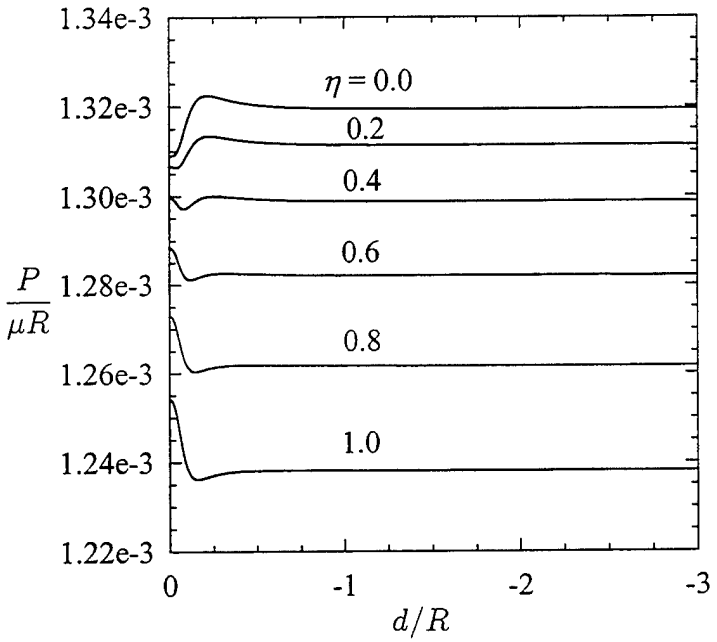


**Figure 49:** Normalized force for a homogeneous half-plane containing an edge crack and indented by a circular stamp as shown in Figure 8. $b/R = -0.1$, $a/R = -0.15$, $\nu = 0.25$.

## APPENDIX A

### Coefficients for the eigenvalue problem

Following are the coefficients for the eigenvalue problem to determine the strength of singularity $\alpha$ (see equation (55)).

$$a_{11}(\alpha) = a_{22}(\alpha) = \frac{1}{\sin(\pi\alpha)}\Big(\cos(\pi\alpha) - \big(2\alpha^2 + 4\alpha + 1\big)\Big), \tag{A1a}$$

$$a_{13}(\alpha) = \frac{1}{\sin(\pi\alpha)}\Big(\eta\cos(\pi\alpha/2)(2+\alpha) + \sin(\pi\alpha)(1+\alpha)\Big), \tag{A1b}$$

$$a_{23}(\alpha) = \frac{1}{\sin(\pi\alpha)}\Big(\eta\sin(\pi\alpha/2)(1+\alpha) - \alpha\cos(\pi\alpha/2)\Big), \tag{A1c}$$

$$a_{31}(\alpha) = \frac{2\sin(\pi\alpha/2)(1+\alpha)}{\sin(\pi\alpha)}, \tag{A1d}$$

$$a_{32}(\alpha) = \frac{2\cos(\pi\alpha/2)(2+\alpha)}{\sin(\pi\alpha)}, \tag{A1e}$$

$$a_{33}(\alpha) = \cot(\pi\alpha) - \frac{\kappa - 1}{\kappa + 1}\eta. \tag{A1f}$$

## APPENDIX B

### Mellin transform method for the derivation of the characteristic equation

The characteristic equation given by (58) can also be obtained by considering a 90-degree elastic wedge as shown in Figure 50 and using Mellin transformation.

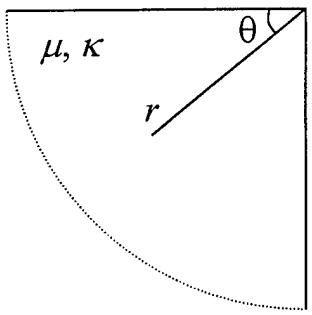


**Figure 50:** 90-degree elastic wedge

The boundary conditions of the problem are given by,

$$\sigma_{r\theta}(r,0) - \eta\sigma_{\theta\theta}(r,0) = 0, \qquad 0 < r < \infty, \tag{B1a}$$

$$\frac{\partial}{\partial r}u_{\theta}(r,0) = f(r), \qquad 0 < r < \infty, \tag{B1b}$$

$$\sigma_{\theta\theta}(r,\pi/2) = 0, \qquad 0 < r < \infty, \tag{B1c}$$

$$\sigma_{r\theta}(r,\pi/2) = 0, \qquad 0 < r < \infty. \tag{B1d}$$

In polar coordinates, following definition of the stresses in terms of a stress function $\chi$ identically satisfies the equilibrium equations,

$$\sigma_{rr}(r,\theta) = \frac{1}{r}\frac{\partial\chi(r,\theta)}{\partial r} + \frac{1}{r^2}\frac{\partial^2\chi(r,\theta)}{\partial\theta^2}, \tag{B2a}$$

$$\sigma_{\theta\theta}(r,\theta) = \frac{\partial^2\chi(r,\theta)}{\partial r^2}, \tag{B2b}$$

$$\sigma_{r\theta}(r,\theta) = -\frac{\partial}{\partial r}\Big(\frac{1}{r}\frac{\partial \chi(r,\theta)}{\partial \theta}\Big). \tag{B2c}$$

Thus, the compatibility condition becomes,

$$\nabla^2\nabla^2\chi(r,\theta) = 0, \tag{B3}$$

where,

$$\nabla^2 = \frac{\partial^2}{\partial r^2} + \frac{1}{r}\frac{\partial}{\partial r} + \frac{1}{r^2}\frac{\partial^2}{\partial \theta^2}\,. \tag{B4}$$

It is also known that (see for example Hein and Erdogan [7]), displacements can be expressed in terms of this biharmonic stress function $\chi$ and another harmonic function $\phi$ in the following form,

$$2\mu u_r(r,\theta) = -\frac{\partial \chi(r,\theta)}{\partial r} + \Big(\frac{\kappa+1}{4}\Big) r\frac{\partial \phi(r,\theta)}{\partial \theta}, \tag{B5a}$$

$$2\mu u_\theta(r,\theta) = -\frac{1}{r}\frac{\partial \chi(r,\theta)}{\partial \theta} + \Big(\frac{\kappa+1}{4}\Big) r^2\frac{\partial \phi(r,\theta)}{\partial r}, \tag{B5b}$$

$\chi(r,\theta)$ and $\phi(r,\theta)$ are related by

$$\nabla^2\chi(r,\theta) = \frac{\partial}{\partial r}\Big(r\frac{\partial \phi(r,\theta)}{\partial \theta}\Big), \tag{B6}$$

and $\phi(r,\theta)$ is a harmonic function

$$\nabla^2\phi(r,\theta) = 0. \tag{B7}$$

Mellin transform of a function $f(r)$ and its inverse are defined as

$$\widehat{f}(p) = \int_0^\infty f(r)r^{p-1}dr, \qquad f(r) = \frac{1}{2\pi i}\int_{c-i\infty}^{c+i\infty}\widehat{f}(p)r^{-p}dp. \tag{B8}$$

Mellin transform of the derivative can be expressed as follows:

$$\int_0^\infty \frac{d^n f(r)}{dr^n} r^{p-1+n}dr = (-1)^n\frac{\Gamma(p+n)}{\Gamma(p)}\widehat{f}(p), \tag{B9}$$

provided that

$$r^{p+m-1}\frac{d^{m-1}}{dr^{m-1}}f(r)=0, \tag{B10}$$

as, $r\to 0$ and $r\to\infty$ for $m=1,2,3,...,n$.

Taking the Mellin transform of equations (B3), (B6) and (B7), following equations are obtained,

$$\frac{d^4\widehat{\chi}(\theta,p)}{d\theta^4}+\left(p^2+(p+2)^2\right)\frac{d^2\widehat{\chi}(\theta,p)}{d\theta^2}+p^2(p+2)^2\widehat{\chi}(\theta,p)=0, \tag{B11a}$$

$$\frac{d^2\widehat{\phi}(\theta,p)}{d\theta^2}+p^2\widehat{\phi}(\theta,p)=0, \tag{B11b}$$

$$\frac{d}{d\theta}\widehat{\phi}(\theta,p+2)=-\frac{1}{p+2}\left(p^2\widehat{\chi}(\theta,p)+\frac{d^2\widehat{\chi}(\theta,p)}{d\theta^2}\right). \tag{B11c}$$

Solving equations (B11a) and (B11b) and using (B11c) displacements and stresses can be expressed in the following form,

$$\mu r^2\left(\frac{\partial u_r}{\partial r}+i\frac{\partial u_\theta}{\partial r}\right)=$$

$$-\frac{1}{2\pi i}\int_{c-i\infty}^{c+i\infty}(p+1)\left(Ape^{ip\theta}+B(p+1)e^{i(p+2)\theta}+\kappa\overline{B}e^{-i(p+2)\theta}\right)r^{-p}dp, \tag{B12a}$$

$$\frac{r^2}{2i}\left(\sigma_{r\theta}+i\sigma_{\theta\theta}\right)=$$

$$\frac{1}{2\pi i}\int_{c-i\infty}^{c+i\infty}(p+1)\left(Ape^{ip\theta}+B(p+1)e^{i(p+2)\theta}-\overline{B}e^{-i(p+2)\theta}\right)r^{-p}dp, \tag{B12b}$$

In equations (B12), $A$ and $B$ are complex constants and $\overline{B}$ is the complex conjugate of $B$. Using equations (B12) and boundary conditions (B1) following expressions are obtained

$$\frac{\sigma_{\theta\theta}(r,0)}{4\mu} = \int_0^\infty f(t)dt \frac{1}{2\pi i}\int_{c-i\infty}^{c+i\infty} \frac{2\alpha^2+4\alpha+1-\cos(\pi\alpha)}{D(\alpha)} \frac{r^\alpha}{t^{\alpha+1}} d\alpha, \tag{B13a}$$

$$\frac{1}{2(\kappa+1)}\frac{\partial}{\partial r}u_\theta(r,\pi/2) =$$

$$\int_0^\infty f(t)dt \frac{1}{2\pi i}\int_{c-i\infty}^{c+i\infty} \frac{\eta\cos(\pi\alpha)(\alpha+2)+\sin(\pi\alpha/2)(\alpha+1)}{D(\alpha)} \frac{r^\alpha}{t^{\alpha+1}} d\alpha, \tag{B13b}$$

where,

$$D(\alpha) = \eta(4\alpha^2+10\alpha+5+(\kappa-1)\cos(\pi\alpha)+\kappa(2\alpha+3))+(\kappa+1)\sin(\pi\alpha). \tag{B14}$$

Note that $D(\alpha)$ is same as the characteristic equation (58). If one performs the inversions in (B13) by using the theory of residues, then negative roots of $D(\alpha)$ give stresses that are singular as $r$ approaches zero. Thus, $D(\alpha) = 0$ is the characteristic equation of the problem.

## APPENDIX C

### Kernels of the integral equations

The integral equations for are given by and the kernels are given by (22) and (23) respectively. In this section we will give the transformed form of the kernels and other terms for the three cases considered.

Flat stamp, $b = 0$

The transformed form of the kernels used in equations (63a,c) are given by,

$$G_{11}(r, s_1) = -\frac{1}{\pi}\frac{d}{2}K_{11}\left(\frac{d}{2}r + \frac{d}{2}, \frac{d}{2}s_1 + \frac{d}{2}\right), \tag{C1a}$$

$$G_{13}(r, s_1) = -\frac{1}{\pi}\frac{a}{2}K_{13}\left(\frac{a}{2}r + \frac{a}{2}, \frac{d}{2}s_1 + \frac{d}{2}\right), \tag{C1b}$$

$$G_{22}(r, s_2) = -\frac{1}{\pi}\frac{d}{2}K_{22}\left(\frac{d}{2}r + \frac{d}{2}, \frac{d}{2}s_2 + \frac{d}{2}\right), \tag{C1c}$$

$$G_{23}(r, s_2) = -\frac{1}{\pi}\frac{a}{2}K_{23}\left(\frac{a}{2}r + \frac{a}{2}, \frac{d}{2}s_2 + \frac{d}{2}\right), \tag{C1d}$$

$$G_{31}(r, s_3) = -\frac{1}{\pi}\frac{d}{2}K_{31}\left(\frac{d}{2}r + \frac{d}{2}, \frac{a}{2}s_3 + \frac{a}{2}\right), \tag{C1e}$$

$$G_{32}(r, s_3) = -\frac{1}{\pi}\frac{d}{2}K_{32}\left(\frac{d}{2}r + \frac{d}{2}, \frac{a}{2}s_3 + \frac{a}{2}\right). \tag{C1f}$$

The terms used in equations (68) are in the following form

$$h_{11n}(s_1) = \int_{-1}^{1} G_{11}(r, s_1)(1-r)^{-1/2}(1+r)^{\alpha}P_n^{(-1/2,\alpha)}(r)dr, \tag{C2a}$$

$$h_{13n}(s_1) = \int_{-1}^{1} G_{13}(r, s_1)(1-r)^{\beta}(1+r)^{\alpha}P_n^{(\beta,\alpha)}(r)dr, \tag{C2b}$$

$$h_{22n}(s_2) = \int_{-1}^{1} G_{22}(r, s_2)(1-r)^{-1/2}(1+r)^{\alpha}P_n^{(-1/2,\alpha)}(r)dr, \tag{C2c}$$

$$h_{23n}(s_2) = \int_{-1}^{1} G_{23}(r, s_2)(1-r)^{\beta}(1+r)^{\alpha} P_n^{(\beta,\alpha)}(r)dr, \tag{C2d}$$

$$h_{31n}(s_3) = \int_{-1}^{1} G_{31}(r, s_3)(1-r)^{-1/2}(1+r)^{\alpha} P_n^{(-1/2,\alpha)}(r)dr, \tag{C2e}$$

$$h_{32n}(s_3) = \int_{-1}^{1} G_{32}(r, s_3)(1-r)^{-1/2}(1+r)^{\alpha} P_n^{(-1/2,\alpha)}(r)dr. \tag{C2f}$$

*Flat stamp, $b < 0$*

The transformed form of the kernels used in equations (79a,c) are given by,

$$M_{11}(r, s_1) = -\frac{1}{\pi}\frac{d}{2} K_{11}\Big(\frac{d}{2}r + \frac{d}{2}, \frac{d}{2}s_1 + \frac{d}{2}\Big), \tag{C3a}$$

$$M_{13}(r, s_1) = -\frac{1}{\pi}\frac{a-b}{2} K_{13}\Big(\frac{a-b}{2}r + \frac{a+b}{2}, \frac{d}{2}s_1 + \frac{d}{2}\Big), \tag{C3b}$$

$$M_{22}(r, s_2) = -\frac{1}{\pi}\frac{d}{2} K_{22}\Big(\frac{d}{2}r + \frac{d}{2}, \frac{d}{2}s_2 + \frac{d}{2}\Big), \tag{C3c}$$

$$M_{23}(r, s_2) = -\frac{1}{\pi}\frac{a-b}{2} K_{23}\Big(\frac{a-b}{2}r + \frac{a+b}{2}, \frac{d}{2}s_2 + \frac{d}{2}\Big), \tag{C3d}$$

$$M_{31}(r, s_3) = -\frac{1}{\pi}\frac{d}{2} K_{31}\Big(\frac{d}{2}r + \frac{d}{2}, \frac{a-b}{2}s_3 + \frac{a+b}{2}\Big), \tag{C3e}$$

$$M_{32}(r, s_3) = -\frac{1}{\pi}\frac{d}{2} K_{32}\Big(\frac{d}{2}r + \frac{d}{2}, \frac{a-b}{2}s_3 + \frac{a+b}{2}\Big). \tag{C3f}$$

The terms used in equations (84) are in the following form

$$p_{11n}(s_1) = \int_{-1}^{1} M_{11}(r, s_1)(1-r)^{-1/2} P_n^{(-1/2,0)}(r)dr, \tag{C4a}$$

$$p_{13n}(s_1) = \int_{-1}^{1} M_{13}(r, s_1)(1-r)^{\beta}(1+r)^{\omega} P_n^{(\beta,\omega)}(r)dr, \tag{C4b}$$

$$p_{22n}(s_2) = \int_{-1}^{1} M_{22}(r, s_2)(1-r)^{-1/2} P_n^{(-1/2,0)}(r)dr. \tag{C4c}$$

$$p_{23n}(s_2) = \int_{-1}^{1} M_{23}(r, s_2)(1-r)^{\beta}(1+r)^{\omega} P_n^{(\beta,\omega)}(r)dr, \tag{C4d}$$

$$p_{31n}(s_3) = \int_{-1}^{1} M_{31}(r, s_3)(1-r)^{-1/2} P_n^{(-1/2,0)}(r)dr, \tag{C4e}$$

$$p_{32n}(s_3) = \int_{-1}^{1} M_{32}(r, s_3)(1-r)^{-1/2} P_n^{(-1/2,0)}(r)dr. \tag{C4f}$$

C.3 *Circular stamp*

The transformed form of the kernels used in equations (90a,c) are given by,

$$W_{11}(r, s_1) = -\frac{1}{\pi}\frac{d}{2} K_{11}\Big(\frac{d}{2}r + \frac{d}{2}, \frac{d}{2}s_1 + \frac{d}{2}\Big), \tag{C5a}$$

$$W_{13}(r, s_1) = -\frac{1}{\pi}\frac{a-b}{2} K_{13}\Big(\frac{a-b}{2}r + \frac{a-b}{2}, \frac{d}{2}s_1 + \frac{d}{2}\Big), \tag{C5b}$$

$$W_{22}(r, s_2) = -\frac{1}{\pi}\frac{d}{2} K_{22}\Big(\frac{d}{2}r + \frac{d}{2}, \frac{d}{2}s_2 + \frac{d}{2}\Big), \tag{C5c}$$

$$W_{23}(r, s_2) = -\frac{1}{\pi}\frac{a-b}{2} K_{23}\Big(\frac{a-b}{2}r + \frac{a-b}{2}, \frac{d}{2}s_2 + \frac{d}{2}\Big), \tag{C5d}$$

$$W_{31}(r, s_3) = -\frac{1}{\pi}\frac{d}{2} K_{31}\Big(\frac{d}{2}r + \frac{d}{2}, \frac{a-b}{2}s_3 + \frac{a-b}{2}\Big), \tag{C5e}$$

$$W_{32}(r, s_3) = -\frac{1}{\pi}\frac{d}{2} K_{32}\Big(\frac{d}{2}r + \frac{d}{2}, \frac{a-b}{2}s_3 + \frac{a-b}{2}\Big). \tag{C5f}$$

The terms used in equations (99) are in the following form

$$q_{11n}(s_1) = \int_{-1}^{1} W_{11}(r, s_1)(1-r)^{-1/2} P_n^{(-1/2,0)}(r)dr, \tag{C6a}$$

$$q_{13n}(s_1) = \int_{-1}^{1} W_{13}(r, s_1)(1-r)^{\beta}(1+r)^{\omega} P_n^{(\beta,\omega)}(r)dr, \tag{C6b}$$

$$q_{22n}(s_2) = \int_{-1}^{1} W_{22}(r, s_2)(1-r)^{-1/2} P_n^{(-1/2,0)}(r)dr, \tag{C6c}$$

$$q_{23n}(s_2) = \int_{-1}^{1} W_{23}(r, s_2)(1-r)^{\beta}(1+r)^{\omega} P_n^{(\beta,\omega)}(r)dr, \tag{C6d}$$

$$q_{31n}(s_3) = \int_{-1}^{1} W_{31}(r, s_3)(1-r)^{-1/2} P_n^{(-1/2,0)}(r)dr, \tag{C6e}$$

$$q_{32n}(s_3) = \int_{-1}^{1} W_{32}(r, s_3)(1-r)^{-1/2} P_n^{(-1/2,0)}(r)dr. \tag{C6f}$$

## APPENDIX D

### Closed form expressions for Cauchy principal value integrals

Following result which is given by Tricomi [8], is the basic expression that is used to evaluate the Cauchy principal value integrals involving Jacobi Polynomials,

$$\frac{1}{\pi}\int_{-1}^{1}(1-t)^{\alpha}(1+t)^{\beta}P_n^{(\alpha,\beta)}(t)\frac{dt}{t-x} =$$

$$\cot(\pi\alpha)(1-x)^{\alpha}(1+x)^{\beta}P_n^{(\alpha,\beta)}(x) -$$

$$-\frac{2^{(\alpha+\beta)}\Gamma(\alpha)\Gamma(n+\beta+1)}{\pi\Gamma(n+\alpha+\beta+1)}\mathrm{F}\Big(n+1,\ -n-\alpha-\beta;1-\alpha;\frac{1-x}{2}\Big), \tag{D1}$$

where $\alpha > -1, \beta > -1, \alpha \neq 0, 1, 2, ....$, $\Gamma$ is the gamma function and F() is hypergeometric function. If $(\alpha+\beta)$ is equal to $-1, 0$ or 1, (D1) can be further simplified as follows,

$$\frac{1}{\pi}\int_{-1}^{1}(1-t)^{\alpha}(1+t)^{\beta}P_n^{(\alpha,\beta)}(t)\frac{dt}{t-x} =$$

$$= \cot(\pi\alpha)(1-x)^{\alpha}(1+x)^{\beta}P_n^{(\alpha,\beta)}(x) - \frac{2^{-\chi}}{\sin(\pi\alpha)}P_{n-\chi}^{(-\alpha,-\beta)}(x), \tag{D2}$$

where, $\chi = -(\alpha+\beta)$.

## APPENDIX E

### Indentation of a homogeneous half-plane by a circular stamp

The expressions for the contact stress $\sigma_{yy}(x,0)$, in-plane stress $\sigma_{xx}(x,0)$ and normalized force $P/\mu R$ can be obtained in closed form for the problem shown in Figure 51. The governing equations can be written as,

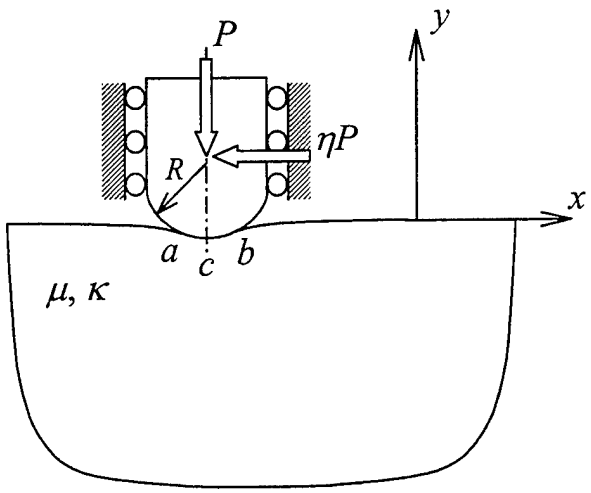


**Figure 51:** Homogeneous half-plane indented by a circular stamp

$$\frac{1}{\pi}\int_a^b \frac{\sigma_{yy}(t,0)}{t-x}dt - \eta\frac{\kappa-1}{\kappa+1}\sigma_{yy}(x) = \frac{4\mu}{\kappa+1}\frac{x-c}{R}, \quad a<x<b, \tag{E1a}$$

$$\int_a^b \sigma_{yy}(x,0)dx = -P. \tag{E1b}$$

(E1a) and (E1b) can be solved in closed form and following results can be obtained

$$x^* = 2x/(a-b) - (a+b)/(a-b), \tag{E2a}$$

$$\sigma_{yy}(x^*,0) = \mu\frac{2\sin(\pi\beta)}{\kappa+1}\frac{(a-b)}{R}\left(1-x^*\right)^{\beta}\left(1+x^*\right)^{\omega}, \qquad -1<x^*<1, \tag{E2b}$$

$$\frac{P}{\mu R} = \frac{2\pi}{\kappa+1}\Big(\frac{a-b}{R}\Big)^2\beta(1-\beta), \tag{E2c}$$

$$c = \frac{1}{2}\big\{(a-b)(2\beta-1)+(a+b)\big\}, \tag{E2c}$$

where,

$$\cot(\pi\beta) = -\frac{\eta(\kappa-1)}{\kappa+1}, \tag{E3a}$$

$$\cot(\pi\omega) = \frac{\eta(\kappa-1)}{\kappa+1}, \tag{E3b}$$

and, $\beta > 0$, $\omega > 0$, $\beta+\omega = 1$. It can be seen that if $a$ and $b$ are known, normalized force can be obtained using (E2b) and position of the centerline of the stamp can be obtained from (E2c). The in-plane stress $\sigma_{xx}(x,0)$ can also be determined in closed form (for the details of the derivation of $\sigma_{xx}(x,0)$, see Guler [9]). For $-\infty < x^* < -1$, we can write,

$$\sigma_{xx}(x^*,0) = -C_1(-x^*+1)^{\beta}(-x^*-1)^{\omega} - x^* + \beta - \omega, \tag{E4a}$$

for $-1 < x^* < 1$,

$$\sigma_{xx}(x^*,0) = C_1(1-x^*)^{\beta}(1+x^*)^{\omega}\cos(\pi\beta) - x^* + \beta - \omega + C_0(1-x^*)^{\beta}(1+x^*)^{\omega}, \tag{E4b}$$

and for $1 < x^* < \infty$,

$$\sigma_{xx}(x^*,0) = C_1(x^*-1)^{\beta}(x^*+1)^{\omega} - x^* + \beta - \omega, \tag{E4c}$$

where

$$C_0 = \mu\frac{(a-b)}{R}\frac{2\sin(\pi\beta)}{\kappa+1}, \qquad C_1 = -\frac{2C_0}{\sin(\pi\beta)}\eta. \tag{E5a,b}$$